Lipophilic nucleic acids – Building blocks for lipid-based multicompartment systems

Dissertation

zur Erlangung des akademischen Grades
d o c t o r r e r u m n a t u r a l i u m
(Dr. rer. nat.)
im Fach Biophysik

eingereicht an der
Mathematisch-Naturwissenschaftlichen Fakultät I
der Humboldt Universität zu Berlin

von
Diplom-Chemiker
Martin Loew

Präsident der Humboldt-Universität zu Berlin
Prof. Dr. Jan-Hendrik Olbertz

Dekan der Mathematisch-Naturwissenschaftlichen Fakultät I
Prof. Dr. Andreas Herrmann

Gutachter: 1. Prof. Dr. Andreas Herrmann

2. Prof. Dr. Jürgen Liebscher

3. Prof. Dr. Daniel Huster

eingereicht: 04.11.2010

Datum der Promotion: 07.12.2010

Ich will, ein für alle Mal, Vieles n i c h t wissen. – Die Weisheit zieht auch der Erkenntniss Grenzen.
(Friedrich Nietzsche, „Götzendämmerung“)

Abstract

Lipid membranes are versatile tools for the spatial organization of biomolecules. On one hand, lipid vesicles represent enclosed compartments to maintain chemical environments and allow the efficient entrapment of substances. On the other hand, lateral inhomogeneous membranes provide the two dimensional sorting of membrane-bound compounds. In this work, lipophilic nucleic acids were used to build multicompartment systems based on lipid membranes by the controlled assembly of vesicles and the domain specific functionalization of inhomogeneous membranes. Three dimensional architectures of vesicles were formed by the sequential assembly of vesicles on layer-by-layer coated particles. Upon binding of the vesicles to the particles the vesicles remained stable – they did not fuse neither became leaky. Molecules could be entrapped inside the vesicles and released on demand. It was shown that the vesicles assembled on a particle can be transported to a defined destiny using an optical tweezer. Thus, the targeted delivery and the release of encapsulated molecules on site was achieved. It was also shown that vesicles immobilized on the particles can be fused by remote control, resulting in a mixing of membrane associated compounds. Different lipophilic nucleic acids were arranged in two dimensional patterns by incorporation into domain-forming vesicles. Cholesterol-modified DNA revealed an equal distribution to both domains in liquid-liquid phase-separated membranes, whereas palmitoylated peptide nucleic acid partitioned into the liquid-ordered domain, which resembles lipid rafts of cellular membranes. Using the palmitoylated peptide nucleic acid and tocopherol-modified DNA both domains of liquid-liquid phase-separated vesicles were functionalized with different DNA recognitions sites. Both constructs could be mixed and separated by temperature control.

Key words: Lipophilic nucleic acids, DNA, PNA, Lipid vesicles, Assembly

Zusammenfassung

Lipidmembranen ermöglichen die räumliche Anordnung von Biomolekülen. Einerseits repräsentieren Lipidvesikel Kompartimente zur Aufrechterhaltung chemischer Milieus und dienen der Verkapselung verschiedenster Substanzen. Anderseits stellen inhomogene Membranen Matrizen für eine laterale Organisation von Membrankomponenten dar. In der vorliegenden Arbeit wurden lipophile Nukleinsäuren zum Aufbau kompartimentalisierter Strukturen auf der Basis von Lipidmembranen benutzt, erstens, für die geordnete, dreidimensionale Assemblierung von Vesikeln, zweitens, für eine spezifische Funktionalisierung inhomogener Lipidmembranen.

Definierte Schichten stabiler Lipidvesikel wurden auf „layer-by-layer“ beschichteten Silikapartikeln angeordnet. Mit Hilfe einer optischen Pinzette wurde der gerichtete Transport der mit Vesikeln beschichteten Partikel demonstriert. Moleküle konnten in den Vesikeln verkapselt und bei Bedarf vor Ort freigesetzt werden. Zudem wurde die kontrollierte Fusion der immobilisierten Veskel gezeigt, die eine Durchmischung von verschiedenen Membrankomponenten zur Folge hatte.

Lipophile Nukleinsäuren wurden in die Membranen von lipiddomänenbildenden Vesikeln inkorporiert. Cholesterolbasierte DNS verteilte sich hierbei homogen über die gesamte Membran. Palmitoylierte Peptid-Nukleinsäure konzentrierte sich hingegen in der flüssig-geordneten Phase von flüssig-flüssig phasenseparierten Membranen, welche sogenannten Lipid Rafts in Zellmembranen ähnelt. Mittels der palmitoylierten Peptid-Nukleinsäure und tocopherolmodifizierter DNS wurden lateral inhomogene Membranen domänenspezifisch funktionalisiert. Beide Konstrukte konnten temperaturabhängig vermischt und separiert werden.

Schlagwörter: Lipophile Nukleinsäuren, DNS, Peptid-Nukleinsäure, Lipidvesikel, Assemblierung

Abbreviations

C6-NBD-PE	1-Palmitoyl-2-{6-[(7-nitro-2-1,3-benzoxadiazol-4 yl)amino]hexanoyl}-*sn*-glycero-3-phosphocholine
CHO-K1	chinese hamster ovary cells
Chol	cholesterol
chol_DNA1	cholesteryl-TEG-modified DNA; sequence: cholesteryl-TEG-5'-TCC GTC GTG CCT TAT TTC TGA TGT CCA-3'
chol_DNA1*	cholesteryl-TEG-modified DNA; sequence: cholesteryl-TEG-5'-TCC GTC GTG CCT TAT TTC TTC (FAM)GA TGT CCA-3'
chol_DNA2	cholesteryl-TEG-modified DNA; sequence: 5'- AGG CAC GAC GGA-3'-TEG-cholesteryl
Cryo-tem	Cryo electron microscopy
DMEM	Dulbecco's Modified Eagle Medium
DNA	deoxyribonucleic acid
DNA1*	DNA oligonucleotide; sequence: 5'-FAM-TGG ACA TCA GAA ATA-3'
DNA2*	DNA oligonucleotide; sequence: 5'-Rh-AAG GAG AAG AA-3'
DNA3*	DNA oligonucleotide; sequence: 5'-FITC-TGG ACA TCA GAA ATA-3'
DNA4*	DNA oligonucleotide; sequence: 5'-TAT TTC TGA TGT CCA-FITC-3'
DOPC	1,2-dioleoyl-*sn*-glycero-3-phosphocholine
dsDNA	double stranded DNA
DTT	dithiothreitol
EDTA	ethylenediaminetetraacetic acid
ET	energy transfer efficiency
FAM	carboxyfluorescein
FBS	fetal bovine serum

FITC	fluoresceine isothiocyanate
FLIM	Fluorescence Lifetime Imaging Microscopy
FRAP	Fluorescence Recovery After Photobleaching
FRET	Förster Resonance Energy Transfer
GPI	glycosylphosphatidylinositol anchor
GPI-mCFP	fusion protein of mCFP with GPI anchor
GPMV	giant plasma membrane vesicle
GUV	giant unilamellar vesicle
HEPES	4-(2-hydroxyethyl)-1-piperazineethanesulfonic acid
IRF	instrument response function
LbL	layer-by-layer
LbL particles	layer-by-layer coated particles
ld	liquid-disordered
lo	liquid-ordered
LSM	laser scanning microscope
LUV	large unilamellar vesicle
mCFP	monomeric cyan fluorescent protein
N-NBD-PE	1,2-dipalmitoyl-*sn*-glycero-3-phosphoethanolamine-*N*-(7-nitro-2-1,3-benzoxadiazol-4-yl)
NBD	7-benzylamino-4-nitrobenz-2-oxa-1,3-diazole moiety
N-Rh-PE	1,2-dipalmitoyl-*sn*-glycero-3-phosphoethanolamine-*N*-(lissamine rhodamine B sulfony)l
palm_PNA	palmitoylated PNA; sequence: Pal-Lys(Pal)-Gly-Glu_2-Gly-ttcttctcctt-Glu_2-Gly-$CONH_2$
PBS	phosphate buffered saline
PDADMAC	poly(diallyldimethylammonium chloride)
PMAA	poly(methacrylic acid)

PMS	plasma membrane sphere
PNA	peptide nucleic acid
POPC	1-palmitoyl-2-oleoyl-*sn*-glycero-3-phosphocholine
POPS	1-palmitoyl-2-oleoyl-*sn*-glycero-3-phospho-L-serine
PS	penicillin/streptomycin
Rh	lissamine rhodamine B (rhodamine) moiety
RNA	ribonucleic acid
siRNA	short interference RNA
SM	sphingomyeline
SNARE	soluble *N*-ethylmaleimide-sensitive factor attachment protein receptor
ssDNA	single stranded DNA
SSM	*N*-stearoyl-D-*erythro*-sphingosylphosphorylcholine
TEG	triethylene glycol
T_m	melting temperature of dsDNA
tocopherol_A17	tocopherol-modified DNA; sequence: 5'-LAA AAA ALA AAA AAA AAA AAA AAA A-3'
tocopherol_DNA1	tocopherol-modified DNA; sequence: 5'-TLT TTT TLT TTT ATT TCT GAT GTC CA-3'
tocopherol_DNA2	tocopherol-modified DNA; sequence: 5'-TGG ACA TCA GAA ATA TTT LTT TTT LT-3'
tocopherol_N16	tocopherol-modified DNA; sequence: 5'-TLC CCC CLT TTT TGT CGC TTC AGC-3'
tocopherol_T18	tocopherol-modified DNA; sequence: 5'-LTT TTT LTT TTT TTT TTT TTT TTT T-3'

Table of contents

1 Introduction and Aim

Compartmentalization on a nano- or micrometer scale is one of the crucial concepts of life. The organization of specific functions is often based on the use of lipid membranes. The concepts known from nature can be transferred into biotechnological approaches to build cargo carriers, nanoscopic reaction volumes, or enclosed chemical environments. To get an impression of the full potential of such lipid-based systems, one can take a view on the eukaryotic cell. The lipid membrane consists mainly of phospho, and sphingolipids, as well as cholesterol, and specific membrane proteins.[1] The spatial organization of the functional compounds is achieved by two different principles. First, lipid membranes of different architecture and composition constitute different compartments: e.g. cytosol, endosomes, Golgi apparatus, endoplasmatic reticulum, mitochondria, and nucleus. On one hand, the membrane represents a barrier separating different environments from each other. Many molecules cannot pass the membrane because of their hydrophilicity or their size. Thus, the compartments form enclosed volumes for the different cellular functions as storage of information, synthesis of biomolecules, or metabolic activities. On the other hand, the compartments stay in contact with each other: Signal transduction pathways are activated by docking of specific molecules to membrane anchored receptor proteins[2] and fusion of vesicles with membranes drives the delivery of molecules from one compartment to the other.[3] Second, membrane compounds are inhomogeneously organized in the membrane by a lateral and transversal sorting. For example, specific membrane proteins are segregated into lipid clusters known as lipid rafts (Figure 1) enriched in cholesterol, saturated lipids, and sphingolipids.[4] Although many questions concerning lipid rafts, like their size, stability, lifetime, or their biophysical properties, are not yet cleared,[5] many membrane proteins partition favorably to rafts,[6] and their biological functions depend on the partitioning behavior.[7]

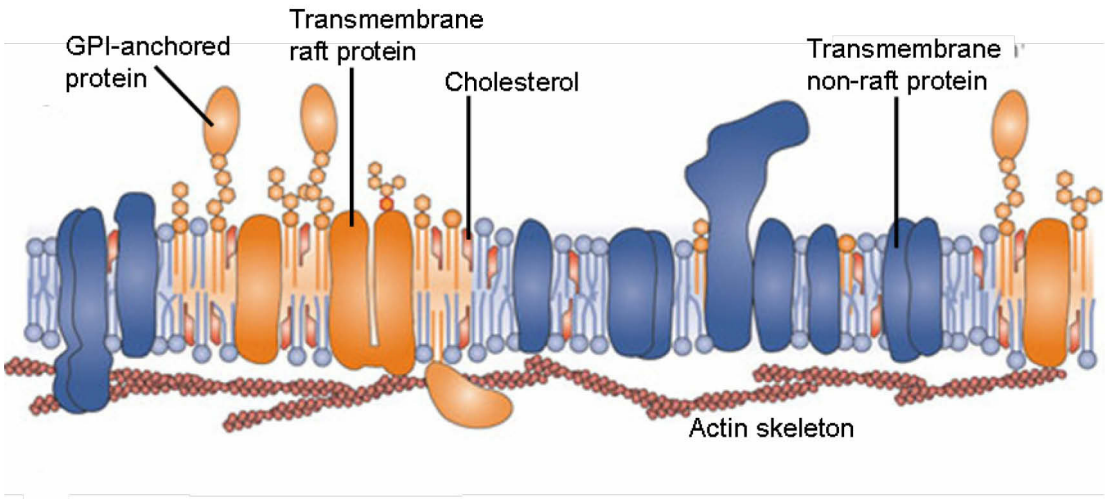

Figure 1: Scheme of a lipid raft in the plasma membrane of a cell. Yellow: lipid rafts; blue: non-raft region. Modified image from[7]

In this work, the two described principles for a spatial organization of functionalities – the formation of enclosed volumes and the lateral sorting mediated by lipid membranes - were explored for biotechnological approaches using lipid vesicles and lipophilic nucleic acids.

1.1 Lipophilic nucleic acids

Lipophilic nucleic acids are conjugates of DNA, RNA, or the artificial peptide nucleic acid (PNA) with a lipophilic moiety. Using specific properties of the nucleic acids, such constructs have already been applied in various biotechnological and biomedical approaches, e.g. for the delivery of short interference RNA (siRNA). During the past decade RNA interference via siRNA has found a great attention because of its potential for therapeutic applications. The main obstacle *in vivo,* concerning the delivery of the siRNA into the cells, is the low permeability of the plasma membrane for the siRNA. To overcome this problem, lipophilic modified siRNA has been shown to be useful.[8] The uptake and gene silencing can be further improved by altering the hydrophobic modification of the siRNA,[9,10] by incorporation of the lipophilic siRNA into high density lipoprotein particles before administration,[9] and by

introduction of a cleavage site between RNA and the lipophilic modification.[11,12] Alternatively, lipophilic PNA can be used. PNA consists of a pseudopeptide backbone that is modified with nucleosides. Figure 2 illustrates the structural differences between DNA and PNA.

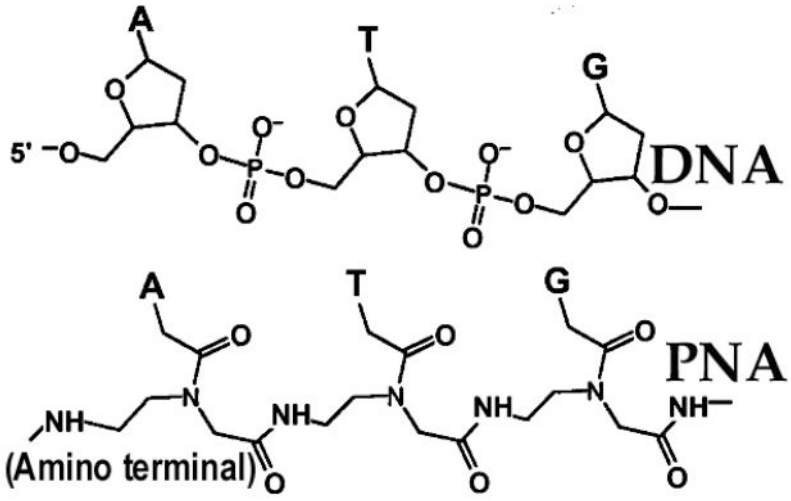

Figure 2: Backbones of DNA and PNA. Image taken from[13]

PNA binds to complementary single stranded DNA (ssDNA) forming PNA/DNA duplexes via Watson-Crick base pairing, as well as to double stranded DNA (dsDNA) by a "strand invasion". In contrary to RNA or DNA, PNA is not charged. The lack of electrostatic repulsion between PNA and DNA results in a high stability of PNA/DNA duplexes.[14] Moreover, PNA is more stable against degradation, as it is not cleavable by enzymes, neither by proteases nor by nucleases, and is more sensitive to single base pair mismatches.[15,16] Due to these specific properties of PNA, lipophilic PNA is a promising tool for the targeting of ssDNA and dsDNA. Incorporated into surfactant micelles, PNA has become a promising candidate for electrophoretic DNA separation.[17 2008] Many different conjugates of PNA with hydrophobic moieties, e.g. adamantyl residues,[18] fatty acids,[19] cholesterol,[20] and lipophilic cations,[21] have also been tested for gene silencing to enhance the low uptake of unmodified PNA into cells. Conjugations of triphenylphosphonium cations via a disulfide

bonding with the PNA has been shown to allow the uptake into the cytosol and block gene expression efficiently.[21]

DNA, being more stable than RNA against hydrolysis and cheaper than PNA, is used for the functionalization of lipid membranes. Lipophilic DNA was found to insert into lipid membranes of cells,[22] vesicles of different size,[23,24,25,26,27,28,29] and supported bilayers,[25,30,31,32] retaining its ability to hybridize with complementary DNA strands. This allows functionalization of membranes with various molecules that are attached to the complementary DNA, as it was demonstrated with dye labeled oligonucleotides.[22,23,24,33] Beyond that, vesicle-vesicle adhesion can be mediated (Figure 3c, d)[27,34,35 2007,36,37,38] and liposomes can be immobilized on solid supports[25,32] or supported lipid bilayers.[35,36] Based on these properties of lipophilic DNA oligonucleotides, various biotechnological approaches have been explored. By the tethering of large unilamellar vesicles (LUVs) on a micro-patterned surface Städler *et al*. arranged vesicles precisely on a micrometer scale providing a method for the making of membrane-based micro arrays.[39] By attaching oligonucleotides to the surface of cells cell-cell adhesion could be triggered to form three-dimensional cell networks (Figure 3a, b).[40]

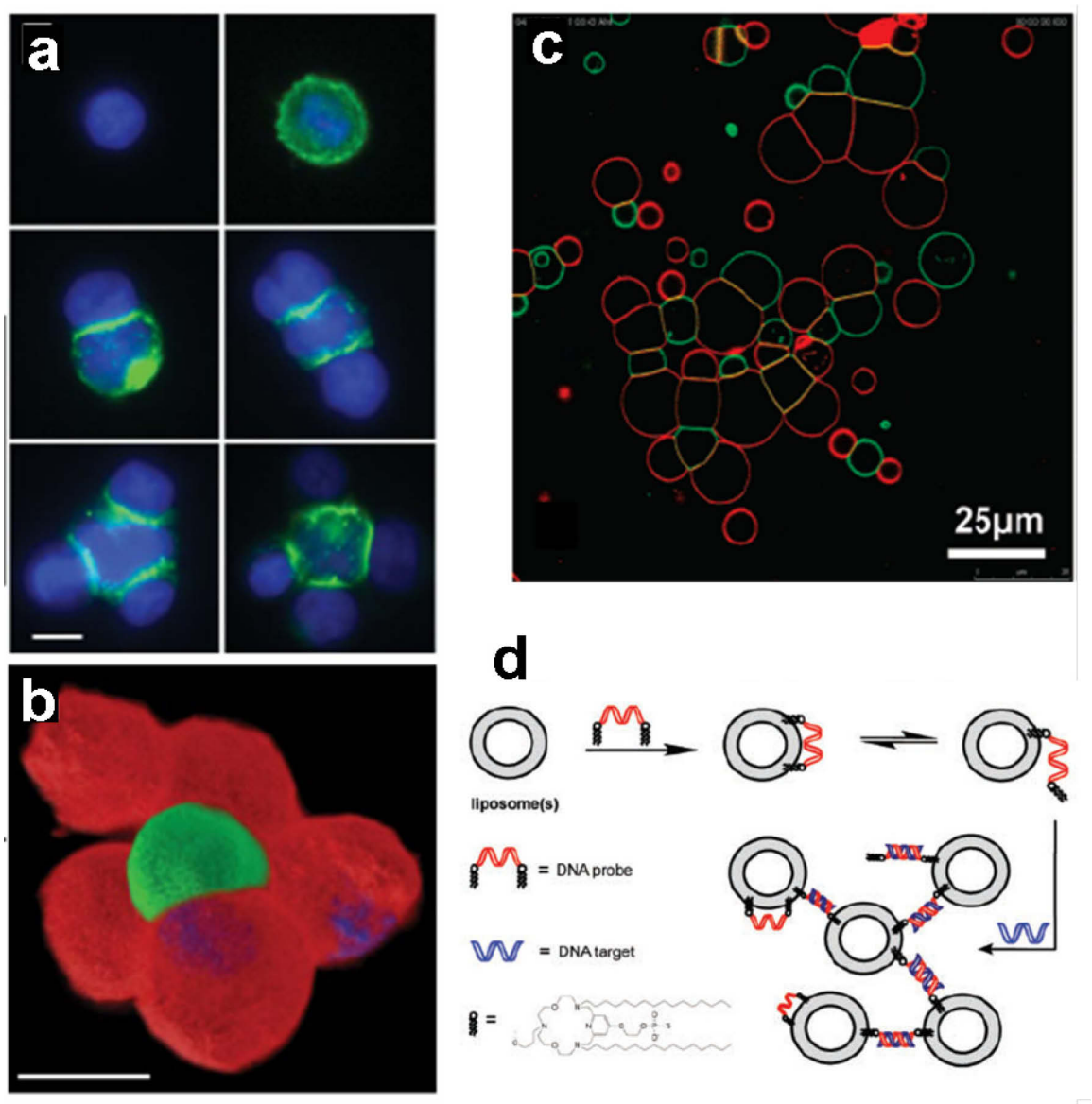

Figure 3: DNA mediated membrane adhesion. (a, b) cells connected by complementary DNA attached to the cell surfaces. (c) Assembly of giant unilamellar vesicles mediated by complementary lipophilic DNA. (d) Principle of DNA aggregation mediated by addition of DNA to vesicles with incorporated lipophilic DNA. Images modified from (a, b),[40] (c),[29,41]

Furthermore, it is possible to mimic some functions of membrane proteins using lipophilic DNA. When two populations of vesicles carrying lipophilic nucleic acids with complementary sequences are mixed, two scenarios are conceivable: Either, upon hybridization both membranes are connected, but still kept in the distance that is given by the dsDNA. In this model the lipophilic DNA acts like a receptor that mediates membrane adhesion in cells (Figure 3).[34] Or, by bringing the membranes in a very close contact,

fusion of the membranes might be promoted in a “SNARE”-like way (SNARE: soluble *N*-ethylmaleimide-sensitive factor attachment protein receptor) (Figure 4).[42 jacs,43] SNAREs are components in protein complexes that mediate membrane fusion in eukaryotic cells.[3] Thus, mixing of membrane compounds or the vesicles' content can be obtained.

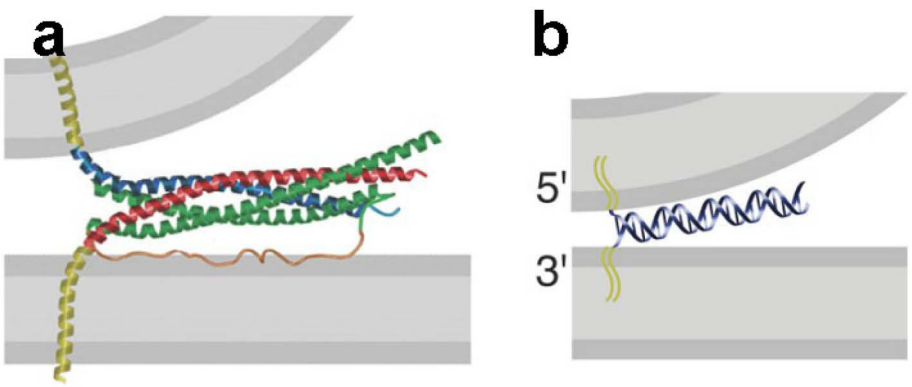

Figure 4: Fusion of lipid vesicles mediated by (a) SNAREs, (b) cholesterol-modified DNA. Image modified from [44] and [43]

Therefore, lipophilic RNA, PNA, and DNA have the potential to facilitate the construction of lipid-based systems that mimic the structures found in nature. Lipid vesicles can serve as potential building blocks even for complex hierarchical structures.

1.2 Lipid vesicles, polymersomes, and polymer capsules

The production of vesicles is quite variable: Applying different methods, size and morphology can be altered, and the use of different lipids allows the tuning of the charge, rigidity of the lipid bilayers, temperature- and pH -sensitivity. As it is possible to encapsulate various types of molecules inside the vesicles, liposomes are used in cosmetic and pharmaceutical application as drug carriers. For instance, liposome systems are under development for coatings of contact lenses,[45] and as drug delivery systems for antibiotics,[46] and are already approved for cancer therapy.[47] In the latter cases the use of

liposomes improves the delivery to the tumor site, and reduces the toxicity of the drugs.[46] An active targeting can be achieved by surface modification with specific ligands.[47] Furthermore, the triggered release of the drug molecules in distinct environments is an important issue of recent research. Studies report on liposome formulations liberating encapsulated molecules in presence of phospholipases,[48] reductive environments,[49], and low pH.[50] Nanoreactors can also be build using lipid vesicles, e.g. by the encapsulation of enzymes. By external stimuli the enzymes can be released to catalyze a distinct reaction. Alternatively, when the substrate is able to pass the membrane barrier, the reaction can be catalyzed inside the vesicle. Till now, enzyme containing vesicles have found applications in the field of biomedicine and the cheese ripening process.[51]

When lipid vesicles are described concerning their applicability for biotechnology, similar approaches based on polymers should not be excluded. The so-called polymersomes are vesicles consisting of amphiphilic block copolymers, that can be loaded with biomolecules, integral membrane proteins can be incorporated into the polymer membrane, and active enzymes can be entrapped inside the polymersomes.[52,53] This enables the positioning of different enzymes to separated sites: inside and outside the polymersome, as well as inside the polymer membrane. In this way, nanoreactors for cascade reactions were constructed (Figure 5a).[54,55]

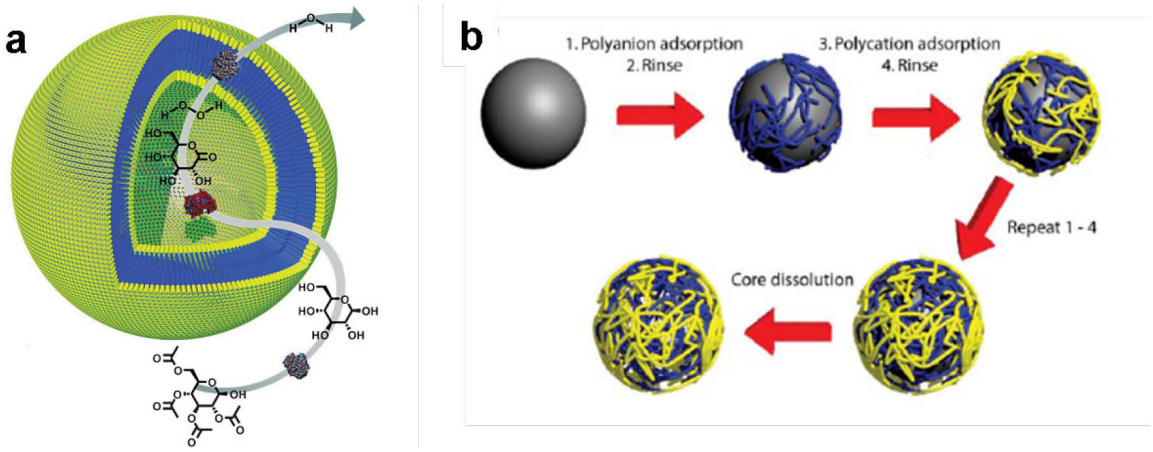

Figure 5: (a) Scheme of a polymersome used as a nanoreactor for a cascade reaction. Enzymes are placed inside, and outside the polymersome, as well as inside the membrane. Image modified from[54] (b) Formation of LbL capsules by the coating of a positively charged support. Image modified from[56]

Another versatile approach to build micrometer sized capsules is the layer-by-layer (LbL) technology. By the step wise adsorption of several layers of oligomers or polymers, surfaces can be coated with a precise control of the coating's thickness.[56] The adhesion of the layers can be mediated by diverse interactions, like electrostatic interactions, hydrogen bondings, DNA hybridization, sequential chemical reactions, metal–ligand complexation, or hydrophobic interactions.[56] For biotechnological applications bioactive substances, like nucleic acids,[57] peptides,[58] or even virus particles[59] can be incorporated inside the layers. When particles are coated by the LbL technique, capsules can be obtained by the dissolution of the core (Figure 5b).[56,60] The capsules can be filled, e.g. with DNA,[61,62] enzymes,[63] or antigens,[64] and the cargo by can released by remote control.[62] Thus, LbL-based capsules might find application as drug delivery systems or microreactors.

1.3 Artificial multicompartment systems

By the assembly of the described lipid or polymer based vesicles, multicompartment systems can be constructed – mimicking the compartments of eukaryotic cells. Different cargos can be

encapsulated into different containers for a co-delivery of active substances. Tuning the physical and chemical properties of the capsules' walls, the release rate of the different cargos can be controlled.[65] The Assembly of lipid vesicles is one possibility to reach that goal. This can be obtained by the use of lipophilic DNA, as described above,[27,29,37], other DNA mediated aggregation,[66] or avidin-biotin interactions.[67] Apart of that, vesicles can be entrapped within larger vesicles: For instance, Bolinger *et al.* invented a method for the loading of large unilamellar vesicles with small unilamellar vesicles without disturbing the vesicles integrity.[68] Molecules inside the small unilamellar vesicles stayed encapsulated until release into the larger vesicle was triggered by temperature change. This approach demonstrates the controlled separation and mixing of compounds on a nanometer scale. Comparable systems were produced using the ethanol-induced interdigitation of phospholipid bilayers. The resulting micrometer-sized "vesosomes" show separated lipid compartments inside an enveloping lipid bilayer (Figure 6a).[69] Due to the shielding of the outer membrane, the inner vesicles are protected from degradation, e.g. by phospholipases, and retain cargo molecules longer than unilamellar vesicles.[70] Therefore, vesosomes are more stable in a physiological environment making them suitable for biomedical application.

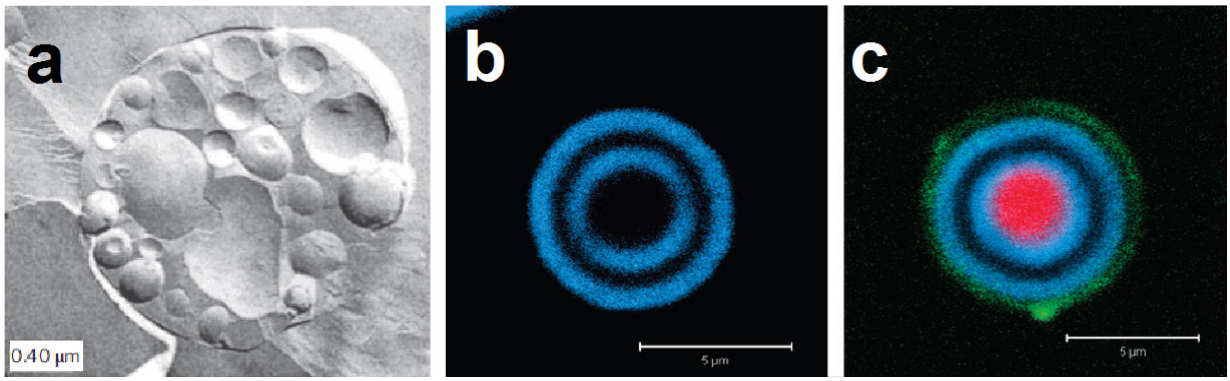

Figure 6: (a) Freeze fracture tunnel electron microscopy images of a vesosome, a lipid-based multicompartment system, white bar corresponds to 0.4 µm;[69] (b, c) Fluorescence microscopy images of a microreactor consisting of five concentric compartments, before (b) and after (c) a cascade reaction, green and red fluorescence indicate different reaction products; bars correspond to 5 µm.[71]

Concentric capsules display another form of multicompartment systems. These onion-like structures are produced in a step wise manner by repeating several coating steps, including the precipitation of an inorganic support. After the formation of the layers, the support can be dissolved leaving the concentric compartments that are separated by polyelectrolyte layers[72] or matrices of biopolymers.[71] Figure 6b and c show such a system used as a nanoreactor for a cascade reaction.[71] Finally, different materials can be combined to obtain multicompartment systems. For instance, Städler *et al.* used solid LbL coated particles as a support for the immobilization of liposomes loaded with active enzymes.[73] The binding of the liposomes was mediated by hydrophobic interactions due to cholesterol moieties attached to the surface of the particles. Thus, several thousands of nanoreactors could be assembled on the solid support.

In the above described examples, multicompartment systems were constructed by the assembly of different capsules or vesicles. An alternative is the use of particles bearing two sides of different chemistry or polarity, so-called Janus particles (Figure 7a).[74]

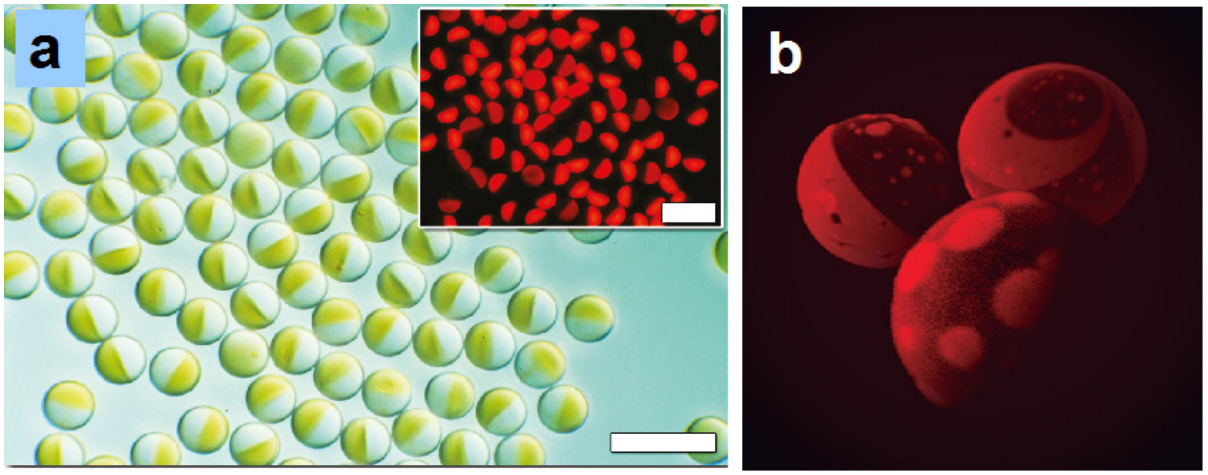

Figure 7: Janus particles, (a) DIC and fluorescence microscopy image (insert) of polymer-based Janus particles, one side containing magnetic nanoparticles (yellow), the other labeled with rhodamine (red), bars correspond to 100 µm;[75] (b) Fluorescence microscopy images of Janus particles based on polymersomes (size around tens of micrometers), domain formation was induced by addition of divalent cations.[76]

These particles can be synthesized with various methods using materials like homopolymers, block copolymers, or silica particles.[77] The Janus particles can be amphiphilic when

hydrophilic and hydrophobic polymers are combined. Such particles could find use as solid surfactants.[78] Using two polymers carrying different charges, zwitterionic Janus particles were produced.[74] Both sides can also carry different functionalizations as magnetic particles, fluorophores,[75] or protein modifications like streptavidin.[79] Specific polymersomes also show a separation into distinct domains. For instance, Christian *et al.* reported on the generation of Janus assemblies made of polymersomes containing polyanionic amphiphiles (Figure 7b).[76] Here, the domain formation was driven by the addition of divalent cations that act as a crossbridge between the negatively charged side chains of the polymers.

1.4 Constructing multicompartment systems with lipophilic nucleic acids

As described above, the ability of many lipophilic nucleic acids to insert spontaneously into lipid membranes and to hybridize with complementary DNA opens the way to realize different biotechnological approaches. First, the lipophilic nucleic acids display receptors for complementary DNA, RNA, or conjugates of DNA or RNA with different molecules or nanocrystals, e.g. organic dyes,[80] quantum dots,[81] peptides,[82] or proteins.[80] The functionalization of the lipid membrane is limited only by the availability of the DNA or RNA conjugate and its potential to hybridize with the lipophilic nucleic acid. Second, different membranes can be linked when lipophilic nucleic acids with a complementary sequence are used.[22,26,28,29,30,35,36,39] Finally, lipid vesicles might be immobilized on a surface that exposes DNA complementary to the lipophilic nucleic acids inserted into the membrane.[83] Here, the described concepts will be applied to build multicompartment systems on a nano- and micrometer scale. A lateral inhomogeneous organization of lipophilic nucleic acids in heterogeneous lipid membranes might be achieved by a specific design of

their lipophilic anchors, whereas three dimensional architectures of lipid vesicles can be built on a solid support using lipophilic DNA.

1.5 Assembly of vesicles on a solid support using lipophilic nucleic acids

The assembly of lipid vesicles allows the formation of multicompartment systems in which different vesicles carry different functions. The vesicles can be arranged on demand, using for example biotin-antibody interactions,[84] biotin-avidin interactions,[67] or lipophilic DNA.[26,38] The use of lipophilic DNA has the advantage that it allows an alteration of the inter-vesicle distance, as well as the possibility to reverse the assembly by several external stimuli like a temperature change, the reduction of ionic strength, or enzymatic treatment.[28] The assembly of the lipid vesicles can be obtained by mixing two populations of vesicles that carry complementary lipophilic nucleic acids resulting in vesicle aggregates.[28,29] Although size and composition of the aggregates can be controlled to some extent, the aggregation process does not lead to a hierarchical architecture of liposomes that would provide a precise regulation of the stoichiometry and the defined spatial organization of the vesicles. Granéli *et al.*[85] solved this problem by assembling layers of vesicles on a solid support: The first layer of vesicles was immobilized on a planar DNA-modified surface by hybridization of cholesterol-tagged DNA incorporated into the vesicles' membrane with the DNA on the support. On that first layer additional 4 layers of vesicles could be assembled in a stepwise manner based on the hybridization of cholesterol-modified DNA conjugates inserted into the vesicles' membranes (Figure 8).

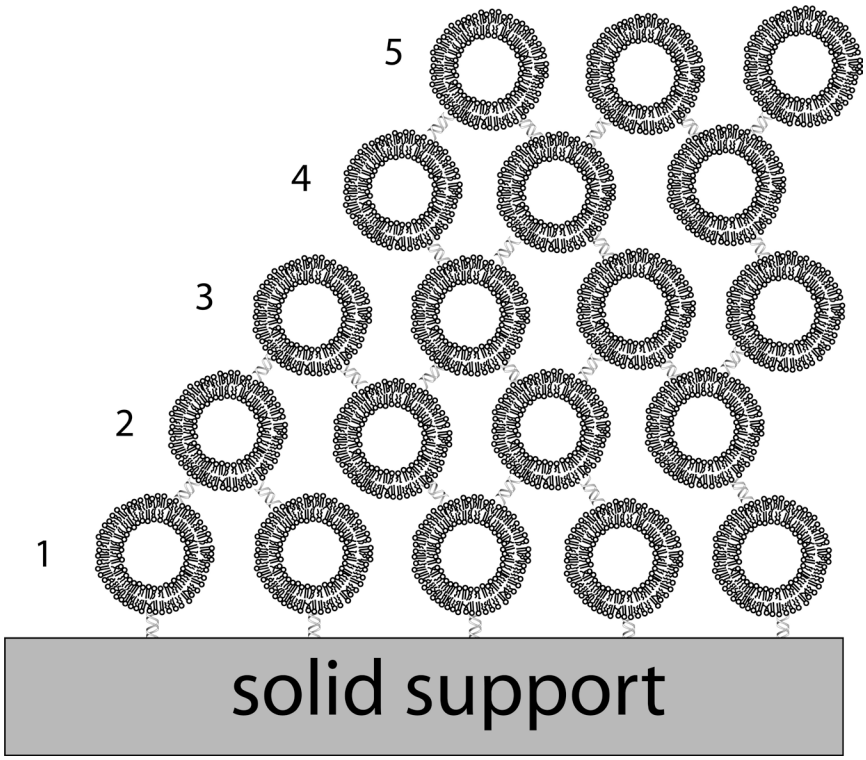

Figure 8: DNA mediated assembly of vesicles layers on a solid support. Modified from[85]

For many approaches, however, like the transport of active molecules to a target, the assembly of vesicles has to be mobile. This is possibly given for the vesicle aggregates but not for the immobilization of layers of vesicles on a planar solid support. To solve this problem the concepts can be combined (see aim): By the assembly of multiple layers of vesicless on micrometer sized particles the formation of a rational designed vesicle architecture can be realized that might be used as a delivery vehicle for co-delivery of bioactive molecules.

1.6 Lateral organization of lipophilic nucleic acids in model membrane systems

For a lateral organization of lipophilic nucleic acids in lipid membranes, the membrane itself can function as a template. Indeed, lateral inhomogeneities in lipid membranes known as lipid domains or lipid rafts are observed in artificial membranes like supported lipid bilayers[86] and giant unilamellar vesicles (GUVs)[87] as well as in the plasma membrane of eukaryotic

cells. Bilayers consisting of mixtures of lipids that differ in their phase transition temperature often show a phase-separation. In binary mixtures a solid-fluid phase-separation can be observed (Figure 9c).[88]

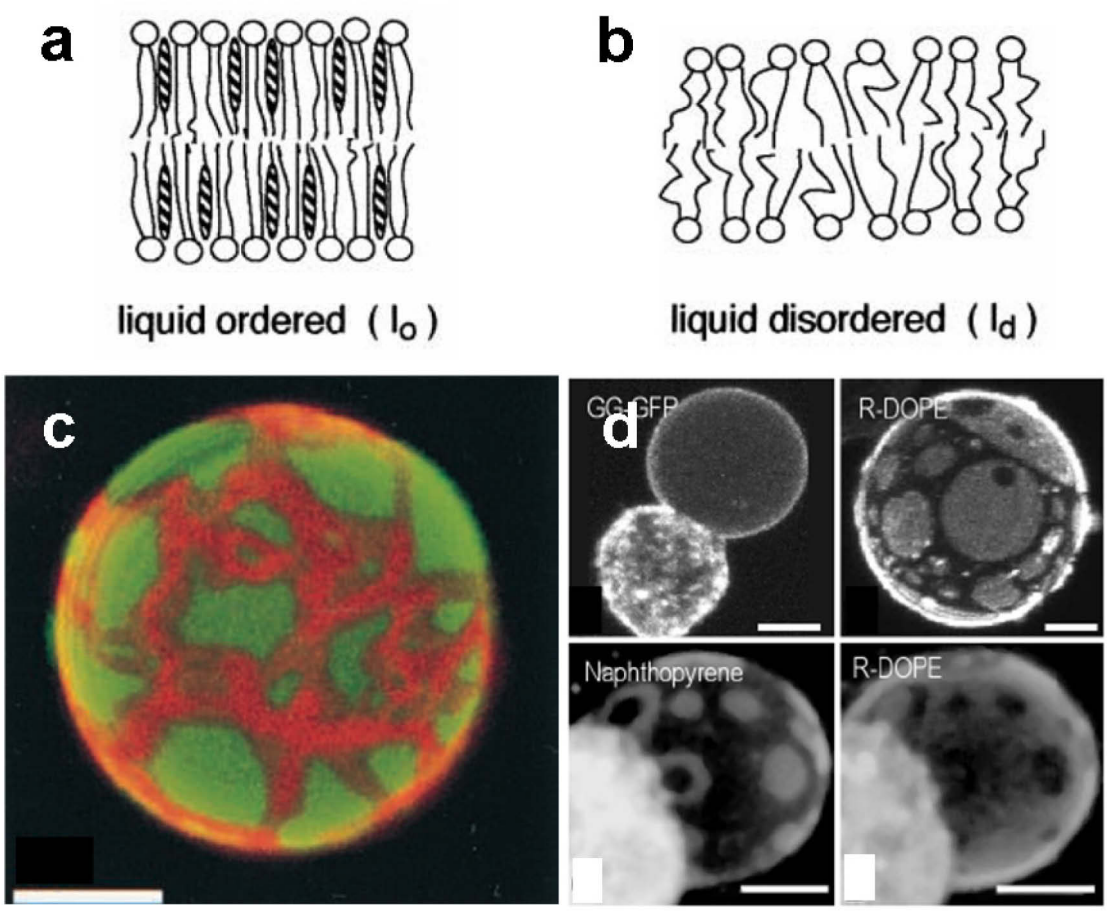

Figure 9: Phase-separation in lipid membrane. (a, b) scheme of lipid chain orientation in the liquid-ordered phase (a), shaded ovals represent cholesterol, and the liquid-disordered phase of a lipid membrane (b);[89] (c) fluorescence microscopy image of a liquid-solid phase-separated GUV;[88] (d) fluorescence microscopy images of giant plasma membrane vesicles (GPMVs) showing phase-separation, vesicles are still attached to the cells.[90] White bars correspond to 10 (c) and 5 μm (d), respectively.

In contrary to the liquid phase, the solid phase shows a long range order concerning the conformation of the lipid chains.[91] In lipid membranes made from ternary mixtures including a lipid with a low phase transition temperature and a lipid with a high transition temperature, cholesterol often triggers a liquid-liquid phase-separation into a liquid-ordered (*lo*, Figure 9a), and a liquid-disordered (*ld*, Figure 9b) phase.[89] In the *lo* domain the lipids

are more tightly packed. For instance, GUVs prepared from a 1:1:1 mixture of dioleylphosphatidylcholine (DOPC), sphingomyelin (SM), and cholesterol (Chol) show a liquid-liquid phase-separation resulting in micrometer-sized domains at room temperature.[89] Here, the *lo* phase is enriched in Chol and SM, whereas the *ld* domain mainly consist of DOPC. Concerning the high content of Chol and SM, the *lo* phase of the GUVs resembles lipid rafts.[92] For the visualization of the *lo* and the *ld* phase with fluorescence microscopy, several fluorescent lipid analogues have been described, that favorably partition into one lipid phase,[93] and, thus, act as domain markers. Domain-separated GUVs can act as model membrane systems to investigate the lateral partitioning of membrane proteins in cellular membranes. The composition of the lipid membrane of the GUVs, however, is quite simple, and cannot simulate the complex lipid-protein and protein-protein interactions in cellular membranes.[94] To this end, other model membrane systems were developed. Both giant plasma membrane vesicles (GPMVs)[90] and plasma membrane spheres (PMS)[95] are directly derived from the plasma membrane of eukaryotic cells, retaining lipid and membrane protein composition. In both systems a phase-separation into microscopic *lo* and *ld* phases can be triggerd by cooling (GPMVs, Figure 9d),[90] or by the clustering of typical raft markers (PMS).[95] By incorporating of lipophilic nucleic acids into the membrane of these model systems – phase-separated GUVs, GPMVs, and PMS – the lateral organization of the lipophilic nucleic acids could be achieved. To tune the phase partitioning behavior of the lipophilic nucleic acids, the chemical structure of the membrane anchor can be altered. Tocopherol modified DNA segregates to the *ld* phase of liquid-liquid phase-separated GUVs.[23] To address both domains, nucleic acids partitioning into the *lo* domain are demanded. Furthermore, targeting of lipid rafts with lipophilic nucleic acids could alter the uptake into cells as lipid rafts are involved in clathrin-independent endocytosis.[96] Beales and Vanderlick reported on the lateral partitioning of cholesterol-modified oligonucleotides in GUVs showing phase-separation.[97] The cholesterol-based DNA showed

segregation into the fluid phase of liquid-solid phase-separated GUVs, whereas the construct showed a 2:1 preference for the *lo* phase in liquid-liquid phase-separated GUVs consisting of DOPC, dipalmitoyl phosphatidylcholine, and Chol. Moreover, it is known that cholesterol is enriched in lipid rafts. Against this background, it is reasonable to assume that a cholesterol modification of lipophilic nucleic acids would drive the partitioning into lipid rafts or the *lo* phase of model membrane systems. The raft association of membrane proteins is, however, often dependent on the palmitoylation of the proteins.[98] Therefore, coupling of palmitoyl chains to nucleic acids might also be a possible modification to access rafts or *lo* domains of phase-separated membranes.

In summary, liquid-liquid phase-separated vesicles might function as templates for the lateral organization of lipophilic nucleic acids. This would allow the formation of a two dimensional multicompartment system, where different compartments are addressable by sequence specific hybridization of DNA.

1.7 Aim

Complex reaction pathways, e.g. signaling pathways in cells, require a strict spatial organization of functional entities. The separation of different compounds and chemical environments can be achieved using lipid membranes. Two principles might be applied to realize the spatial organization: The building of lipid vesicle assemblies and the lateral organization of membrane-bound compounds. In this work lipophilic nucleic acids should be used to realize both concepts.

First, lipid vesicles can act as compartments, where different contents are entrapped in the lumen or the membrane of the vesicles. The assembly of these vesicles on a mobil support would result in a three dimensional architecture of functional units that can be transported to a defined destiny. Different molecules might be encapsulated into different vesicles and released on demand for the targeted delivery of bioactive molecules. Furthermore, by the triggered fusion of the assembled vesicles membrane compounds could be mixed to start specific reactions.

Second, lateral inhomogeneous lipid membranes might act as a template for a two dimensional sorting of membrane compounds. Using lipophilic oligonucleotides that reveal a distinct partitioning behavior into lipid phases, lipid domains become addressable by DNA or DNA-conjugates. Until now, no lipophilic nucleic acids have been described that partition exclusively into the *lo* phase of liquid-liquid phase-separated lipid membranes. These molecules would not only provide a functionalization of lipid rafts in the membrane of eukaryotic cells. Incorporation of two different lipophilic nucleic acids partitioning into the *ld* and the *lo* domain of domain-forming vesicles would result in two-sided vesicles where both domains can be functionalized with a wide variety of molecules attached to the complementary DNA.

2 Materials and Methods

2.1 Chemicals

1-Palmitoyl-2-{6-[(7-nitro-2-1,3-benzoxadiazol-4-yl)amino]hexanoyl}-*sn*-glycero-3-phosphocholine (C6-NBD-PC), 1,2-dipalmitoyl-*sn*-glycero-3-phosphoethanolamine-*N*-(7-nitro-2-1,3-benzoxadiazol-4-yl) (*N*-NBD-PE), 1,2-dipalmitoyl-*sn*-glycero-3-phosphoethanolamine-*N*-(lissamine rhodamine B sulfonyl) (*N*-Rh-PE), 1-palmitoyl-2-oleoyl-*sn*-glycero-3-phosphocholine (POPC), 1-palmitoyl-2-oleoyl-*sn*-glycero-3-phospho-L-serine (POPS), 1,2-dioleoyl-*sn*-glycero-3-phosphocholine (DOPC), *N*-stearoyl-*D*-*erythro*-sphingosylphosphorylcholine (SSM), and cholesterol (Chol) were obtained from Avanti Polar Lipids, Inc., (Alabaster, USA). Chloroform and KCl was purchased from Merck (Darmstadt, Germany). Neomycin, Sucrose, calcein, dithiothreitol (DTT), Sephadex G50 fine, Triton X-100 and ethylenediaminetetraacetic acid (EDTA) was obtained from Sigma-Aldrich (Taufkirchen, Germany), 2-[4-(2-hydroxyethyl)piperazin-1-yl]ethanesulfonic acid (HEPES) was obtained from Carl Roth GmbH + CO. KG (Karlsruhe, Germany), Dulbecco's Modified Eagle Medium (DMEM) and penicillin/streptomycin (PS) were from PAN (Aidenbach, Germany), fetal bovine serum (FBS) and Hoechst 33342 was from Invitrogen (Carlsbad, CA, USA).

LbL coated particles were produced by Surflay Nanotec GmbH (Berlin, Germany). The particles consisted of a silica core (Ø = 4.3 µm) coated with 6 alternating layers of the positively charged poly(diallyldimethylammonium chloride) (PDADMAC) and the negatively charged poly(methacrylic acid) (PMAA) as described elsewhere.[99] The negatively charged last layer was modified by the covalent attachment of 5'-adenosine 21mers.

Nucleic acids

DNA oligonucleotides were purchased from BioTeZ (Berlin, Germany) or from Eurogentec S.A. (Belgium), tocopherol-modified deoxyuridine was synthesized in the group of Prof. Dr. Jürgen Liebscher (department of chemistry, Humboldt University, Berlin) as described elsewhere.[100] Cholesteryl-TEG-modified oligonucleotides and FAM-modified oligonucleotides were obtained from Eurogentec S.A. (Belgium). The palmitoylated PNA (palm_PNA) was synthesized as described elsewhere by solid phase synthesis by the groups of Prof. Dr. Jürgen Liebscher and Prof. Dr. Oliver Seitz (department of chemistry, Humboldt University, Berlin).[99] The oligonucleotides are listed in Table 1. The lipophilic anchors are presented in Figure 10.

Table 1: All nucleic acids were based on DNA, except of palm_PNA that is based on PNA. DNA1*, and chol_DNA1* were labeled with the green fluorescent dye carboxyfluorescein (FAM), DNA3*, and DNA4* were labeled with the green fluorescent dye fluoresceinisothiocyanate (FITC), DNA2*, an adenosine 20mer, and a thymidine 20mer were labeled with the red fluorescent dye rhodamine (Rh). L indicates lipophilic modifications.

Abbreviation	Sequence	lipophilic modification
DNA1*	5'-FAM-TGG ACA TCA GAA ATA-3'	-
DNA2*	5'-Rh-AAG GAG AAG AA-3'	-
DNA3*	5'-FITC-TGG ACA TCA GAA ATA-3'	-
DNA4*	5'-TAT TTC TGA TGT CCA-FITC-3'	-
	5'-TTT TTT TTT TTT TTT TTT TT-Rh-3'	-
	5'-AAA AAA AAA AAA AAA AAA AA-Rh-3'	-
tocopherol_T18	5'-**L**TT TTT **L**TT TTT TTT TTT TTT TTT T-3'	tocopherol
tocopherol_A17	5'-**L**AA AAA A**L**A AAA AAA AAA AAA AAA A-3'	tocopherol
tocopherol_N16	5'-T**L**C CCC C**L**T TTT TGT CGC TTC AGC-3'	tocopherol
tocopherol_DNA1	5'-T**L**T TTT T**L**T TTT ATT TCT GAT GTC CA-3'	tocopherol
tocopherol_DNA2	5'-TGG ACA TCA GAA ATA TTT **L**TT TTT **L**T-3'	tocopherol
chol_DNA1	5'-**L**TC CGT CGT GCC TTA TTT CTG ATG TCC A-3'	cholesteryl-TEG
chol_DNA1*	5'-**L**TC CGT CGT GCC TTA TTT CTT C(FAM)GA TGT CCA-3'	cholesteryl-TEG
chol_DNA2	5'-AGG CAC GAC GGA **L**-3'	cholesteryl-TEG
palm_PNA	**L**-Lys(**L**)-Gly-Glu_2-Gly-ttcttctcctt-Glu_2-Gly-$CONH_2$	palmitoyl

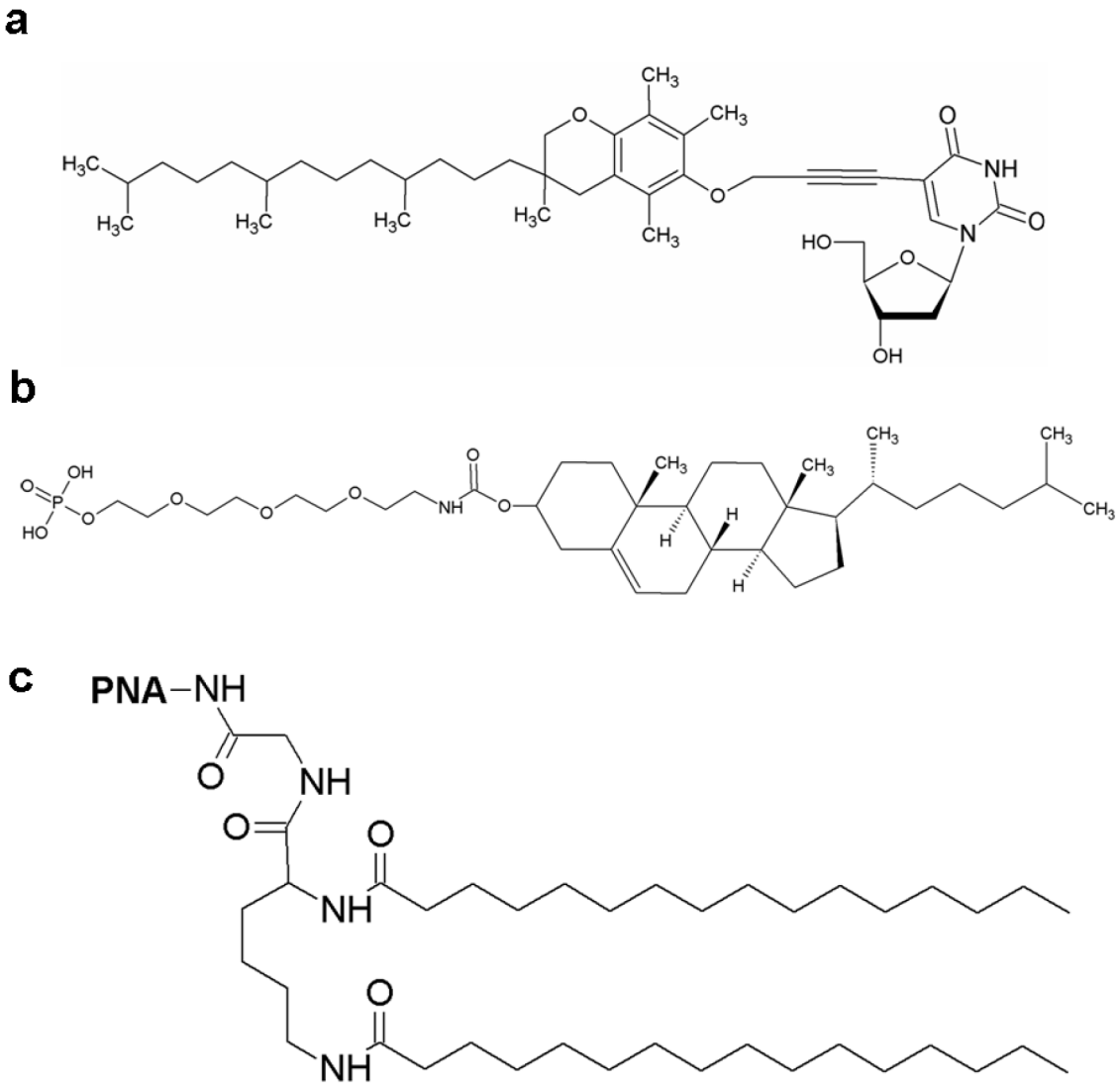

Figure 10: Lipophilic anchors of lipophilic nucleic acids. (a) tocopherol-modified deoxyuridine, used for tocopherol_T18, tocopherol_A17, tocopherol_N16, tocopherol_DNA1, and tocopherol_DNA2. (b) TEG-cholesteryl anchor of chol_DNA1*, chol_DNA1, and chol_DNA2. (c) Double-palmitoylated lysine of palm_PNA.

2.2 Buffers

1. GUV buffer contained 250 mM sucrose, 10 mM Hepes, pH 7.4.
2. Glucose buffer contained 280 mM glucose, 10 mM HEPES, pH 7.4
3. KCl buffer contained 100 mM KCl, 10 mM Hepes, pH 7.4.
4. Sucrose buffer contained 176 mM sucrose, 10 mM HEPES, pH 7.4; optional 0.5 mM calcein and 1 mM EDTA was added.
5. Phosphate buffered saline (PBS) without Ca^{2+} and Mg^{2+}, pH 7.4, was obtained from PAA (Pasching, Austria).
6. Calcein buffer was 70 mM calcein, 10 mM Hepes, 1 mM EDTA, pH 7.4, 230 mOsm.
7. Calcein exchange buffer was 10 mM KCl, 50 mM citric acid, 1 mM EDTA, pH 7.4, 230 mOsm.

2.3 Large unilamellar vesicles (LUVs)

LUVs were produced by extrusion.[101] 2 µmol POPC in about 1 ml $CHCl_3$ was added to a round bottom flask. $CHCl_3$ was removed at 40 °C at low pressure (~10 mbar) under constant rotation to obtain a homogeneous lipid film. Fluorescently labeled POPC vesicles were obtained by using lipid mixtures containing 0.1-1mol% *N*-NBD-PE or *N*-Rh-PE, or a mixture of both lipid analogues. Table 2 shows the compositions of fluorescently labeled LUVs.

Table 2: Composition of fluorescently labeled LUVs

Composition	Used in Chapter
1.0mol% *N*-NBD-PE, 99.0 mol% POPC	3.1.4, 3.1.7
0.1mol% *N*-Rh-PE, 99.9 mol% POPC	3.1.4
0.3mol% *N*-NBD-PE, 0.3mol% *N*-Rh-PE, 99.4 mol% POPC	3.1.7
0.6mol% *N*-NBD-PE, 0.6mol% *N*-Rh-PE, 98.8 mol% POPC	3.1.7
0.6mol% *N*-NBD-PE, 99.4 mol% POPC	3.1.7

After 30 min the flask was ventilated. The lipid film was suspended in 1 ml sucrose, KCl, or calcein buffer. The lipid suspension was transfered into a cryo tube. 5 freeze-thaw cycles were performed by shock freezing the samples in a dry ice/isopropanol mixture and thawing in a water bath (T = 50 °C) for 3-5 min. The lipid suspension was eleven times extruded using a mini extruder from Avanti Polar Lipids, Inc., (Alabaster, USA) with a polycarbonate filter (pore size 100 nm) resulting in LUVs with a mean diameter of 100 nm.[101] The LUVs were mixed with tocopherol-modified oligonucleotides (molar ratio lipid:oligonucleotide = 200:1). The samples were incubated overnight at 4 °C. To separate the LUVs from free lipophilic oligonucleotides and lipid aggregates, two different methods were applied:

1. Sucrose loaded vesicles (1 ml) were diluted in KCl buffer (4 ml) and centrifugated for 1 h at 100'000 g. The supernatant was removed and the pellet consisting of the vesicles with incorporated lipophilic oligonucleotides was resuspended with the isoosmotic KCl buffer (1 ml).[72]
2. Vesicles suspended in KCl buffer or calcein buffer were separated from unbound lipophilic oligonucleotides and lipid aggregates by column centrifugation. To this end, the matrix (Sephadex G50 fine) was incubated with a buffer that was isoosmotic to the buffer used for the vesicles' preparation for at least 30 min (LUVs prepared in KCl buffer: KCl buffer; LUVs prepared in calcein buffer: calcein exchange buffer). 1 ml columns (Qiagen, Hilden, Germany) were filled with the matrix. After precentrifugation of the columns for 2 min at 530 g, the samples were added and centrifugated for 3 min at 530 g. The eluate containing the vesicles was collected and the volume of the eluate was determined. To restore the sample volume before the centrifugation step, KCl buffer or calcein exchange buffer was added, respectively.

Sucrose-loaded LUVs were used for the assembly of one to three layers of LUVs on LbL particles (Chapter 3.1.4), the release and fusion assays of immobilized LUVs on LbL particles

(Chapters 3.1.5, 3.1.7) except for the time resolved calcein release assay and for the assembly of LUVs for cryo electron microscopy (Chapter 3.1.3). Assembly of LUVs on LbL particles was reproduced using LUVs produced with KCl buffer showing that column centrifugation did not affect binding of the LUVs to the particles. Calcein-loaded LUVs were used for the time resolved calcein release assay (Chapters 3.1.5, 3.1.6).

2.4 Coating of LbL particles with LUVs

The LbL particles (5% (w/v) in water) were sonified in a bath sonifier for 20 min. The particles (2.5 µl) were mixed gently with tocopherol_T18 containing LUVs or tocopherol_A17 containing LUVs (30 µL, 2 mM total lipid) and KCl buffer (217 µl). When LUVs were filled with calcein buffer, calcein exchange buffer was used instead of KCl buffer. The suspension was incubated under constant motion using Labquake (Barnstead Thermolyne) for at least 1 h or overnight at 4 °C. To separate the coated LbL particles from unbound LUVs, KCl buffer (750 µl) was added and the mixture was centrifuged for 1 min at 326 g. The supernatant was removed, the pellet containing the particles was resuspended in KCl buffer (1000 µl), mixed gently, and centrifuged again. Washing was repeated three times. After the last centrifugation step only 750 µl of the supernatant were removed to obtain a 250 µl suspension of the coated LbL particles for microscopy or fluorescence spectroscopy. To build a second (or third) layer, 780 ml of the supernatant were removed and tocopherol_T18 containing LUVs or tocopherol_A17 containing LUVs (30 µl, 2 mM total lipidv concentration) were added, proceeding as described above.

2.5 Giant unilamellar vesicles (GUVs)

Giant unilamellar vesicles (GUVs) were prepared by the electroformation method[102] in a titanium chamber.[103] A 100 nmol aliquot of pure lipids or a lipid mixture in chloroform was spotted onto a titanium plate and heated to 50 °C to remove the solvent. Traces of chloroform were removed under vacuum for at least 1 h. After sealing, the titanium chamber was filled with 1 ml of GUV buffer. An alternating electrical field of 10 Hz, rising from 0.02 to 1.1 V in the first 30 min, was applied for at least 150 min, followed by 30 min of 4 Hz and 1.3 V to detach the formed liposomes. The process was carried out at 50-60 °C when lipid mixtures including cholesterol and SSM were used. When incorporation of lipophilic PNA in POPC GUVs was investigated (Chapter 3.2.2) lipophilic PNA (as a dry powder) was added to the lipid film before addition of GUV buffer.

The following lipids or lipid mixtures were used:

- POPC
- DOPC/SSM/Chol (1/1/1 molar ratios)
- POPC/SSM/Chol (1/1/1 molar ratios)
- DOPC/SSM/Chol/POPS (1/1/1/1 molar ratios).

In lipid mixtures, 0.1 mol% *N*-Rh-PE or 0.5 mol% C6-NBD-PC was used as a marker for the liquid-disordered domains. A 20 µl portion of GUV solution was mixed with 80 µl of a microscopy buffer (see below) and 0.13 µl of 10 µM lipophilic oligonucleotides or PNA, and a stoichiometric amount of complementary DNA (lipophilic oligonucleotide to lipid molar ratio of 1:3000 or 1:300) and incubated at room temperature for 15 min (lipophilic DNA oligonucleotide) or 1 h (lipophilic PNA). As a microscopy buffer, glucose buffer, PBS, or mixtures of both with different ionic strengths was used.

2.6 Cell culture and giant plasma membrane vesicle (GPMV) preparation

Chinese hamster ovary cells (CHO-K1) cells were grown in DMEM without phenol red and supplied with 2 mM L-glutamine, 10% FBS, and 5% PS (complete medium) and incubated at 37 °C and 5% CO_2. Some CHO-K1 cells used were stably transfected with GPI-mCFP, a fusion protein of the monomeric cyan fluorescent protein (mCFP) and a glycosylphosphatidylinositol anchor (GPI). Note, the mCFP carries A206K mutation, which abolishes the natural tendency of fluorescent proteins to dimerize.[104] These cells were cultured in DMEM complete supplied with 250 µg/ml neomycin. Cells were forced to produce giant plasma membrane vesicles (GPMVs) or "blebs" upon treatment with buffer containing dithiothreitol (DTT) and formaldehyde as previously described.[90,94] Briefly, almost confluent cells (T25 flask) were washed twice with PBS, then 1.5 ml of PBS containing 2 mM DTT and 25 mM formaldehyde were added and flasks were incubated at 37 °C for 1 hour, under gentle shaking (60-80 cycles per minute). GPMVs detached from cells were then collected from the bottom of the flask and transferred into a conical glass tube where they were allowed to sediment at 4 °C for about 30 min. For microscopy 30 µl of GPMV suspension were incubated with lipophilic PNA and complementary DNA (both 1 µl, 10 µM) at 4 °C for 30 minutes, CHO-K1 cells at 37 °C for 1 hour. Vesicles were imaged in ibidi-dishes (ibidi GmbH, München, Germany). Images of the equatorial plane of the blebs were taken at 4 °C and the temperature was controlled with a water circulating bath.

2.7 Confocal microscopy

All images were taken using an Olympus Fluoview 1000 with a 60x oil immersion objective. Laser light was directed to sample and separated from emitted light with a dichroic mirror (DM 405/488/559/635). FITC (NBD, FAM) was excited with a 488 nm Argon laser, rhodamine with a laser diode at 559 nm. Green fluorescence (FITC, NBD, or FAM) was separated from red fluorescent light (rhodamine) with a dichroic long pass filter (SDM 560) reflecting light with a wavelength below 560 nm. FITC (NBD, FAM) fluorescence was recorded between 500 and 545 nm, rhodamine fluorescence was recorded between 570 and 670 nm. To avoid crosstalk of FITC (NBD, FAM) fluorescence in the rhodamine channel and vice versa, sequential scanning mode was used. Here, the sample is excited successively with the 488 nm and the 559 nm lasers while the green and the red fluorescence is recorded only during excitation with the 488 nm and the 559 nm laser, respectively. Heating and cooling (Chapter 3.2.5) was achieved using a water circulating bath and a heating block (self-construction) fitting ibidi µ-Slide VI (ibidi GmbH, München, Germany).

2.8 Fluorescence Lifetime Imaging Microscopy (FLIM)

Förster Resonance Energy Transfer (FRET) between NBD (Chapter 3.1.7) or FAM (Chapter 3.2.1) as the fluorescence donor and rhodamine as the fluorescence acceptor was measured via Fluorescence Lifetime Imaging Microscopy (FLIM) of the donor fluorescence. Images were acquired using the time-resolved LSM Upgrade Kit from PicoQuant (Berlin, Germany) on the microscope. NBD and FAM were excited at 470 nm using a pulsed laser diode. The fluorescence was detected by a single photon avalanche photodiode with a 540±20 nm filter. Data were analyzed using the SymPhoTime software (PicoQuant).

Measurement of NBD lifetime

NBD lifetimes were measured to estimate whether LUVs fuse upon binding to LbL particles, and upon addition of melittin (Chapter 4.1.7). To this end, NBD lifetimes were not fitted to a two exponential decay,[103] but only to a one exponential decay to compare the lifetimes qualitatively. FLIM pictures were accumulated for 90 s. NBD fluorescence lifetime was fitted to a mono exponential decay, by a "tail-fit", meaning that only the part which was not affected by the instrument response function (IRF) was used for the fit. Goodness of the fits was judged by visual examination of the residuals.

Measurement of FAM lifetime

FLIM pictures were accumulated for 60 s. The best two-exponential fit to the averaged fluorescence decay curve as judged by visual examination of the residuals was used. Here, also, a tail-fit was performed. For the calculation of energy transfer efficiency (ET), the amplitude weighted average lifetime $<\tau>$ was used (Equation 1):[105]

$$<\tau>=\frac{A_1\tau_1 + A_2\tau_2}{A_1 + A_2} \qquad (1)$$

where τ_1 and τ_2 are the first and second lifetime components and A_1 and A_2 are the corresponding amplitudes. ET was calculated using Equation 2:[105]

$$ET = 1 - {<\tau_{DA}>}\Big/{<\tau_D>} \qquad (2)$$

where $<\tau_D>$ is the amplitude weighted average fluorescence lifetime of the donor in the absence of an acceptor (lifetime of FAM without rhodamine (*N*-Rh-PE)) and $<\tau_{DA}>$ is the amplitude weighted average fluorescence lifetime of the donor in the presence of the acceptor.

2.9 Moving LbL particles with an optical tweezer and monitoring calcein release with fluorescence microscopy

LbL particles were coated with one layer of POPC LUVs with incorporated tocopherol_T18. In order to monitor the transient release of encapsulated molecules the LUVs were loaded with calcein at a self-quenching concentration (70 mM). The coated particles were diluted in buffer, and the suspension was placed on a glass slide. The particles were arranged to a pattern using an optical tweezer by capturing single particles before sedimenting onto the surface of the glass slides, and dropping the particles at defined place. Particles already settling on the glass surface could not be moved, most likely due to van der Waals attractions between the lipid membranes and the glass surface. To manipulate micrometer scaled particles with an optical tweezer, the particles have to consist of a material that (i) is transparent for the trapping laser, and (ii) has a different refraction index as the surrounding medium. This is valid for the LbL particles that are based on silica and are suspended in an aqueous milieu.

An optical trap implemented into an inverted Olympus IX70 microscope equipped with an 100x oil immersion objective was used. The trapping laser was a Nd:YAG-Laser (TEM_{00}, $\lambda = 1064$ nm).

To monitor calcein release of LUVs immobilized on LbL particles, a Nikon fluorescence microscope equipped with a 60x oil immersion objective was used. The sample was excited with a xenon arc fluorescence lamp using a 470±20 nm excitation filter. The emitted calcein fluorescence was recorded from 500 to 550 nm with a CCD camera. To enhance the time resolution, the optical resolution was reduced to 16*16 binning. Thus, single particles appeared as green dots instead of green open circles (Figure 19) although only the surface was fluorescently labeled with LUVs containing calcein. Time resolution was 12.5 ms. To release

the calcein, melittin (solution in H_2O, final concentration 0.18 µM) was cautiously added to the particles.

2.10 Fluorescence spectroscopy

Fluorescence of Hoechst 33342 (Chapter 3.1.2) and calcein (Chapter 3.1.5) was measured by fluorescence spectroscopy. The fluorescence spectra were acquired with a Fluoromax-4 spectrofluorometer (Jobin Yvon) at 25 °C using quartz cuvettes from Hellma (Müllheim, Germany). For excitation a xenon arc-lamp was used. Spectra were recorded with a R928P photomultiplier tube under continuous stirring. Fluorescence spectra were corrected regarding to the intensity fluctuations of the xenon arc-lamp and the wavelength dependent detection efficiency of the photomultiplier tube. Baseline spectrum of KCl buffer was subtracted from the spectra.

Fluorescence spectra of Hoechst 33342

Hoechst 33342 is a minor groove binding fluorescent dye, that shows a strongly increased fluorescence in presence of dsDNA.[72]

Sample preparation

Sample (1): 2.5 µl LbL particles (10% (w/v)) were mixed with 6 µl tocopherol_T18 containing LUVs (lipid concentration 1mM) in 1 ml KCl buffer. The suspension was shaken with a Labquake for 90 min at 25 °C. Afterwards 1 µl Hoechst 33342 (162 µM, solution in H_2O) was added, and the suspension was incubated for 120 min under constant shaking. For fluorescence measurements 1 ml KCl buffer was added. For control measurements the following probes were incubated with Hoechst 33342 instead of LbL particles and tocopherol_T18 containing LUVs: (2) 6 µl tocopherol_T18 containing LUVs; (3) 6 µl LUVs

(no lipophilic oligonucleotide incorporated) with 2.5 µl LbL particles; (4) 6 µl LUVs (no lipophilic oligonucleotide incorporated); (5) 6 µl tocopherol_N16 containing LUVs with 2.5 µl LbL-A21 particles; (6) 6 µl tocopherol_N16-LUVs; (7) 3 µl tocopherol_T18 (10 µM); (8) 3 µl tocopherol_N16 (10 µM); (9) 2.5 µl LbL particles; (10) only Hoechst 33342. Acquisition of fluorescence spectra: Hoechst 33342 was excited at 350 nm (slit 5 nm). Spectra were recorded from 360-550 nm (1 nm increment, 5 nm slit).

Fluorescence spectra of calcein

Samples were prepared according Chapter 2.3 and 2.4. 20 µl of LbL particles (0.4% (w/v)) coated with calcein loaded LUVs were mixed with 1 ml calcein exchange buffer. Time resolved calcein fluorescence was detected for 1800 s (1 s integration time, 1 s increment). Calcein was excited at 492 nm, emission was detected at 515 nm, slits were 1 nm both for excitation and emission. After about 3 min 5 µl melittin (3.5 µM) was added. When a constant fluorescence level was reached 10 µl Triton X-100 (10% (w/v)) was added.

2.11 Calculation of calcein release

Calcein release from LUVs assembled on LbL particles (Chapter 3.1.5) was calculated from the calcein fluorescence intensity spectra (2.10). Calcein release R was calculated using Equation 3, assuming that no calcein is released before melittin addition according to the previous results:[72]

$$R = \frac{F(t) - F_0}{F_{max} - F_0} \cdot 100 \qquad (3)$$

R: release of calcein from immoblized LUVs in percent

F(t): calcein fluorescence at time t

F_0: fluorescence at the beginning of the measurement

F_{max}: maximal fluorescence after addition of Triton X-100

To estimate the release of encapsulated calcein during the storage time, the calcein release R' was calculated using Equation 4:

$$R' = \frac{F'(t) \cdot (F_{max} / F'_{max}) - F_0}{F_{max} - F_0} \cdot 100 \qquad (4)$$

R': release of calcein from immoblized LUVs (after one week storage) in percent

F'(t): calcein fluorescence at time t (after one week storage)

F'_{max}: maximal fluorescence after addition of Triton X-100 (after one week storage)

F_0: fluorescence at the beginning of the measurement (without storage)

F_{max}: maximal fluorescence after addition of Triton X-100 (without storage)

2.12 Cryo electron microscopy (Cryo-TEM)

Sample preparation

Two different kinds of sucrose loaded LUVs were produced as described in Chapter 2.3 (100% POPC, lipid concentration 2 mM): One sample with incorporated tocopherol_T18, the other with incorporated tocopherol_A17. LUVs were mixed at RT and incubated for at least 2 h at 4 °C (ratio tocopherol_T18 containing LUVs:tocopherol_A17 containing LUVs = 2:1).

Cryo-TEM preparation

Droplets of the sample (5 µl) were applied to perforated (1.5 µm hole diameter) carbon film covered 200 mesh grids (R1/4 batch of Quantifoil Micro Tools GmbH, Jena, Germany), which had been hydrophilized before use by 60 s plasma treatment at 8 W in a BALTEC MED 020 device. The supernatant fluid was removed with a filter paper until an ultra thin layer of the sample solution was obtained spanning the holes of the carbon film. The samples were immediately vitrified by propelling the grids into liquid ethane at its freezing point (90 K) operating a guillotine-like plunging device.

Cryo-TEM measurement

The vitrified samples were subsequently transferred under liquid nitrogen into a Tecnai F20 FEG transmission electron microscope (FEI Company, Oregon, USA) using the Gatan (Gatan Inc., California, USA) cryoholder and -stage (Model 626). Microscopy was carried out at 94 K sample temperature using the microscopes low dose protocol at a calibrated primary magnification of 62,000X and an accelerating voltage of 160 kV (FEG-illumination). Images were recorded using an EAGLE 2k-CCD device (FEI Company, Oregon, USA) at full 2048 by 2048 pixel size. The defocus was chosen in all cases to be 1.96 µm. Cryo-TEM preparation

and measurements were performed by Dr. Kai Ludwig and Dr. Christoph Böttcher (Institute of Chemistry and Biochemistry, Freie Universität Berlin).

3 Results

3.1 Assembly of lipid vesicles on LbL particles

LUVs with incorporated lipophilic DNA oligonuleotides were assembled on a solid support via sequence specific hybridization (Figure 11). As a solid support LbL coated silica particles were chosen. To allow the binding of the LUVs onto the particles via DNA hybridization the LbL particles were covalently modified with DNA oligonucleotides. First, precursor experiments were performed to test whether (i) complementary DNA binds to the LbL particles, (ii) vesicles with incorporated complementary lipophilic nucleic acids bind to the LbL particles by the formation of double stranded DNA, and (iii) vesicles can be aggregated by sequence specific hybridization of complementary lipophilic DNA. It was then tested whether a rational architecture of several vesicle layers can be constructed on the LbL particles by a step wise coating procedure. Finally, biotechnological questions were addressed: Encapsulation of molecules inside vesicles assembled on LbL particles and their controlled release, positioning of the system with an optical tweezer, as well as the triggered fusion of assembled vesicles.

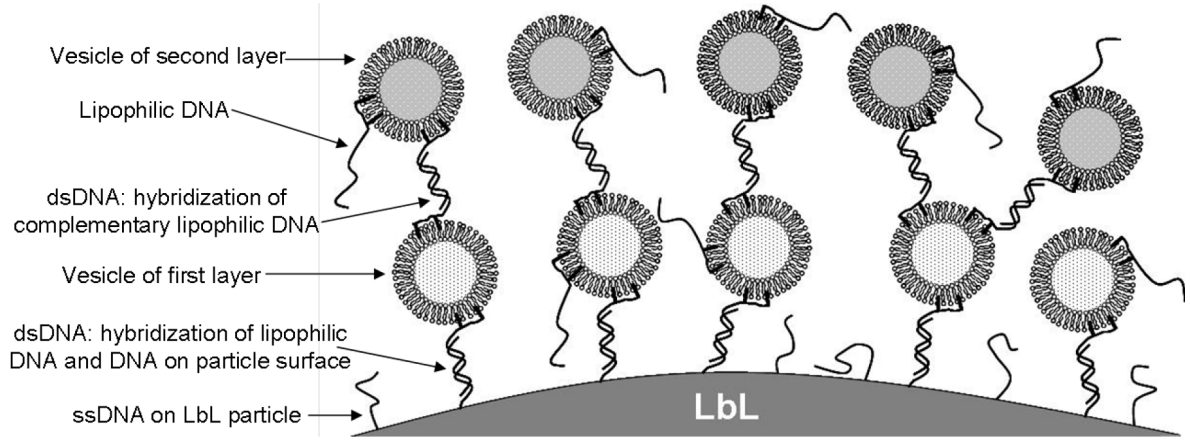

Figure 11: Scheme, detail of the assembly of two layers of vesicles on the surface of an LbL particle by sequence specific DNA hybridization.

3.1.1 Sequence specific binding of DNA to LbL particles funtionalized with complementary DNA

To immobilize vesicles on particles via DNA hybridization, their surface had to be functionalized with DNA. For that purpose LbL particles were used. The particles consisted of a silica core (Ø = 4.3 µm) coated with 6 alternating layers of the positively charged poly(diallyldimethylammonium chloride) (PDADMAC) and the negatively charged poly(methacrylic acid) (PMAA) as described elsewhere.[99] The negatively charged outermost layer was modified by covalent attachment of a 5'-adenosine 21mer.

First, it was tested whether the adenosine 21mer on the outermost polyelectrolyte layer was accessible for hybridization of complementary DNA. Addition of the complementary 3'-rhodamine thymidine 20mer resulted in rhodamine fluorescence (red) on the surface of the particles (Figure 12a and b). Note, in this experiment the LbL particles were labeled by the covalent attachment of the green fluorescence dye FITC to the outermost polyelectrolyte layer for a better visualization of the particles. As a negative control the particles were mixed with a non-complementary 3'-rhodamine adenosine 20mer. Here, no red fluorescence of rhodamine was observed on the particles' surface (Figure 12c and d). This proves that there was no unspecific binding of DNA to the LbL particles.

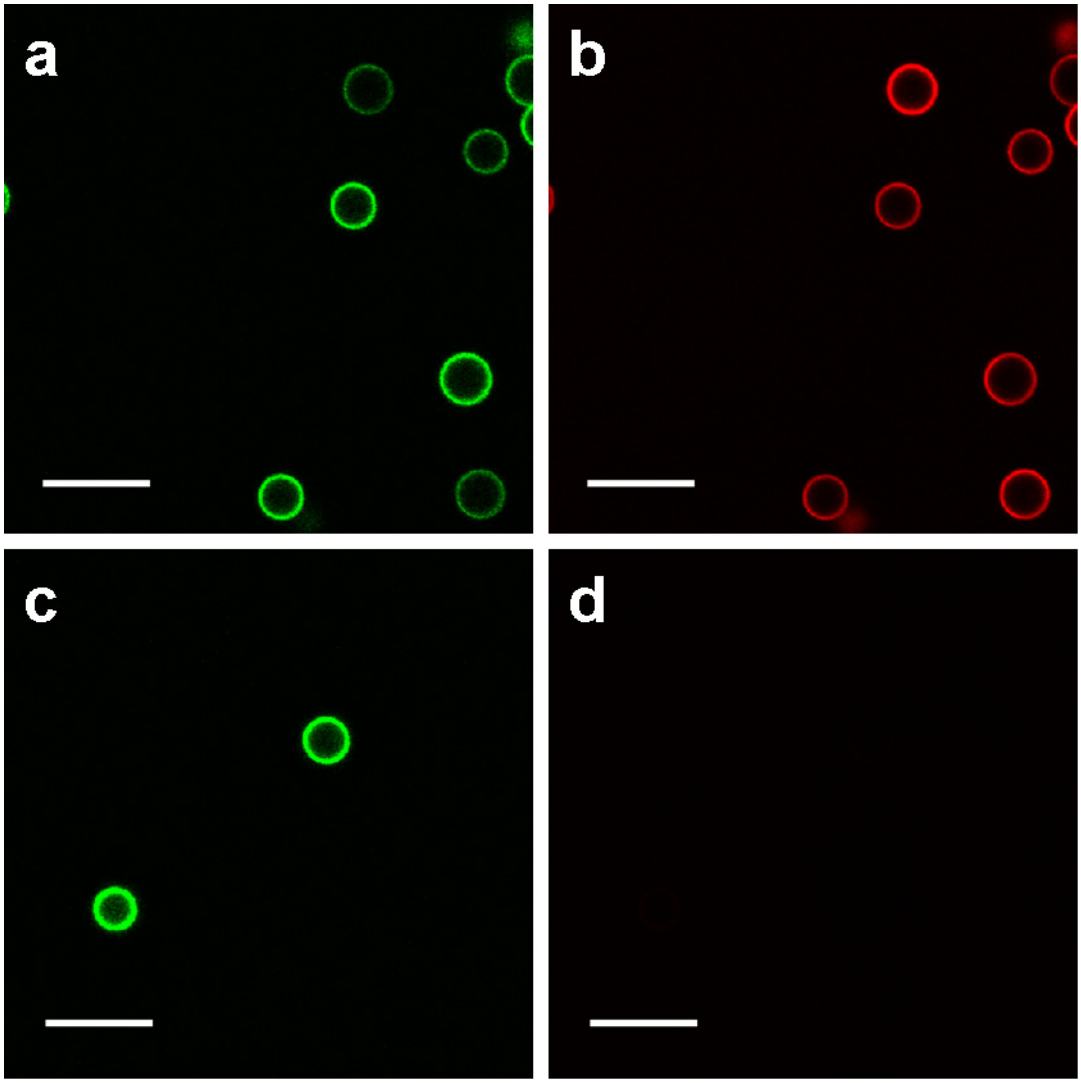

Figure 12: Confocal fluorescence microscopy images of LbL particles modified by the covalent attachment of an adenosine 21mer and the green fluorescent dye FITC to the outermost polyelectrolyte layer. Addition of a rhodamine labeled complementary oligonucleotide led to rhodamine fluorescence (red) on the particles' surface (a, b). The absence of fluorescence after addition of a rhodamine labeled non-complementary oligonucleotide (c, d) proves that no unspecific binding of DNA to the particles took place. White bars correspond to 10 μm.

3.1.2 Attachment of LUVs with incorporated lipophilic oligonucleotides to LbL particles by sequence specific hybridization of complementary DNA

To build several layers of vesicles on LbL particles via DNA hybridization, it is a prerequisite that vesicles with incorporated lipophilic oligonucleotides complementary to the DNA on the LbL particles bind to the LbL particles. For the immobilization and assembly on the LbL particles LUVs made from 1-palmitoyl-2-oleoyl-*sn*-glycerophosphocholine (POPC) produced by the extrusion method[101] were used: Because of their relatively small size (Ø~100 nm)[101] compared to the LbL particles (Ø = 4.3 µm), many vesicles can be assembled on the particles' surface. Furthermore, LUVs show a narrow size distribution[72] and are already well described for pharmaceutical applications[46,47] and as nanoreactors.[51] The LUVs were functionalized by the incorporation of lipophilic DNA that had a complementary sequence to the DNA on the LbL particles. The lipophilic oligonucleotide consisted of a DNA oligonucleotide conjugated with two lipophilic, tocopherol-modified deoxyuridine moieties. It was already shown that such lipophilic oligonucleotides incorporate spontaneously and stably into lipid vesicles and hybridize sequence specifically with complementary DNA.[23,24] The following sequence was used: 5'-LTT TTT LTT TTT TTT TTT TTT TTT T-3' (tocopherol_T18, L corresponds to the tocopherol-modified deoxyuridine moiety). LUVs with incorporated tocopherol_T18 were incubated with LbL particles. Unbound LUVs were removed from the LbL particles by several washing steps.

To elucidate whether the LUVs bind to the LbL particles via sequence specific hybridization, a minor groove binding fluorescent dye (Hoechst 33342) was added to the suspension, that shows a strongly increased fluorescence in presence of dsDNA.[72] It was already shown that hybridization of a lipophilic oligonucleotide incorporated into the membrane of GUVs with a

complementary DNA strand can be monitored using Hoechst 33342.[23] Thus, hybridization of the lipophilic oligonucleotides incorporated into the LUVs' membrane with the adonesine 21mer on the LbL particles should result in an increase of the fluorescence of Hoechst 33342. As negative controls the LbL particles were incubated with POPC LUVs without lipophilic oligonucleotides, and LUVs with an incorporated, non-complementary lipophilic oligonucleotide (sequence: 5'-TLC CCC CLT TTT TGT CGC TTC AGC-3'; abbreviation: tocopherol_N16; L corresponds to the to the tocopherol-modified deoxyuridine moiety). Furthermore, Hoechst 33342 fluorescence was measured in presence of tocopherol_T18 and tocopherol_N16, without LUVs and incorporated into LUVs, as well as in presence of the LbL particles without further additives.

Fluorescence intensity of Hoechst 33342 is only remarkably enhanced when LbL particles and tocopherol_T18 containing LUVs were present (Table 3, sample 1) compared to the fluorescence of Hoechst 33342 in buffer (Table 3, sample 10) and to the fluorescence in other control samples (Table 3, samples 2-9). Therefore, it can be concluded that binding of tocopherol_T18 containing LUVs to LbL particles led to the formation of dsDNA between lipophilic DNA (tocopherol_T18) and the DNA adenosine 21mer covalently bound to the LbL particles' surface. All samples containing the LbL particles with 4.3 µm diameter (samples 3, 5, 8, and 9) showed increased background fluorescence, very likely caused by light scattering. The slight increase of fluorescence in the samples containing LN16 is most probably due to possible hairpin formation of the oligonucleotide.

Table 3: Fluorescence maxima of Hoechst 33342 in the presence of LbL particles, LUVs, and different lipophilic oligonucleotides; tocopherol_N16 refers to a lipophilic oligonucleotide that is non-complementary to LbL particles (sequence: 5'-TLC CCC CLT TTT TGT CGC TTC AGC-3'; L refers to the lipophilic deoxyuridine moiety). Data represent the mean of two measurements (x_1 and x_2), displayed in counts per second (cps/10^5). Errors represent the deviation of the two measurements x_1-x_2.

No.	LbL particles	LUVs	Lipophilic oligonucleotide	Fluorescence intensity (cps/10^5)
1	+	+	tocopherol_T18	10.1±0.1
2	-	+	tocopherol_T18	2.6±0.3
3	+	+	-	5.3±0.3
4	-	+	-	3.3±0.4
5	+	+	tocopherol_N16	5.7±0.8
6	-	+	tocopherol_N16	2.8±0.1
7	-	-	tocopherol_T18	2.9±0.2
8	-	-	tocopherol_N16	4.5±0.4
9	+	-	-	5.2±0.2
10	-	-	-	2.9±0.2

3.1.3 Aggregation of LUVs by hybridization of complementary lipophilic oligonucleotides

To allow the formation of a three dimensional architecture of LUVs on LbL particles by hybridization of complementary tocopherol-based oligonucleotides, these lipophilic oligonucleotides should be able to mediate sequence specific vesicle-vesicle interactions without disturbing the vesicles' integrity. This was tested by mixing tocopherol_T18 containing POPC LUVs and POPC LUVs carrying the complementary lipophilic DNA, tocopherol_A17 (sequence: 5'-LAA AAA ALA AAA AAA AAA AAA AAA A-3'; L corresponds to the to the tocopherol-modified deoxyuridine moiety). The samples were studied by transmission electron cryomicroscopy (Cryo-TEM). Figure 13a and c show large and densely packed assemblies of intact vesicles. Dark spots are visible, mainly localized at the membrane's surface (Figure 14b, arrows point to dark spots), that most likely originate from dsDNA. In contrast, when only one kind of vesicles (LUVs with incorporated

tocopherol_A17) was present, no aggregation was observed, the LUVs were loosely spread (Figure 13b, arrows point to single vesicles). Here, none of the dark spots were found (Figure 14a). In conclusion, complementary tocopherol-modified oligonucleotides mediated the formation of LUV aggregates by sequence specific hybridization; the vesicles did not aggregate if only one lipophilic oligonucleotide was present. Furthermore, the microscopic studies show that the binding did not interfere with the stability of the LUVs.

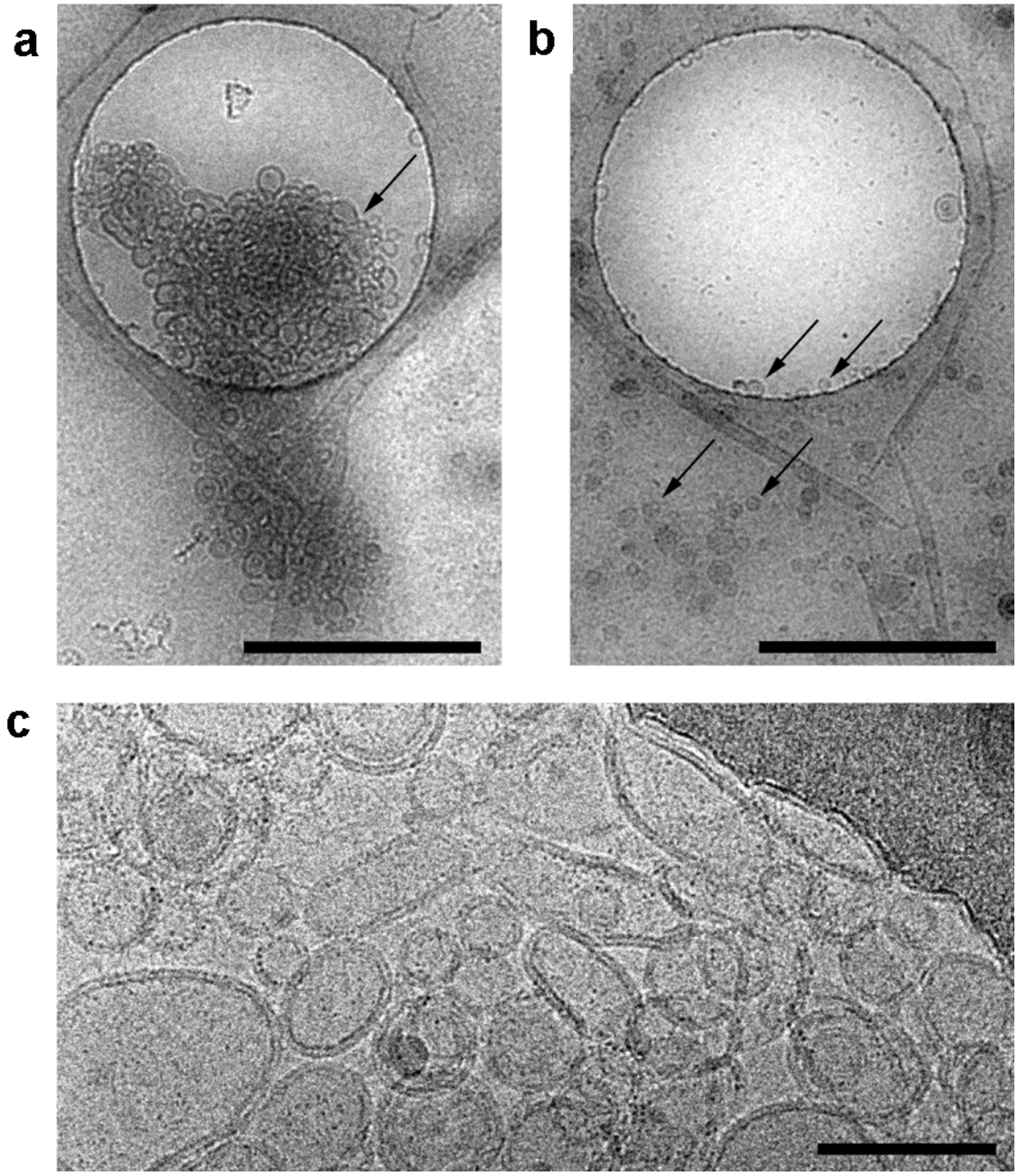

Figure 13: Cryo-TEM images: Intact vesicles are attached to each other via DNA hybridization. Vitrified samples of a 2:1 mixture of tocopherol_T18 containing LUVs and tocopherol_A17 containing LUVs (a, c) and of tocopherol_A17-LUVs (b) spanning the 1.5 µm holes of a perforated carbon film imaged by TEM. Bars correspond to 1 µm in (a) and (b) and 100 nm in (c). Whereas large assemblies of intact vesicles in the micrometer scale can be seen for the mixed sample in (a) and (c), see arrow in (a), only single unassembled vesicles (some marked by arrows) are found in (b). Cryo-TEM measurements were performed by Dr. Kai Ludwig and Dr. Christoph Böttcher (Institute of Chemistry and Biochemistry, Freie Universität Berlin).

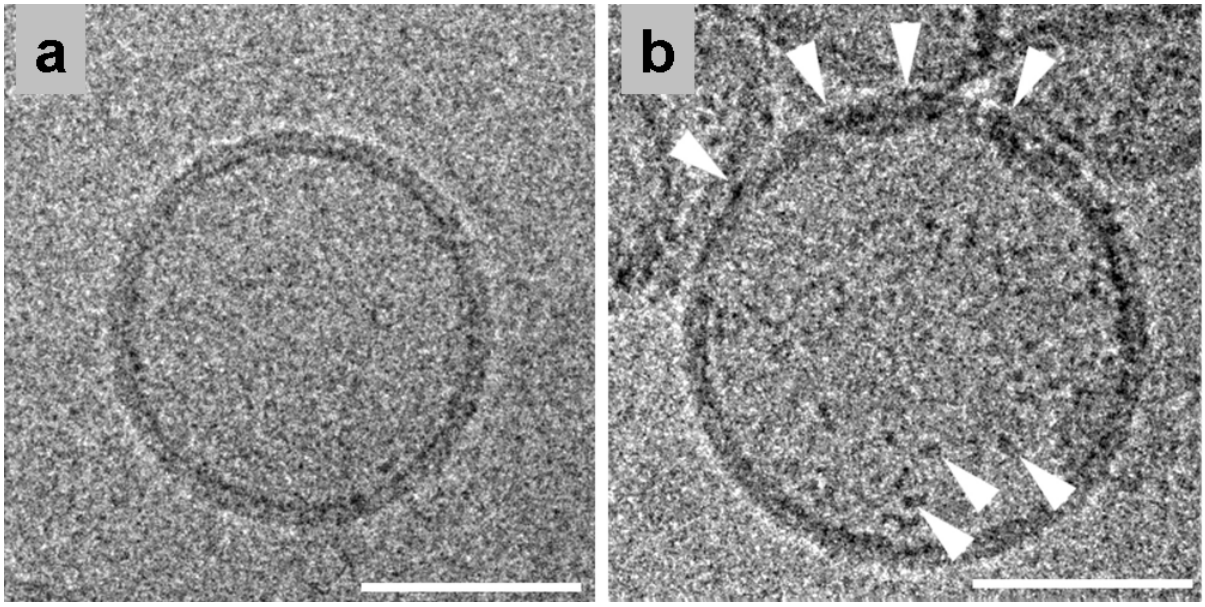

Figure 14: Cryo-TEM images: (a) Image of one control vesicle carrying only single DNA strands and therefore no spots of high density. (b) Image of a vesicle in an aggregate from the mixed sample with double-stranded DNA. Dark sports of high density (some indicated by arrows) most probably originate from double stranded DNA. Bars correspond to 50 nm. Cryo-TEM measurements were performed by Dr. Kai Ludwig and Dr. Christoph Böttcher (Institute of Chemistry and Biochemistry, Freie Universität Berlin).

3.1.4 Assembly of several layers of LUVs on LbL particles by DNA hybridization

It was aimed to assemble sequential layers of distinct vesicles on the LbL particles functionalized with the adenosine 21mer. First, the particles were coated with one layer of POPC LUVs. In order to fabricate a complete and homogeneous coating of vesicles on the LbL particles, it was necessary to add an excess of LUVs to the particles. To calculate the amount of LUVs that is needed to saturate the surface of a particle, it was assumed that all LUVs have a diameter of 100 nm, are not deformed upon binding to the particles, and are densely packed. According to this calculation, a fourfold excess of LUVs containing tocopherol_T18 was gently mixed with the LbL particles. Unbound LUVs were removed by washing. A second layer of vesicles with lipophilic oligonucleotides was assembled by repeating the above-mentioned procedure starting from the LbL particles coated with one

layer of vesicles carrying tocopherol_T18. For this purpose, LUVs with oligonucleotides complementary to that of the first layer, tocopherol_A17, were used. A third layer of LUVs, with tocopherol_T18, was assembled on the particles coated with two layers. To visualize the liposome layers, the LUVs contained fluorescent lipids, either 1,2-dipalmitoyl-*sn*-glycero-3-phosphoethanolamine-N-(7-nitro-2-1,3-benzoxadiazol-4-yl) (*N*-NBD-PE, green fluorescence) or 1,2-dipalmitoyl-*sn*-glycero-3-phosphoethanolamine-*N*-(lissamine rhodamine B sulfonyl) (*N*-Rh-PE, red fluorescence).

Figure 15a shows the confocal fluorescence microscope image of LbL particles covered with an almost homogeneous layer of *N*-NBD-PE labeled vesicles with incorporated complementary oligonucleotides (tocopherol_T18). This demonstrates the DNA mediated binding of LUVs to the LbL particles. In the absence of lipophilic oligonucleotides, *N*-NBD-PE labeled LUVs did not bind to the LbL particles (not shown). The occasional non-specific binding of *N*-NBD-PE labeled vesicles carrying the non-complementary tocopherol_A17 oligonucleotides (Figure 15b) can be explained by defects of the outermost negatively charged polymer layer that led to exposure of the underlying positively charged polymer layer of the LbL particles. Figure 15c and 17e show LbL coated particles with 2 and 3 layers of LUVs, respectively. On the first layer of *N*-NBD-PE labeled vesicles (containing tocopherol_T18), a second layer of *N*-Rh-PE labeled LUVs containing the complementary tocopherol_A17 was assembled (Figure 15c). In a control experiment, *N*-Rh-PE labeled LUVs containing tocopherol_T18, that is non-complementary to the first layer, were added. In this case, no red fluorescence was observed (Figure 15d). When three layers of LUVs were built, the LUVs of the first layer (containing tocopherol_T18) were labeled with *N*-NBD-PE, the LUVs of the second layer (containing tocopherol_A17) were not labeled, and the LUVs of the third layer (containing again tocopherol_T18) were labeled with *N*-Rh-PE (Figure 15c). As a control measurement *N*-Rh-PE labeled vesicles containing tocopherol_A17 were added to the LbL particles yet coated with two vesicle layers (Figure 15f). Note, that some

rhodamine fluorescence was observed on the particles due to unspecific binding. Presumably, tocopherol_A17 can hybridize with tocopherol_T18 incorporated into the first layer of LUVs, indicating defects of the second layer that make oligonucleotides from the first layer accessible. Due to this unspecific binding more than three layers could not be assembled on the LbL particles by sequence specific hybridization (not shown). This can be certainly avoided by using another pair of lipophilic oligonucleotides with different sequences that are non-complementary to any previous layer.

In summary, up to three layers of LUVs were assembled on LbL particles. It could be shown that the formation of the layers is mediated by the sequence specific hybridzation of complementary DNA.

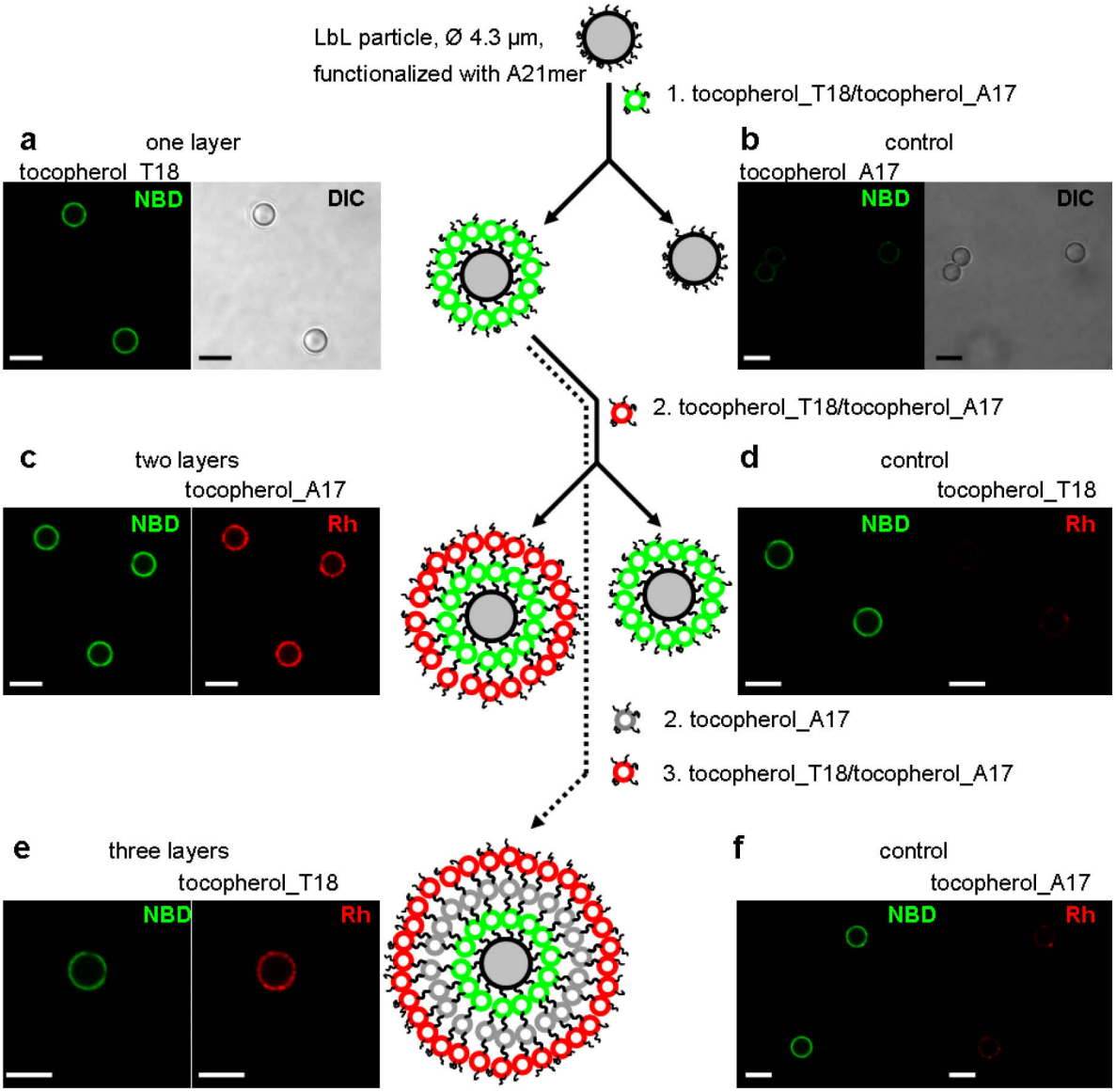

Figure 15: Coating of the LbL particles with oligonucleotide-containing vesicles: a scheme (not to scale) of the sequential layer-on-layer coating with 100 nm LUVs and images of the 4.3 µm particles obtained by differential interference contrast (DIC) and confocal fluorescence microscopy. The fluorescence originates from the lipid analogues *N*-NBD-PE (green) and *N*-Rh-PE (red) incorporated into LUVs that are attached to the LbL particles. Bars correspond to 5 µm. (a) One layer of tocopherol_T18 containing *N*-NBD-PE labeled LUVs. (b) Control for a nonspecific binding: addition of non-complementary tocopherol_A17 containing *N*-NBD-PE labeled LUVs: no binding. (c) Two layers (the first layer: tocopherol_T18 containing *N*-NBD-PE labeled LUVs, the second layer: tocopherol_A17 containing *N*-Rh-PE labeled LUVs). (d) Control addition of non-complementary tocopherol_T18 containing *N*-Rh-PE labeled LUVs: no binding. (e) Three layers (the first layer: tocopherol_T18 containing *N*-NBD-PE labeled LUVs, the second layer: unlabeled tocopherol_A17 containing LUVs, the third layer: tocopherol_T18 containing *N*-Rh-PE labeled LUVs). (f) Control addition of non-complementary tocopherol_A17 containing *N*-Rh-PE labeled LUVs: some binding is observed.

3.1.5 Encapsulation and release of molecules entrapped in LUVs assembled on LbL particles

LUVs are suitable vehicles for the encapsulation of water soluble molecules.[72] Thus, they can function as delivery vehicles for the entrapped molecule. This concept might be applied to LUVs assembled on LbL particles. However, it needs to be tested whether the LUVs remain stable upon attachment to the surface of the LbL particles, that is, they do not loose content. For instance, small vesicles are known to fuse spontaneously forming a supported lipid bilayer on charged surfaces such as glass, mica, or LbL layers.[106,107] Apart from this, it is desirable that the system allows a release of the molecules by an external trigger, as it was shown for unbound vesicles, e.g. by the addition of surfactants[108] or specific peptides,[109] or a temperature change.[110]

To demonstrate that small molecules remain entrapped in the lumen of LUVs attached to LbL particles via DNA hybridization, LUVs with incorporated tocopherol_T18 containing calcein (0.5 mM), a small water soluble dye, were attached to the LbL particles. Calcein is often used at a high self-quenching concentration of about 50-70 mM[109] to monitor the increase in calcein fluorescence intensity due to dequenching via fluorescence spectroscopy, when the fluorophore is released. Here, calcein concentration was kept well below the self-quenching concentration to visualize the fluorophore still entrapped inside the LUVs by fluorescence microscopy. Indeed, confocal fluorescence microscopy reveals calcein fluorescence on the surface of the LbL particles (Figure 16a, b). The fluorescence intensity did not notably decrease for several hours proving the stability of the immobilized LUVs for small water soluble molecules. In order to trigger calcein release, melittin, an amphipatic membrane pore-forming and fusogenic peptide from bee venom,[111] was used. Addition of melittin led to an immediate calcein leakage and loss of the fluorescence signal (Figure 16c, d).

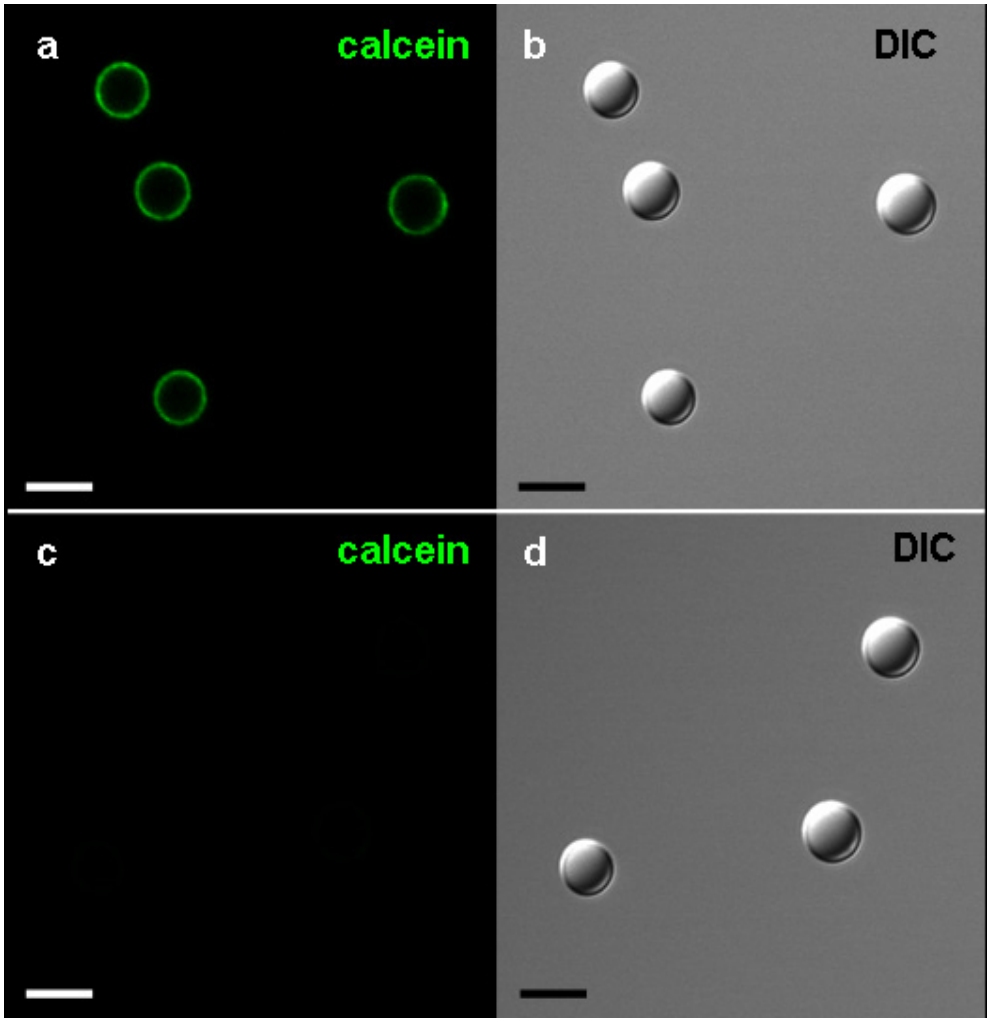

Figure 16: LbL particles coated with calcein-loaded LUVs and triggered release of the content. (a, c) Confocal fluorescence microscopy and (b, d) DIC images of the LbL particles covered with a layer of calcein-loaded tocopherol_T18 containing LUVs before (a, b) and 1 min after addition of an aqueous solution of melittin (c, d; final melittin concentration was 3.5 µM). Bars correspond to 5 µm. Vesicles were prepared by Dr. Anna Arbuzova (Department of Biology, Humboldt University Berlin).

Further, release kinetics and long term stability were investigated. To this end, calcein was entrapped at a self-quenching concentration of 70 mM inside LUVs, which were then incubated with tocopherol_T18. After binding of the LUVs to the LbL particles and subsequent removal of unbound LUVs, the time dependent calcein fluorescence intensity of the particle suspension was measured (Figure 17, black line). Fluorescence intensity remained constant until addition of 2 µM melittin. Addition of Triton-X100 to dissolve the LUVs revealed that melittin caused a complete release within 3 min. Figure 17 (red line) shows the calcein release from tocopherol_T18 containing LUVs bound to LbL particles after one week

of storage at 4 °C. Although LUVs still retained calcein, a loss of calcein from the vesicles of about 30% was detected. Melittin treatment (final concentration 2 µM) led again to an immediate increase of calcein fluorescence reaching a constant level after one minute. Subsequent Triton-X100 addition did not result in a further increase of the fluorescence intensity showing that the added amount of melittin was again sufficient for the complete release of calcein.

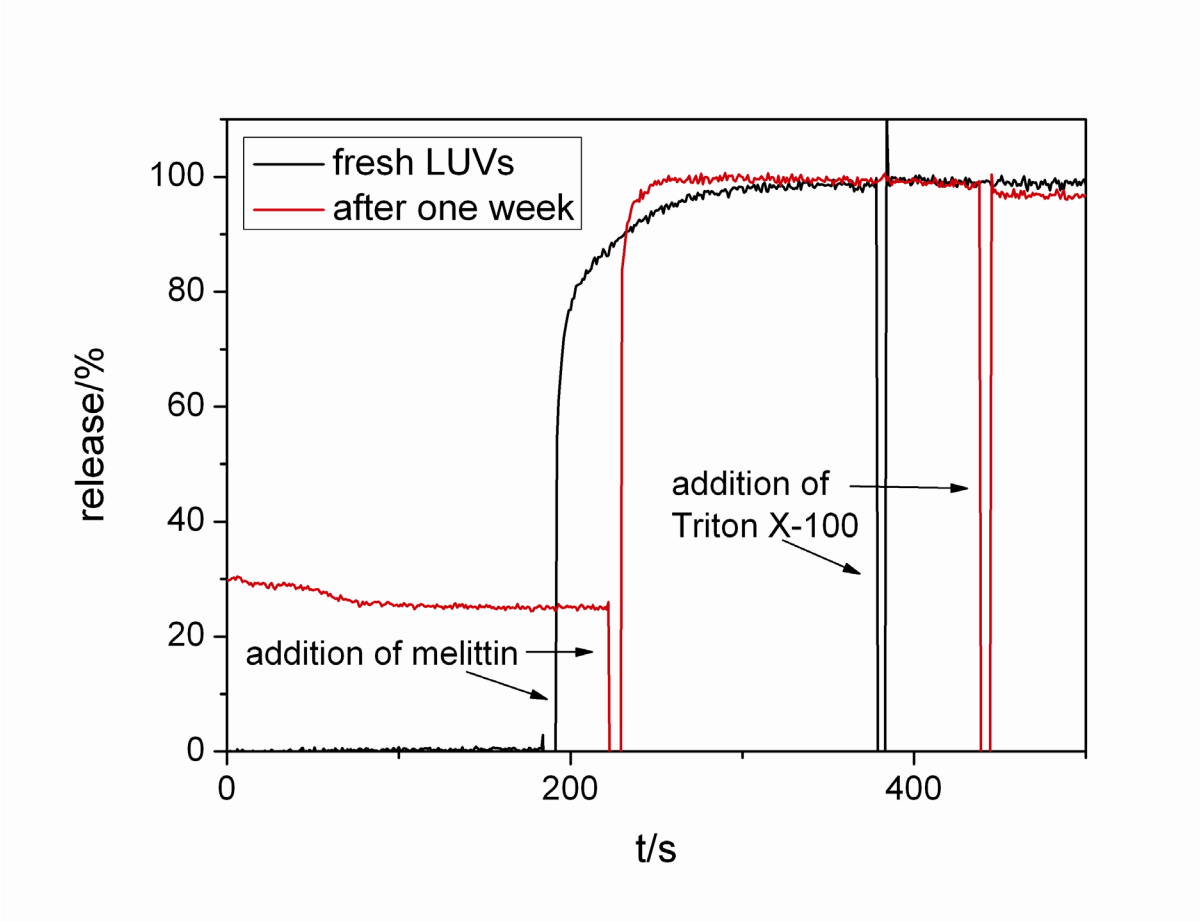

Figure 17: Release kinetic of calcein from LUVs with incorporated tocopherol_T18 immobilized on LbL particles. Release was measured directly after the preparation of the coated particles (black line) or after one week of storage at 4 °C (red line) by monitoring the calcein fluorescence.

3.1.6 Transport of LbL particles coated with LUVs using an optical tweezer and subsequent calcein release

In the previous chapter it was shown that small water soluble molecules can be encapsulated and released by addition of melittin. In this chapter the targeted delivery of LbL particles coated with one layer of LUVs is reported, achieved by the combination of three different approaches: the encapsulation of molecules inside LUVs immobilized on the particles, the controlled transport to a selected destiny by an optical tweezer, and the triggered release of the molecules.

LbL particles were coated with one layer of POPC LUVs with incorporated tocopherol_T18, loaded with calcein at a self-quenching concentration (70 mM). The release of calcein from the particles arranged in a pattern ("Smiley") by an optical tweezer was monitored using fluorescence microscopy. Figure 18 illustrates the formation of the pattern.

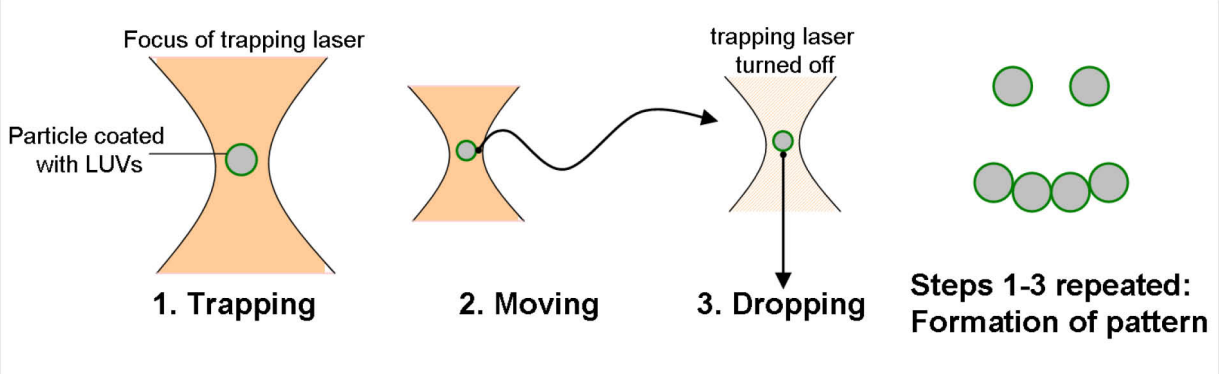

Figure 18: Scheme, positioning of LbL particles coated with one layer of LUVs with an optical tweezer. The particles are trapped in the focus of the trapping laser, moved to a certain destiny, and dropped by switching of the trapping laser. By repetition of these steps patterns of particles were built.

Figure 19a shows the assembly of LbL particles coated with one layer of LUVs before the release of calcein in a false color representation. The green color indicates a relatively low fluorescence that arises from the self-quenched calcein. Melittin was added to the arrangement of particles (Figure 19c). The subsequent calcein release resulted in a rising fluorescence (yellow and red color, Figure 19d and e) in the region around the particles due to

dilution of calcein. Finally, the calcein was completely released and diffused out of the observation area. As a consequence fluorescence faded out and finally disappeared (Figure 19f).

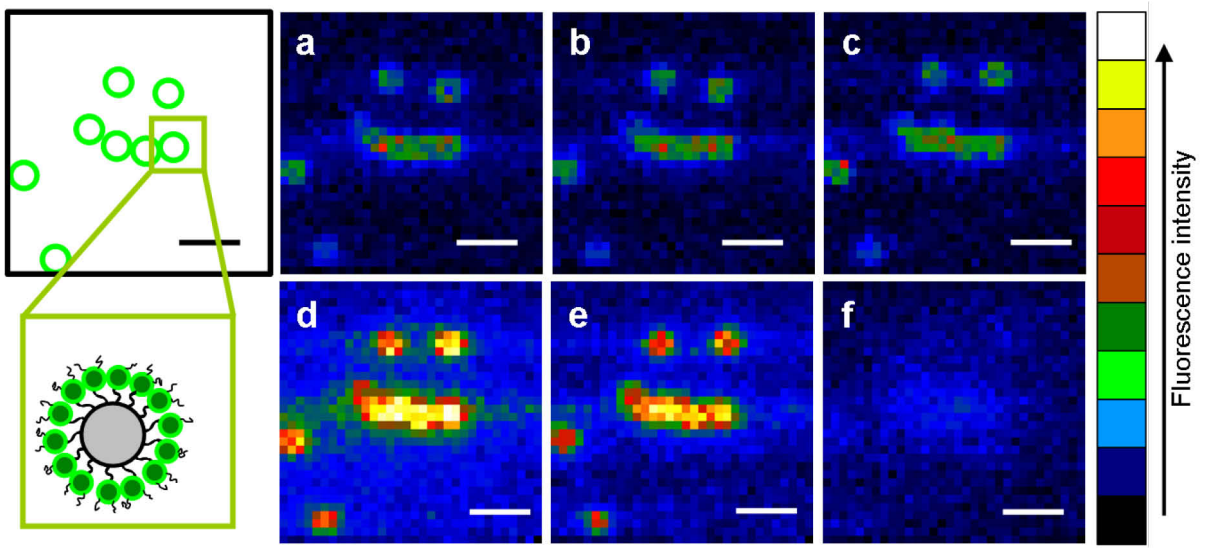

Figure 19: Calcein release from LbL particles coated with one layer of LUVs containing tocopherol_T18 by melittin addition. Particles were arranged to a pattern ("Smiley") using an optical tweezer. Schemes in the upper and lower left shows the position of the single particles and one coated particle, respectively. Fluorescence microscopy images are presented in false colors. The bar on the right side shows the correlation between the fluorescence intensity and the color representation. (a, b): before the melittin addition, low calcein fluorescence due to self quenching of the fluorophore; (c): directly after melittin addition, low fluorescence remains, calcein is not yet released; (d, e): during calcein release fluorescence rises; (f): the fluorescence is diappeared, calcein is completely released and diffused out of the observation area. Please note, optical resolution was reduced to enhance time resolution. Bars correspond to 10 µm.

3.1.7 Induced fusion of vesicles assembled on LbL particles

For specific (bio)technological application fusion of LUVs assembled on LbL particles might be desired. For instance, two different reactants could be entrapped into different LUVs. Fusion of the LUVs would result in mixing of the reactants and start the reaction. Therefore, it is necessary that LUVs do not fuse upon binding to the LbL particles and that fusion can be triggered on demand. Two different fusion assays based on Fluorescence Recovery After

Photobleaching (FRAP) and Förster Resonance Energy Transfer (FRET) were applied to investigate whether the tocopherol_T18 containing LUVs fuse upon binding to the LbL particles or it is possible to trigger such fusion.

For the FRAP assay LbL particles were coated with one layer of POPC LUVs with incorporated tocopherol_T18 containing the green fluorescent lipid analogue *N*-NBD-PE. If the LUVs stay intact upon binding to the LbL particles, the diffusion of the incorporated *N*-NBD-PE molecules will be restricted to the small areas of individual LUVs of about 100 nm, whereas the formation of µm-sized continuous lipid membranes by fusion of the LUVs would enable a free diffusion of the *N*-NBD-PE molecules. Figure 20a-c shows that *N*-NBD-PE diffusion is restricted: When a spot on an LbL particle coated with *N*-NBD-PE labeled LUVs was bleached, no recovery of the fluorescence at this spot was observed. However, after fusion of the LUVs by pre-incubation of the coated LbL particles with melittin, fluorescence recovery was observed, showing that the particles were then covered by a rather continuous lipid coat (Figure 20d-f).

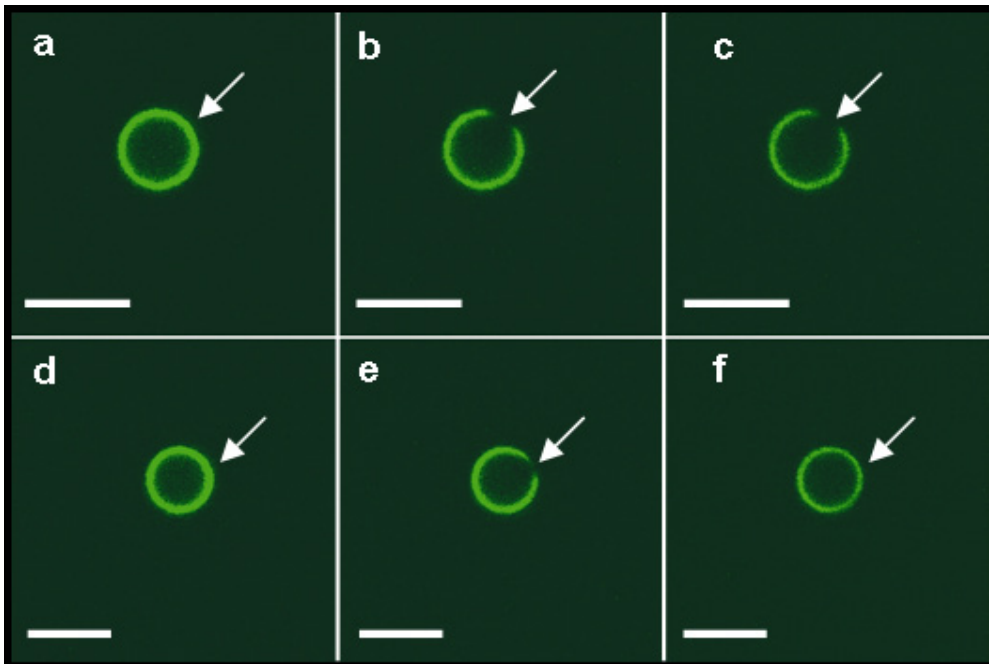

Figure 20: Intact vesicles are stably bound to the LbL particles as demonstrated by FRAP experiments. The LbL particles coated with one layer of *N*-NBD-PE labeled LUVs before (a, d), directly after (b, e), as well as 18 s after (c, f) the bleaching pulse. Bleached areas are indicated with arrows. (a–c) In the absence of melittin no fluorescence recovery on the LbL particles coated with vesicles was observed. (d–f) After pre-incubation with melittin, fluorescence recovery was observed. Bars correspond to 5 µm.

The results of the FRAP assay do not guarantee the complete absence of vesicle fusion: When only a few LUVs fuse in each fusion event, the resulting vesicles or membrane patches have a size below the optical resolution limit of the microscope. Therefore, another fusion assay, based on FRET was applied that is independent of the size of a potential fusion product. The fusion assay was performed using a modified protocol of Düzgüneş *et al.*[112] LbL particles were coated with one layer of a mixture of tocopherol_T18 containing LUVs made from POPC: One part of the LUVs was labeled with 0.6mol% *N*-NBD-PE and *N*-Rh-PE (0.6% NBD-Rh-LUVs), the other vesicles contained no fluorophore (ratio 0.6% NBD-Rh-LUVs: unlabeled LUVs was 1:2). In the fluorescently labeled vesicles *N*-NBD-PE acts as a FRET donor and *N*-Rh-PE as a FRET acceptor. As a consequence the fluorescence lifetime of *N*-NBD-PE is reduced compared to *N*-NBD-PE in the absence of a FRET acceptor. When the fluorescently labeled LUVs fuse with the unlabeled ones, the dyes are diluted in the

membrane. The FRET efficiency is reduced which can be monitored by the raised fluorescence lifetime of *N*-NBD-PE. Therefore, the fusion of the LUVs can be measured by FLIM. For control measurements LbL particles were also coated with LUVs labeled with a) 0.6mol% *N*-NBD-PE (0.6% NBD-LUVs), b) 0.6% *N*-NBD-PE and *N*-Rh-PE, and c) 0.3mol% *N*-NBD-PE and *N*-Rh-PE (0.3% NBD-Rh-LUVs). Table 4 summarizes the results of the FLIM measurements.

Table 4: Fluorescence lifetimes of NBD measured by FLIM of LbL particles coated with one layer of LUVs. LUVs consisted of POPC and contained different amounts of *N*-NBD-PE as FRET donor, and *N*-Rh-PE as FRET acceptor. FLIM was measured in presence and absence of melittin. The data displays the mean of ten measurements. * Lifetime not measured. Errors represent the standard error.

sample	$\langle\tau\rangle$/ns (no addition of melittin)	$\langle\tau\rangle$/ns (addition of melittin)
Mixture 0.6% NBD-Rh-LUVs and unlabeled LUVs	4.0 ± 0.2	5.1 ± 0.4
0.6% NBD-LUVs	7.7 ± 0.4	*
0.6% NBD-Rh-LUVs	4.0 ± 0.2	4.0 ± 0.2
0.3% NBD-Rh-LUVs	4.8 ± 0.3	*

The fluorescence lifetime of *N*-NBD-PE in vesicles containing 0.6 mol% *N*-NBD-PE (no *N*-Rh-PE) attached to the LbL particles was ~ 7.7 ± 0.4 ns. The fluorescence lifetime became shorter due to FRET when *N*-Rh-PE was also incorporated into POPC LUVs: 4.0 ± 0.2 ns and 4.8 ± 0.3 ns for 0.6%-NBD-Rh-LUVs and for 0.3%-NBD-Rh-LUVs, respectively. When a mixture of unlabeled LUVs and 0.6%-NBD-Rh-LUVs was attached to the LbL particles, the lifetime of *N*-NBD-PE was identical to that measured in the absence of unlabeled LUVs. This indicates that LUVs did not fuse spontaneously. When fusion between unlabeled and labeled vesicles was triggered by addition of melittin to these LbL particles, the distance between donor and acceptor increased leading to a reduction of FRET efficiency measured by the enhancement of NBD fluorescence lifetime from 4.0 ± 0.2 ns to 5.1 ± 0.4 ns. Addition of

melittin to the LbL particles coated with only one type of vesicles did not change NBD lifetime. Here vesicles of the same composition fused with each other, the average distance between donor and acceptor was not affected and consequently the lifetime remained constant.

3.2 Lateral organization of lipophilic nucleic acids in model membrane systems

Two different lipophilic nucleic acids were investigated concerning their phase partitioning behavior in phase-separated lipid vesicles. In particular, it was of interest whether the constructs partition into the *lo* phase of liquid-liquid phase-separated membranes, and, thus, are possible candidates for targeting rafts in cellular membranes. First, cholesterol-based DNA, and second, palmitoylated PNA were incorporated into liquid-liquid phase-separated GUVs and GPMVs. Palmitoylated PNA was also tested for its partitioning behavior in GMPVs and its ability to incorporate into the plasma membrane of cells. Finally, using the lipophilic PNA and tocopherol-modified DNA, two-sided vesicles – Janus vesicle – were generated.

3.2.1 Lateral organization of membrane-associated cholesterol-modified-DNA

To investigate the phase partitioning behavior of cholesterol-modified DNA, different cholesterol-based oligonucleotides were incorporated into the membranes of GUVs consisting of a mixture of 1,2-dioleoyl-*sn*-glycero-3-phosphocholine (DOPC), *N*-stearoyl-D-*erythro*-sphingosylphosphorylcholine (SSM), and cholesterol (Chol; molar ratio 1:1:1). GUVs of this composition have been shown to form microscopically visible *lo* and *ld* domains.[89] To visualize domains, GUVs contained 0.1 mol% *N*-Rh-PE as a marker for *ld* domains.[93] The lipophilic oligonucleotides consisted of one cholesterol moiety connected to the DNA oligonucleotide via a triethylene glycol (TEG) linker. The following sequences were used: cholesteryl-TEG-5′-TCC GTC GTG CCT TAT TTC TGA TGT CCA-3′ (chol_DNA1); cholesteryl-TEG-5′-TCC GTC GTG CCT TAT TTC TTC (FAM)GA TGT CCA-3′

(chol_DNA1*); 5′- AGG CAC GAC GGA-3′-TEG-cholesteryl (chol_DNA2); (FAM)- 5′-TGG ACA TCA GAA ATA-3′ (DNA1*). chol_DNA1 and chol_DNA1* display a complementary sequence to chol_DNA2 and DNA1, respectively. To visualize the cholesterol-modified DNA at the membrane, chol_DNA1* and DNA1* were labeled with the green fluorescent dye carboxyfluorescein (FAM). Figure 21 illustrates the constructs that were incorporated into GUV membrane: chol_DNA1* (a), a hybrid of chol_DNA1* and chol_DNA2 (b), as well as a hybrid of chol_DNA1 , chol_DNA2, and DNA1* (c).

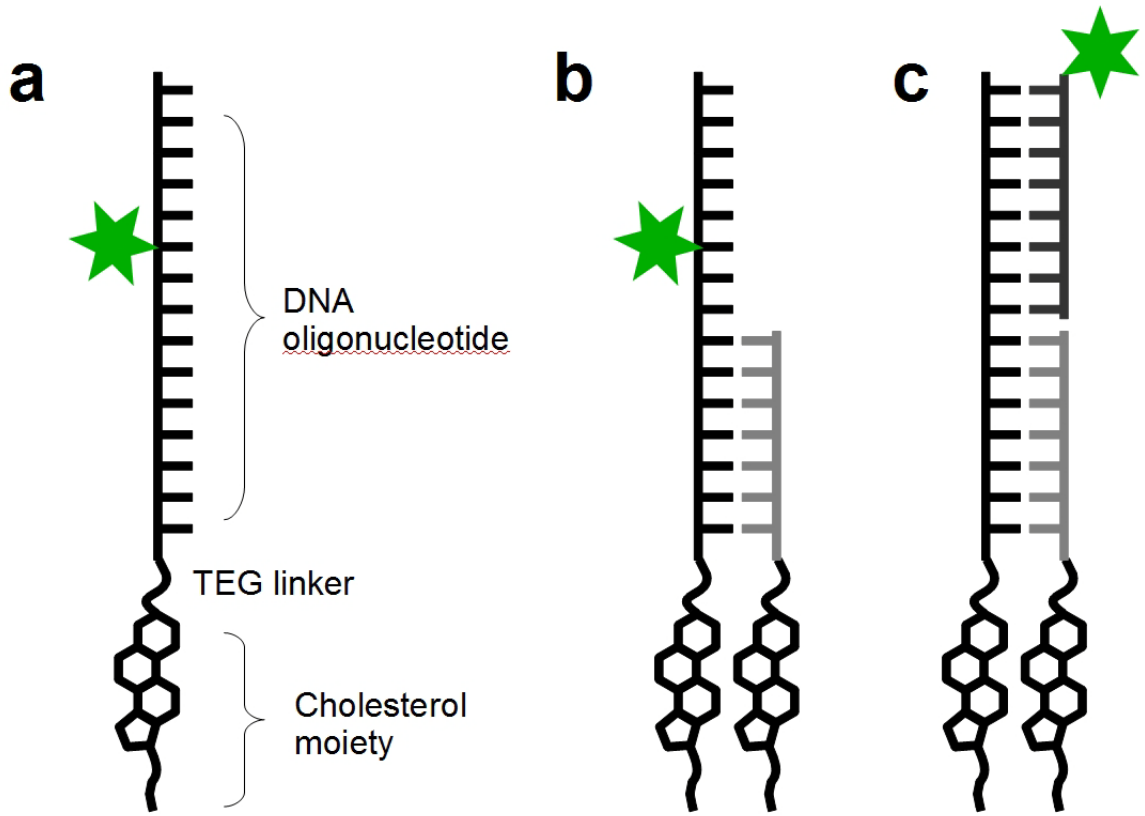

Figure 21: Scheme of cholesterol-based oligonucleotides incorporated into GUV membranes. DNA oligonucleotides are connected to the cholesterol moiety via a TEG linker. (a): chol_DNA1* (black); (b): hybrid of chol_DNA1* and chol_DNA2 (light grey); (c): hybrid of chol_DNA1 (black), chol_DNA2, and DNA1* (dark grey). The green star represents the FAM-label.

As seen in Figure 22 for the chol_DNA1/chol_DNA2/DNA1* complex, the oligonucleotides were equally distributed to the *lo* and *ld* domains. FLIM measurements revealed differences between fluorescence lifetimes of FAM-labeled oligonucleotides in the *lo* and *ld* domains (Table 5). The slightly lower FAM fluorescence and the shorter fluorescence lifetime of FAM

in the *ld* domain are due to FRET between the FAM and rhodamine (Rh). After correction of the intensities, no significant difference between the lateral distribution of the single cholesteryl-TEG-DNA (chol_DNA1*) and hybrids of two complementary cholesteryl-TEG-DNAs (chol_DNA1*/chol_DNA2 or chol_DNA1/chol_DNA2/DNA1*) was observed (Table 5). The decreasing FRET efficiency in the order from chol_DNA1* to chol_DNA1*/chol_DNA2 and to chol_DNA1/chol_DNA2/DNA1* (Table 5) is consistent with the increasing distance between the FAM label on the oligonucleotides and the acceptor Rh in the membrane, due to the formation of a rigid DNA duplex.

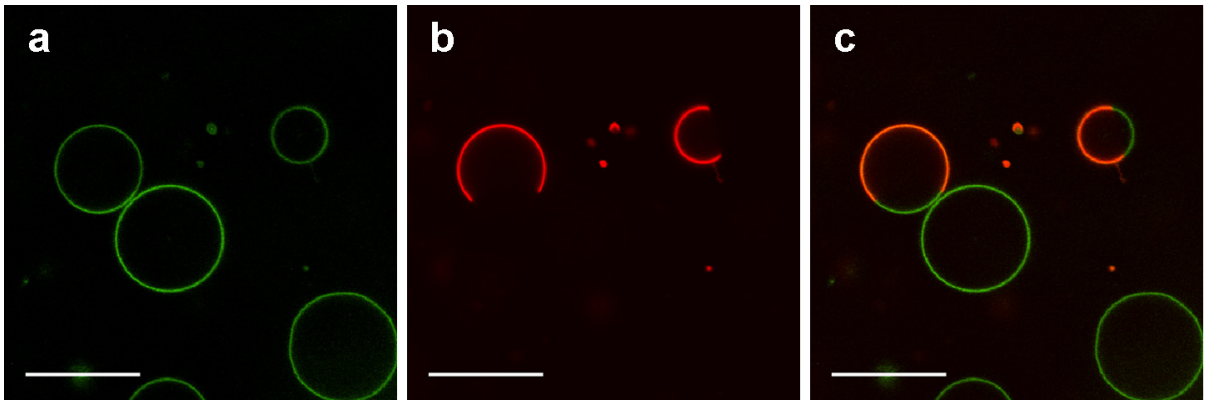

Figure 22: Confocal fluorescence microscopy images of GUVs consisting of DOPC, SSM, and Chol with incorporated chol_DNA1/chol_DNA2/DNA1* hybrid labeled with the green fluorescence dye FAM (a). As a marker for the *ld* phase the red fluorescent lipid analogue *N*-Rh-PE was used (b). (c) shows an overlay of both images. The white bars correspond to 50 µm.

Table 5: Results of FLIM measurements of FAM labeled cholesterol-based oligonucleotides incorporated into GUV membranes and the fraction partitioning into the *lo* phase. $<\tau_{DA}>$: Average lifetime of FAM in the *ld* phase (FRET acceptor Rh present). $<\tau_{D}>$: Average lifetime of FAM in the *lo* phase (FRET acceptor Rh absent). ET: Energy transfer between FAM and Rh due to FRET. *fo*: Fraction of the lipophilic oligonucleotides in the *lo* phase. Errors represent the standard error.

oligonucleotides	$<\tau_{DA}>$/ns	$<\tau_{D}>$/ns	ET (FAM-Rh)	*fo*
chol_DNA1*	3.39±0.04	4.05±0.03	0.16±0.01	0.48±0.06
chol_DNA1*/chol_DNA2	3.36±0.11	3.83±0.04	0.12±0.03	0.50±0.05
chol_DNA1/chol_DNA2/DNA1*	3.66±0.03	3.96±0.03	0.08±0.02	0.47±0.03

To test whether the partitioning behavior can be altered by electrostatic repulsion 1-palmitoyl-2-oleoyl-*sn*-glycero-3-phospho-L-serine (POPS) was incorporated into the membrane. POPS, as a lipid with one unsaturated chain, is localized preferentially in *ld* domains. In PBS buffer, the incorporation of POPS into the lipid mixture (1/1/1/1 DOPC/POPS/SSM/Chol) did not affect the lateral distribution of lipophilic oligonucleotides, either for chol_DNA1* or for chol_DNA1/chol_DNA2/DNA1* (chol_DNA1/chol_DNA2 not tested). The incorporation and lateral distribution of chol_DNA1* in POPS-containing GUVs was also tested at lower ionic strengths. In sucrose buffer (250 mM sucrose, 10 mM Hepes) chol_DNA1* did not incorporate into the lipid membrane, most likely due to electrostatic repulsion. In buffers with higher ionic strength (mixtures of PBS and sucrose buffer), chol_DNA1* incorporated into negatively charged GUVs and was equally distributed between *l*o and *l*d phase, the same as in the zwitterionic membranes.

Independent of the number of cholesterol anchors, cholesterol-modified DNA partitioned equally into the *lo* and the *ld* phase of DOPC/SSM/Chol and DOPC/POPS/SSM/Chol GUVs. The presence of negatively charged headgroups in the *ld* phase had no influence on the lateral partitioning behavior.

3.2.2 Incorporation of palmitoylated PNA into phospholipid membranes and hybridization with complementary DNA

For the functionalization of lipid membranes with PNA, double palmitoylated PNA (palm_PNA) with the following sequence was used: Pal-Lys(Pal)-Gly-Glu_2-Gly-ttcttctcctt-Glu_2-Gly-$CONH_2$. Four glutamat residues were introduced to enhance the solubilty in an aqueous milieu. To test whether palm_PNA incorporates into lipid membranes and is accessible for the hybridization to complementary DNA, GUVs were prepared from a mixture of POPC and palm_PNA (molar ratio lipid:palm_PNA = 300:1). After incubation with a stoichiometric amount of the complementary strand 5´-Rh-AAG GAG AAG AA-3´ (DNA2*), GUVs' membrane showed a bright red Rh fluorescence (Figure 23a, b), indicating that palm_PNA was inserted in the lipid membrane and hybridized with the complementary DNA. In a control measurement the palm_PNA containing GUVs were mixed with a non-complementary Rh-labeled DNA. Here, no fluorescence on the vesicles was observed, proving that no unspecific binding of DNA occurred. Thus, these experiments revealed the sequence specific binding of the complementary DNA to palm_PNA inserted into the lipid membrane.

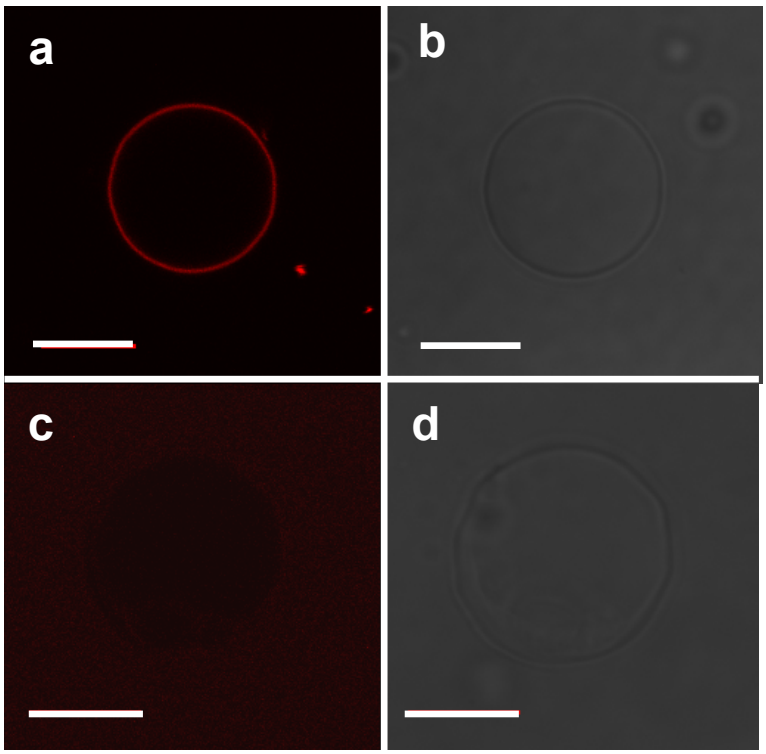

Figure 23: Confocal fluorescence images (a, c) and differential interference contrast images (b, d) of GUVs with incorporated palm_PNA. Addition of the complementary DNA labeled with Rh results in a red fluorescence on the GUV membrane (a, b). Non-complementary Rh-labeled DNA did not bind to GUV surface (c, d). Bars correspond to 10 µm.

3.2.3 Palmitoylated PNA for the targeting of lipid rafts

Palm_PNA was investigated for a possible targeting to lipid rafts in the plasma membrane of eukaryotic cells. First, insertion of palm_PNA hybridized with the Rh-labeled, complementary oligonucleotide DNA2* into the membrane of Chinese hamster ovary (CHO-K1) cells was studied. Palm_PNA was premixed with a stoichiometric amount of DNA2*, and added to the cells. Confocal and differential interference contrast images of CHO-K1 cells after incubation with palm_PNA/DNA2* hybrids are shown in Figure 24a and 24b. Rh fluorescence was mainly localized to the plasma membrane, indicating that the palm_PNA/DNA2* hybrids were inserted into the plasma membrane. Some uptake of the membrane-incorporated palm_ PNA/DNA2* hybrids into endocytic vesicles was found (Figure 24a). In a control experiment, palm_PNA was premixed with a non-complementary

Rh-labeled oligonucleotide and added to CHO-K1 cells. No fluorescence was observed either at the plasma membrane or inside the cells (Figure 24c and 24d). These results show that palm_PNA (i) inserts into the cell plasma membrane, (ii) hybridizes specifically with the complementary DNA2*, and (iii) the inserted palm_PNA/ DNA2* hybrids could be taken up by endocytosis. The inhomogeneous distribution of rhodamine fluorescence on the cell surface might be due to lateral segregation of palm_PNA/DNA2* in rafts or accumulation in early endocytic vesicles.

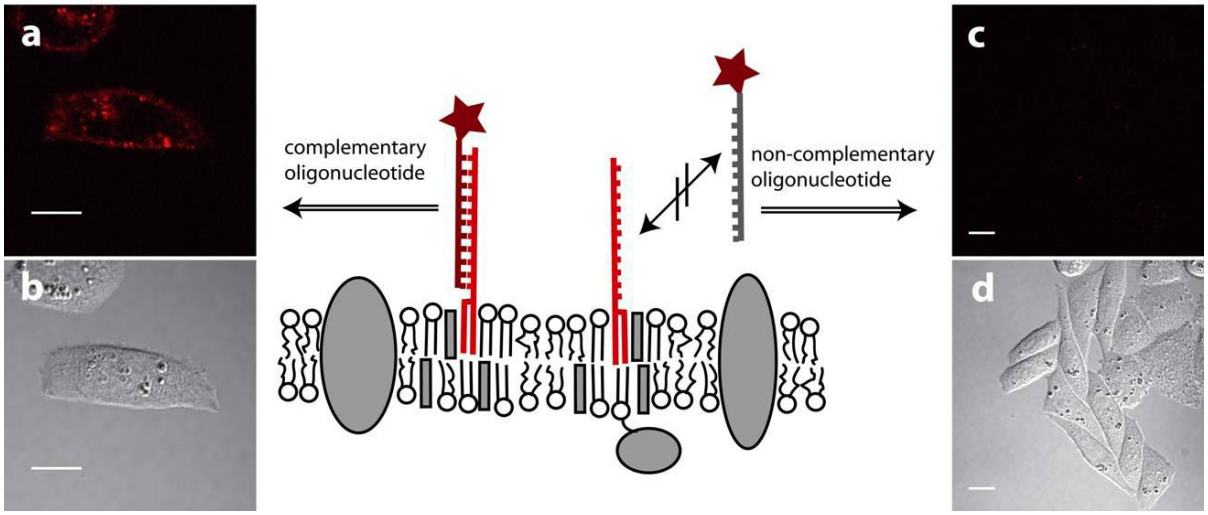

Figure 24: Palmitoyl-anchored PNA incorporates into the plasma membrane of CHO-K1 cells. A confocal fluorescence microscopy image (a; b: differential interference contrast image) shows the localization of a complementary Rh-labeled oligonucleotide complementary to the palm_PNA. In contrast, a non-complementary Rh labeled oligonucleotide did not bind to palm_PNA and no fluorescence could be detected at the cell membrane (c; d: differential interference contrast image). Bars correspond to 10 µm. Cartoon (middle) summarizes the observations (grey rectangles: Chol). Cells were provided by Dr. Silvia Scolari (Department of Biology, Humboldt University Berlin).

As lipid rafts have a size below the resolution limit of conventional fluorescence microscopes, the partitioning behavior of palm_PNA was studied two in model membrane systems showing phase-separation where the *lo* domain mimics lipid rafts:

i. GUVs made from a 1:1:1 mixture of DOPC, SSM, and Chol

ii. GPMVs, derived from the plasma membrane of CHO-K1 cells

The GUVs were labeled with the green fluorescent lipid analogue 1-palmitoyl-2-{6-[(7-nitro-2-1,3-benzoxadiazol-4-yl)amino]hexanoyl}-*sn*-glycero-3-phosphocholine (C6-NBD-PC) that preferentially segregates into the *ld* phase,[72] to distinguish between the *lo* and *ld* phase. Hybrids of palm_PNA and DNA2* were incorporated in the vesicles at a lipid to palm_PNA/DNA2* molar ratio of 300:1 or 3000:1. Figure 25a-c shows a typical domain-forming vesicle with inserted palm_PNA/DNA2* hybrids at 3000:1 molar ratio. Green fluorescence from C6-NBD-PC (Figure 25a) visualizes the *ld* domain, whereas the red fluorescence from Rh on the hybrid palm_PNA/DNA2* was observed in the domain that could not be labeled with C6-NBD-PC (Figure 25b). This suggests that palm_PNA is almost exclusively localized in the *lo* domain as sketched in Figure 25 (see also overlay in Figure 25c). An increase of the palm_PNA/DNA2*:lipid ratio to 1:300 did not change the partitioning behavior of the palm_PNA/DNAc2* hybrid (data not shown). To exclude the possibility of C6-NBD-PC influencing the palm_PNA/DNA2* partitioning, domain-forming vesicles lacking C6-NBD-PC were also prepared. As judged from the distribution of rhodamine fluorescence, almost all palm_PNA/DNAc2* hybrids were segregated into one domain (not shown), i.e. into the *lo* phase when taken into account the results with C6-NBD-PC-labeled vesicles.

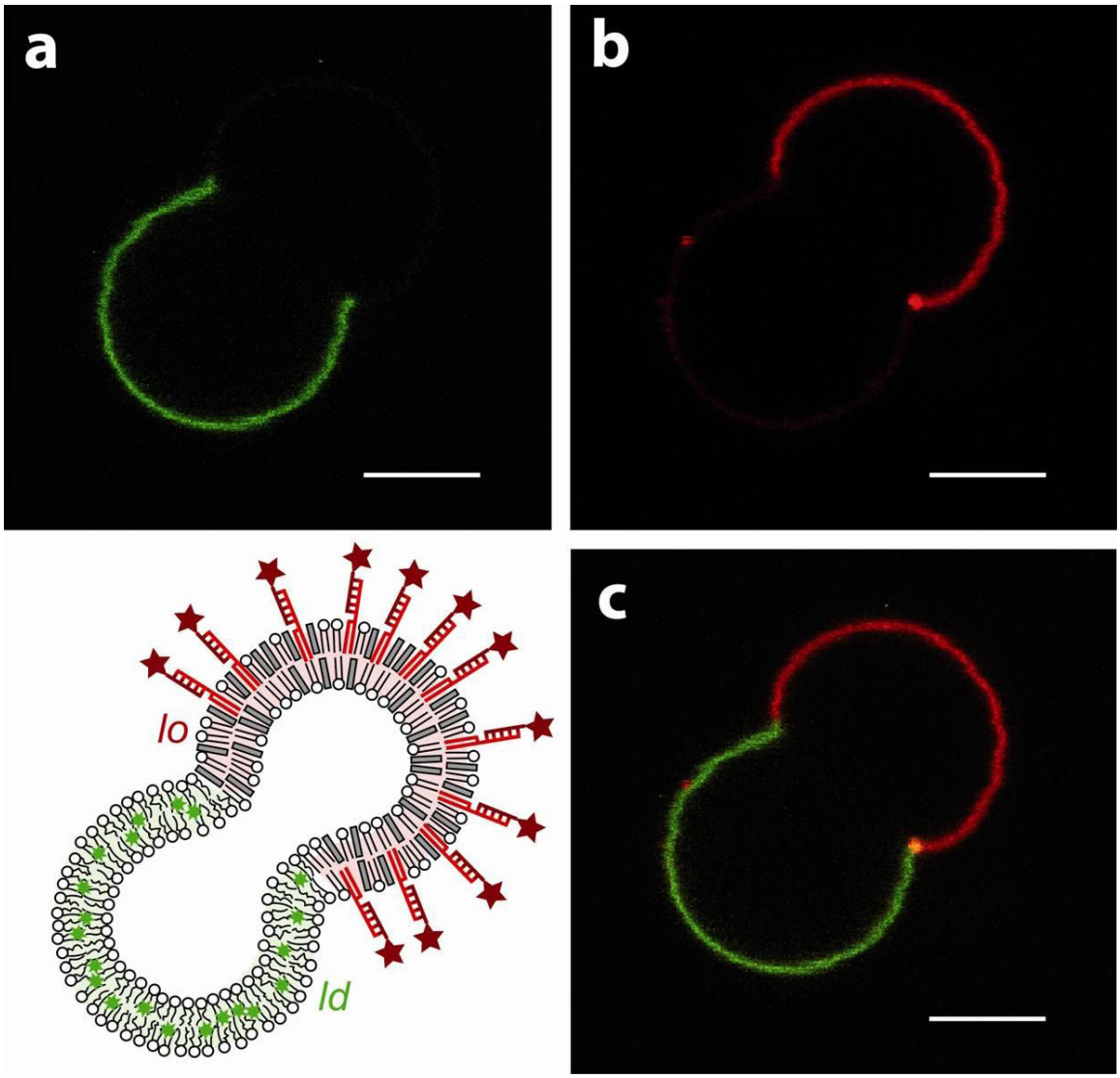

Figure 25: Lateral distribution of the palmitoyl-anchored PNA/DNA hybrid in the domain-forming GUVs made of 1:1:1 DOPC/SSM/Chol (molar ratio palm_PNA:lipid = 1:3000). The panels show confocal fluorescence microscopy images of (a) C6-NBD-PC fluorescence visualizing the *ld* phase, (b) the membrane-inserted palm_PNA/DNA2* hybrids, which are localized in the *lo* phase of the GUV, and (c) an overlay of the images shown in (a) and (b). Bars correspond to 5 µm. Cartoon summarizes the observations: C6-NBD-PC is localized to the *ld* domain (light green), while palm_PNA/DNA2* (rose) is recruited to the cholesterol enriched *lo* domain (grey rectangles: Chol).

GPMVs were derived from CHO-K1 cells stably expressing a fluorescent raft marker, a fusion protein of a glycosylphosphatidylinositol (GPI) anchor and monomeric cyan fluorescent protein (GPI-mCFP). GPI anchored proteins are known to partition into cholesterol-enriched domains in the plasma membrane of cells.[72] At low temperatures, a significant fraction of GPMVs showed phase-separation into micrometer-scaled *lo* and *ld*

domains.[90] As in the experiments with GUVs, hybrids of palm_PNA and DNA2* were incorporated into the vesicles. Palm_PNA/DNA2* co-localized with GPI-mCFP in the phase-separated GPMVs at 4 °C. Therefore, it can be concluded that it partitioned into *lo* phase (Figure 26).

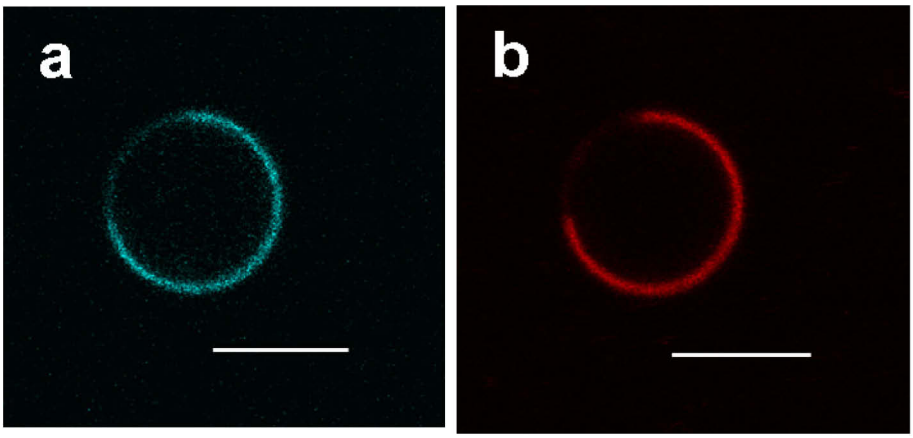

Figure 26: Segregation of palm_PNA/DNA2* in domain-forming GPMVs at 4 °C. As a marker for the *lo* phase the fusion protein GPI-mCFP was used (a). Rh fluorescence of palm_PNA/DNA2* hybrid is co-localized with GPI-mCFP (b) in the *lo* phase. Bars correspond to 5 µm. GPMVs were provided by Dr. Silvia Scolari (Department of Biology, Humboldt University Berlin).

The hybrids of palmitoylated PNA and complementary DNA2* segregated into the *lo* phase of both GUVs and GPMVs. As palm_PNA also inserts into the plasma membrane of cells, it is also likely that the palmitoylated PNA targets lipid rafts.

3.2.4 Construction of Janus vesicles using palmitoylated PNA and tocopherol-based DNA

The specific partitioning behavior of palm_PNA to segregate into the *lo* phase of model membrane systems opened the way to construct two-sided vesicles that exhibit different DNA sequences in different domains – Janus vesicles. For that aim GUVs and GPMVs that show a liquid-liquid phase-separation were functionalized with palm_PNA/DNA2* and the hybrid of

a tocopherol-modified DNA oligonucleotide and a complementary DNA strand. Tocopherol-based oligonucleotides are known to partition into the *ld* phase of GUVs consisting of a DOPC/SM/Chol mixture.[23,24] For the tocopherol-modified oligonucleotide a construct with the following sequence was used: 5′-TLT TTT TLT TTT ATT TCT GAT GTC CA-3′ (tocopherol_DNA1), where L refers to a tocopherol-modified deoxyuridine. The complementary DNA (DNA3*; sequence: 5′-FITC-TGG ACA TCA GAA ATA-3′) was labeled with the green fluorescent dye fluorescein isothiocyanate (FITC) to visualize the tocopherol_DNA1/DNA3* hybrid inside the membrane. Figure 27a-c shows a phase-separated GUV consisting of 1:1:1 mixture of DOPC, SSM, and Chol with incorporated palm_PNA/DNA2* and tocopherol_DNA1/DNA3* hybrids. Tocopherol_DNA/DNA3* (Figure 27a, FITC fluorescence) and the palm_PNA/DNA2* (Figure 27b, Rh fluorescence) partitioned into well separated domains, the *ld* and the *lo* domain, respectively. Figure 27c shows an overlay of both images, whereas Figure 27d represents a three dimensional overlay of the FITC and the Rh channel of another GUV.

Using GPMVs derived from CHO_K1 cells two different types of vesicles where observed: (i) in vesicles presenting no domain-separation green fluorescence of tocopherol_DNA/DNA3* and red fluorescence of palm_PNA/DNA2* were spread over the whole membrane (not shown); (ii) in vesicles showing domain formation tocopherol_DNA/DNA3* (Figure 27e) and palm_PNA/DNA2* (Figure 27f) partitioned into different domains. Figure 27g shows an overlay of both images.

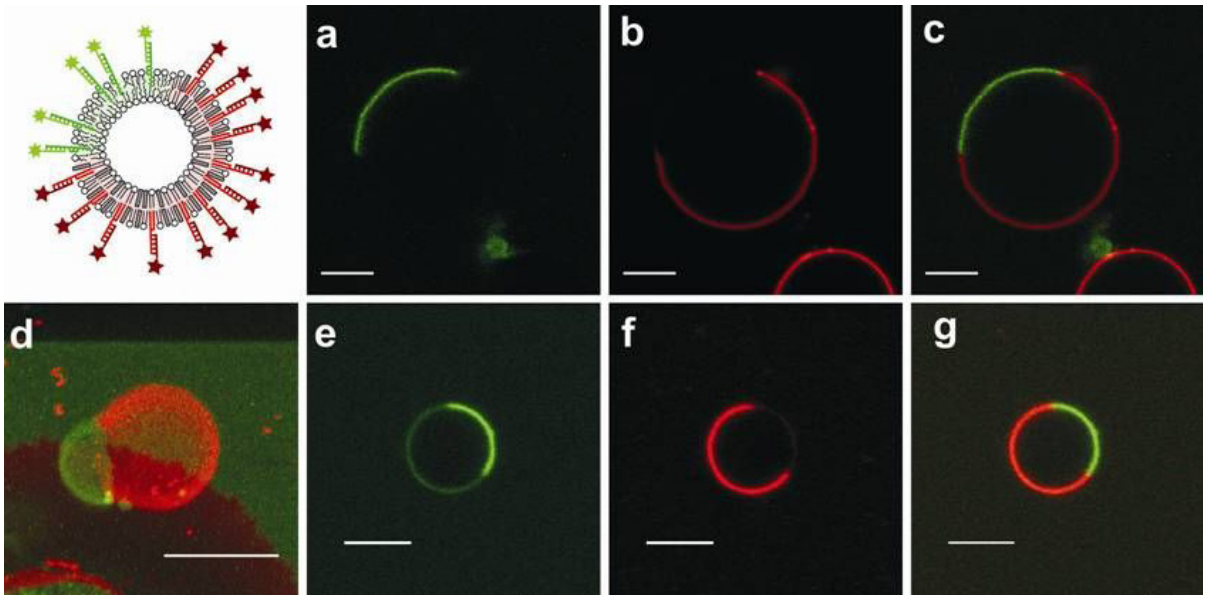

Figure 27: Lateral distribution of hybrids of palmitoyl-modified PNA with complementary DNA (palm_PNA/DNA2*) and tocopherol-modified DNA with complementary DNA (tocopherol_DNA/DNA3*) in domain-forming GUVs made from a 1:1:1 mixture of DOPC, SSM, and Chol (a-d) and GPMVs prepared from CHO-K1 cells (e-g). (a) FITC channel – the membrane-inserted hybrids tocopherol_DNA1/DNA3* are localized in the *ld* domain of a GUV. (b) Rh channel – the membrane inserted hybrids palm_PNA/DNA2* are localized in the *lo* domain. (c) Overlay of the images shown in (a) and (b). (d) The three-dimensional overlay of the confocal images of another domain-forming GUV. (e-g): In domain-forming GPMVs tocopherol_DNA/DNA3* (e) partitioned into another domain than palm_PNA/DNA2* (f). (g) Overlay of the images shown in (e) and (f) Bars represent 5 µm (a-c) and 10 µm (d-g). Cartoon (left, top) illustrates the results: palm_PNA/DNA2* (red) is recruited to the *lo* domain (rose; grey rectangles: Chol), while tocopherol_DNA/DNA3* to the *ld* domain (light green). GPMVs were provided by Dr. Silvia Scolari (Department of Biology, Humboldt University Berlin).

3.2.5 Temperature-controlled mixing and separation of lipophilic nucleic acids in Janus vesicles

In the above presented Janus vesicles two different membrane-incorporated compounds are separated by their partitioning into different lipid domains. When domain-forming vesicles are heated above the phase-separation temperature, the domains vanish resulting in a homogeneous membrane. This phenomenon was used to mix and separate both lipophilic nucleic acids – palmitoylated PNA and tocopherol-modified DNA. For the phase-separated vesicles GUVs were used, made from a 1:1:1 mixture of POPC, SSM, and Chol. This lipid

mixture was chosen because of its lower liquid-liquid phase transition temperature compared to DOPC/SSM/Chol membranes,[89] that is below the melting temperature of the amphiphilic PNA/DNA and DNA/DNA hybrids.

Figure 28 shows a sequence of fluorescence images of a vesicle with incorporated tocopherol_DNA2/DNA4* (sequence: tocopherol_DNA2: 5′-TGG ACA TCA GAA ATA TTT LTT TTT LT-3′; DNA4*: 5′-TAT TTC TGA TGT CCA-FITC-3; L cossreponds to the tocopherol-modified deoxyuridine moiety) (a-d) and palm_PNA/DNA2* (e-h). At temperatures below phase transition both *lo* and *ld* phases were present and the constructs partitioned into different domains (Figure 28a and 28e). Upon heating above phase transition temperature, the two domains merged causing co-localization of tocopherol_DNA2/DNA4* (Figure 28b) and palm_PNA/DNA2* (Figure 28f) hybrids in the entire vesicle. Subsequent cooling led to reformation of several small *lo* and *ld* domains and separation of lipophilic DNA and PNA molecules (Figure 28c, 28g). The small domains tend to fuse minimizing the line tension until again only one *lo* and one *ld* domain remained containing tocopherol_DNA2/DNA4* and palm_PNA/DNA2* (Figure 28d, 28h). Thus, by heating and cooling of Janus vesicles with two different lipophilic nucleic acids incorporated into separated domains, controlled mixing and separation was achieved.

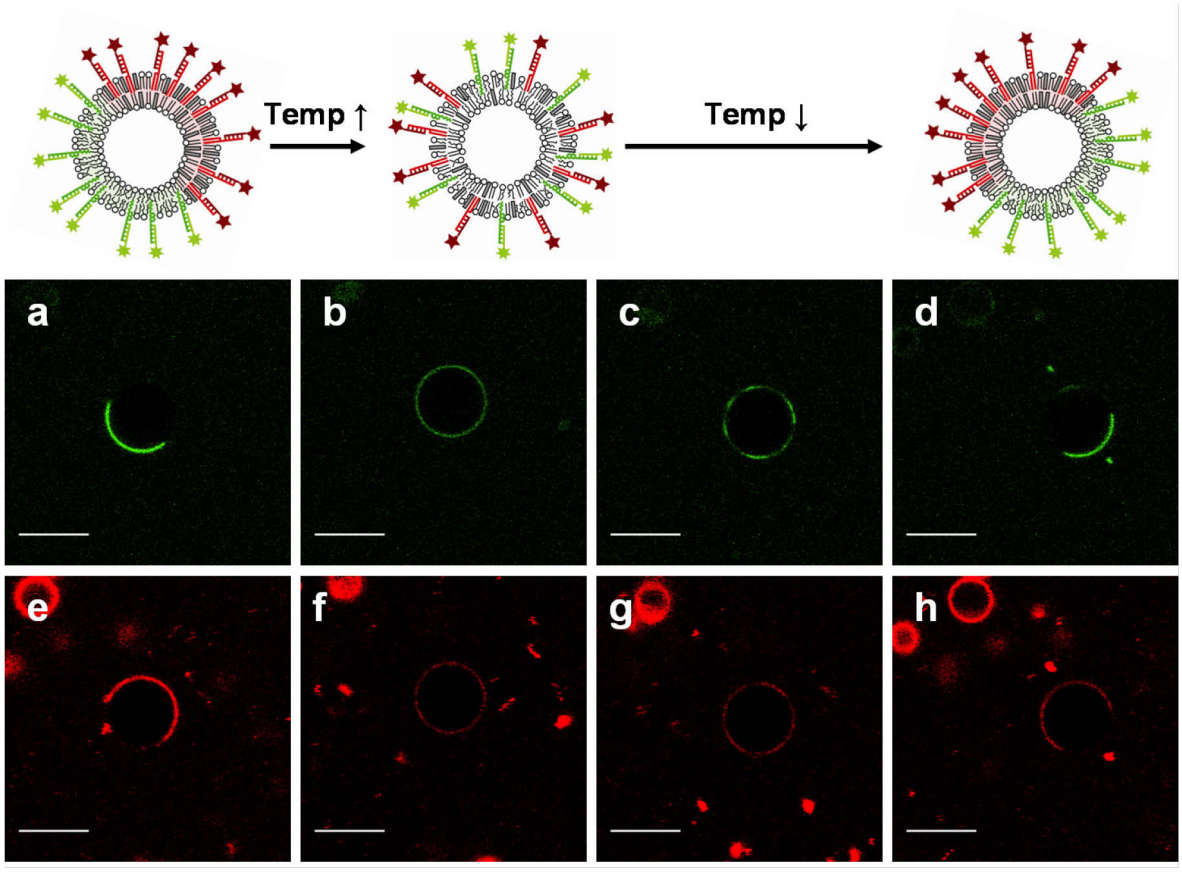

Figure 28: Mixing/demixing of tocopherol_DNA2/DNA4* (a-d) and palm_PNA/DNA2* (e-h) hybrids incorporated in POPC/SSM/Chol GUVs due to temperature increase and decrease. Below phase transition temperature tocopherol_DNA2/DNA4* (a) and palm_PNA/DNA2* (e) are located to different domains (~5 °C). Above the phase transition temperature domains disappeared and both constructs mix (b, f) (~55 °C). After cooling (~46 °C) new smaller domains are formed (c, g), which then merge to larger domains separating again both types of constructs (d, h). Bars correspond to 10 µm. Scheme (top) illustrates the process: left – lipophilic DNA/DNA (green) and PNA/DNA (red) hybrids are separated to different domains (*ld* – light green, *lo* – rose) at low temperatures (corresponding to a and e); middle – upon heating, the whole membrane is in an *ld* state and both constructs intermix (as in b and f); right – subsequent cooling leads to a two-sided vesicle with lipophilic DNA and PNA partitioning into opposing sites (as in d and h).

4 Discussion

In this work, lipid membranes were functionalized using three different kinds of lipophilic nucleic acids – tocopherol- and cholesterol-modified DNA, as well as palmitoylated PNA – to build organized structures on a micro- and nanometer scale: (i) a rational architecture of vesicle complexes, and (ii) the switchable lateral sorting of lipophilic nucleic acids in membranes.

4.1 Controlled assembly of LUVs on a solid support

It was shown that distinct layers of intact lipid vesicles can be built on a solid support given by LbL particles (Figure 29). The formation of the layers was achieved by sequence hybridization of tocopherol-modified DNA oligonucleotides. Up to three layers of different vesicles were formed as indicated by a different fluorescence labeling of the layers.

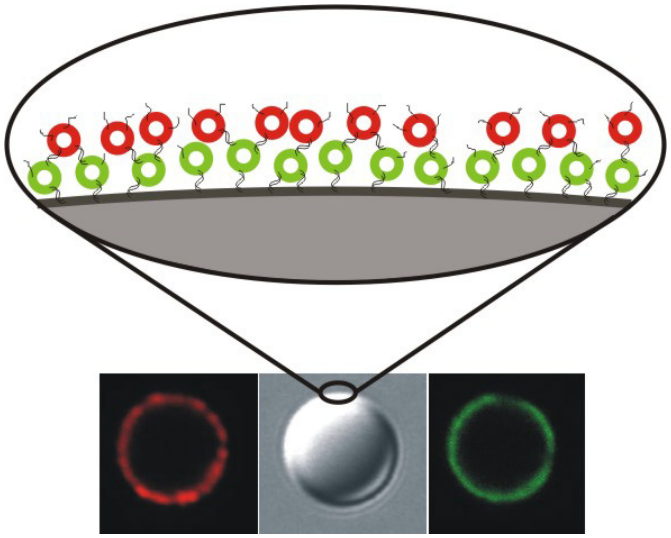

Figure 29: Two layers of vesicles assembled on an LbL particle, scheme and microscopic images: red rhodamine fluorescence of the second layer (left), differential interference contrast image (middle), and green NBD fluorescence of the first layer (right).

When particles, already coated with three vesicle layers, were mixed with vesicles containing lipophilic nucleic acids complementary to those of the last vesicle layer, a binding to the particles was observed. Nevertheless, vesicles with incorporated non-complementary lipophilic DNA to the third layer – but complementary to the second layer – did also bind to these particles. This unspecific binding most probably originates from binding of the vesicles to the second layer, indicating that defects in the third layer were present. To overcome this problem other sequences for the lipophilic nucleic acids could be used, that are non-complementary to any of the previous layers.

The stability, with which the vesicles are attached to the solid support (first vesicle layer), or to other vesicles (second and third layer), is given by the stability of the dsDNA, and the anchoring of the lipophilic DNA molecules in the vesicle membrane. The stability of dsDNA can be characterized by the melting temperature (T_m) of the dsDNA. It has been shown that T_m values and melting profiles of dsDNA attached to nanoparticles,[113] or lipid vesicles[34] are different to dsDNA free in solution. For instance, DNA linked gold nanoparticles that are assembled by the hybridization of complementary DNA show an enhanced T_m and a sharp melting profile of the dsDNA compared to unmodified DNA. In these aggregates, many factors influence the T_m, like the particle size, the inter-particle distances, and the surface density of DNA on the nanoparticles.[113] To estimate the thermal stability of the dsDNA formed upon building of vesicle layers on the LbL particles several aspects have to be considered: (i) The reduced entropy of single stranded DNA when attached to the LbL particle, or of the lipophilic DNA when inserted into the lipid membrane of a vesicle, (ii) the cost of entropy for a vesicle upon tethering to the LbL particle, or another vesicle, (iii) electrostatic repulsion between dsDNA and the negatively charged surface of the LbL particles, (iv) electrostatic repulsion between different dsDNAs that are crowded in the tethering area, (v) reduced lateral mobility of the lipophilic DNA upon dsDNA formation with DNA immobilized on the LbL particles, (vi) inter-vesicle, and vesicle-particle

interactions.[34] Beales and Vanderlick measured the T_m of dsDNA of complementary cholesterol-modified DNA (10mers) incorporated into the membrane of LUVs. [34] They showed that the thermal stability of the vesicle aggregates was determined by T_m of the cholesterol-based DNA. Dependent on the concentration of the lipophilic oligonucleotides the T_m was about 15-20 °C enhanced compared to unmodified DNA free in solution. Thus, the lipophilic 10mers had a T_m of about 45-60 °C (unmodified DNA: ~ 30-40 °C). This can be explained by the reduced impact of entropy when two lipophilic DNA molecules that are already inserted into lipid membranes hybridize. In contrast, using lipophilic nucleic acids with different membrane anchors for vesicle aggregation showed T_m values comparable to those unmodified DNA.[38] Furthermore, duplexes of tocopherol-based DNA incorporated into vesicles and complementary unmodified DNA revealed a slightly lower T_m as dsDNA of unmodified DNA strands.[24] Therefore, T_m of the dsDNA formed upon binding of the vesicles to the LbL particles, or to other vesicles, might be in the range of T_m of unmodified DNA, or – considering entropic effects – slightly higher. The formation of vesicle layers on LbL particles was based on the hybridization of adenosine and thymidine oligomers. When a first layer of vesicles binds to the LbL particles, a duplex is built between an adenosine 21mer and tocopherol_T18. Here, the dsDNA has a maximal length of 18 base pairs, as tocopherol_T18 provides only the 18 thymidines for double strand formation (Dr. Andreas Bunge, Prof. Dr. Daniel Huster, personal communication). The double strand formation between the vesicle layers is mediated by hybridization of tocopherol_T18 and tocopherol_A17, with a maximal length of the dsDNA of 17 base pairs. T_m of dsDNA formed of unmodified adenosine 17mers and thymidine 17mers was calculated to 38.4°C (DNA concentration 250 nM, 100 mM NaCl; IDT oligo analyzer; http://www.idtdna.com/analyzer/Applications/OligoAnalyzer). If that value represented the real T_m of the dsDNA formed upon binding of the vesicles to the LbL particles or to other vesicles, the assembly of the vesicles would be stable at room temperature, but melting would

occur to some extent at physiological temperatures. For an enhanced thermal stability longer or mixed DNA strands containing guanosine and cytidine should be used for the oligonucleotides attached to the LbL particles and the lipophilic DNA. Shorter DNA sequences would not only destabilize the assembly but could also promote vesicle fusion due to a decreased inter-vesicle distance (see below).[28]

The other prerequisite for a stable assembly of vesicles on LbL particles is the firm anchoring of the lipophilic oligonulceotides inside the lipid membranes. Due to the amphiphilic character of tocopherol-modified oligonucleotides these molecules can be solved in aqueous solutions. This finding suggests that in presence of lipid vesicles an equilibrium exists between tocopherol-based DNA in the aqueous solution and inserted into the membrane, although it is assumed that only a small portion is not bound to the vesicles. For cholesterol-modified DNA it was shown that the anchoring of the lipophilic oligonucleotides is reversible when only one lipophilic anchor is present.[114] When two cholesterol moieties anchored the oligonulceotides to the membrane an irreversible insertion into the lipid bilayer was observed.[114]

In this study sequential layers of LUVs were bound to LbL particles by the sequence specific hybridization of complementary tocopherol-based DNA, whereas a reorganization of the vesicles caused by a redistribution of the lipophilic oligonucleotides from one vesicle to another would have resulted in unspecific binding of vesicles. As this was not observed in a significant amount for the first two vesicle layers it can be assumed that such a redistribution of lipophilic oligonucleotides does not often take place. A stable tethering of the vesicles against shear forces is also provided. During the washing steps the particles coated with vesicles were resuspended using a pipette. The strong shear forces appearing at the tip of the pipette did not perturb the assembly of the vesicles. When the particles coated with one layer of vesicles (labeled with *N*-NBD-PE) were mixed with an excess with *N*-Rh-PE labeled vesicles, the *N*-Rh-PE labeled vesicles did bind to the LbL particles (see Figure 15d). This

observation indicates that the vesicles are tethered not only by one but by several dsDNA strands formed between lipophilic DNA and DNA attached to the LbL particles. The replacement of already immobilized vesicles could be achieved, however, when the coated particles (coated with *N*-NBD-PE labeled vesicles) were mixed with an excess of vesicles (labeled with *N*-Rh-PE labeled) by vigorous shaking ("vortexing"). Here, the shear forces were too strong, the vesicles were pulled out of the assembly, and binding places for new vesicles were free.

One important question of this study was, whether LUVs neither loose their content nor fuse upon binding to the particles. Applying different methods it was shown that LUVs retained entrapped molecules and fusion did not happen. These methods complement each other: Cryo-TEM measurements clearly showed that vesicles did not fuse upon DNA directed aggregation, as it was also demonstrated for the LUVs bound to the LbL particles with the FLIM and FRAP experiments. In addition, calcein self-quenching assays not only showed that molecules stayed entrapped when the vesicles bound to the LbL particles, but also confirmed that no fusion process took place: It is known that lipid vesicles often show a transient leakage upon fusion.[48] Thus, the absence of any spontaneous calcein release strongly indicates that LUVs did not fuse upon binding to the particles. At first sight, this phenomenon seems quite surprising: Membranes tend to fuse when brought in close proximity,[28] and vesicles often rupture on solid supports forming supported lipid bilayers.[107] Indeed, Stengel *et al.*,[42] and Chan *et al.*[43] recently reported on vesicle fusion mediated by DNA in a SNARE-like manner, where lipophilic oligonucleotides triggered a close membrane-membrane contact. This was achieved by using oligonucleotides that carry the lipophilic modification on the 3'- and 5'-end of the DNA (Figure 30a).

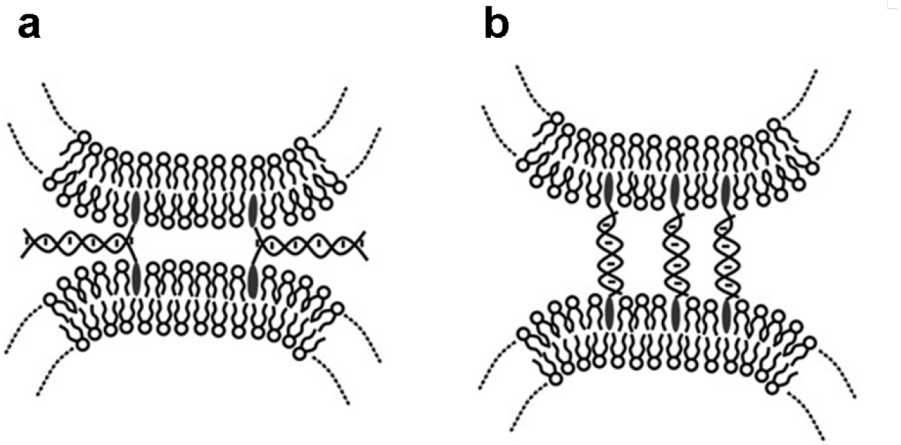

Figure 30: Membrane-membrane adhesion caused by lipophilic nucleic acids. (a) When one lipophilic anchors is situated at the 3'-end, and the other at the 5'-end fusion is triggered in a SNARE-like way. (b) When both lipohilic nucleic acids are lipophilic modified at the 3' or the 5'-end, the membranes are kept in distance. Modified scheme from [34]

When both anchors are situated at the 3’- or the 5’-ends, the membranes are separated (Figure 30b). When short sequences were used, however, fusion was also observed:[28] Vesicles aggregated with complementary lipophilic DNA 12mers showed vesicle fusion within 24 h, whereas DNA 24mers did not promote fusion. This can be explained by the increased distance between aggregated vesicles. In the case of the lipophilic nucleic acids used in this work (tocopherol_T18 and tocopherol_A17), the distance between connected membranes is 17 base pairs, and no fusion was observed. Assuming that the complementary lipophilic nucleic acids form duplexes of a B-DNA conformation, the distance between the membranes was at least 5.8 nm. According to our results, this is enough to separate membranes and prevent fusion. The stability of the LUVs upon immobilization on LbL particles is most probably caused by electrostatic repulsion of the oligonucleotides on the vesicles' surface and the stiff double helix forming between the tocopherol_T18 containing LUVs and LbL particles or tocopherol_A17 containing LUVs. After one week storage at 4°C, however, the LUVs lost about 30% of the cargo. This is comparable to the loss from POPC LUVs free in solution, within the same time.(unpublished results) Using other lipid mixtures, e.g. including

cholesterol, it should be possible to minimize this loss, as it is known that cholesterol stabilizes lipid membranes.[115]

It was shown that particles can be arranged to a pre-defined pattern using an optical tweezer. Thus, reservoirs with bioactive molecules can be organized on a micrometer scale. For example, in tissue regeneration, cell growth could be directed by loading the vesicles assembled on the particles with growth factors and nutrients. The arrangement of particles coated with vesicles could also be fixed by embedding the particles into a matrix, e.g. gels or polymers, for the building of micro-patterned coatings (Figure 31). Such films would sense changes in the chemical micro-environment and respond releasing distinct molecules just at the defined place.

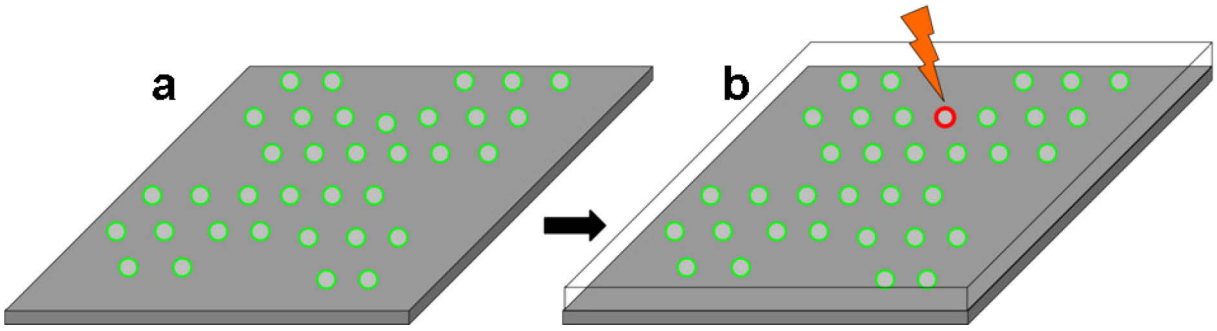

Figure 31: Formation of micro-patterned films. (a) Positioning of LbL particles coated with vesicles on a surface. (b) The arrangement is fixed by the embedding of the particles in gels or polymers. Function of single particles can be activated by remote control, or local changes in the chemical environment (red arrow).

For biotechnological applications, the system might also be tuned to allow other transport and release mechanisms. For instance, the particles could also be moved with micromanipulators or microfluidic devices. For cellular uptake smaller particles could be used, and to target specific tissues in living organisms magnetic particles could replace the silica core. Release of molecules could also be assessed by alternative methods. Vesicles become leaky when heated through the phase transition temperature of their lipid mixture.[116] Thus, using specific lipid mixtures for the LUVs assembled on the LbL particles, would result in a temperature

sensitive system. The release in a defined biochemical environment is also possible. For instance, in the microenvironment of tumors the pH is reduced.[117] Liposomes that are sensitive for low pH values[50] could be used to release drugs at the tumor site. The combination of the maneuverable LbL particles with LUVs designed for the release of molecules under specific conditions would result in potential delivery systems for drugs. Moreover, the co-delivery of different substances could be achieved, e.g. of a pro-drug and an enzyme converting the pro-drug to the active substance at the desired place after release from the vesicles.

Fusion of the vesicles assembled on the LbL particles was demonstrated: Using FRAP and FLIM measurements the mixing of the lipid bilayers upon addition of melittin was proven. The stability of liposomes and the abilty to trigger fusion in a controlled manner opens the way for application: Two reactants, or an enzyme and its substrate could be incorporated into the membranes of different LUVs. Fusion of the LUVs would result in the mixing of both compounds to start the reaction.

LbL particles coated with several layers of vesicles are biomimetic structures. The vesicles represent lipid compartments or organelles able to store biomolecules, to retain specific chemical environments, and provide an enclosed place for distinct enzymatic reactions. By the combination of several vesicle-based reactors that work in tandem, complex micro factories can be constructed. The system is responsive to outer influences as it was demonstrated by the addition of melittin, and the different compartments can communicate with each other by mixing of molecules associated to membranes or entrapped inside the vesicles. Thus, the assembly of vesicles on LbL particles is not only a versatile approach that can find use as simple nanoreactor or drug delivery systems, it can also be a tool to simulate and study the complex interplay of cellular reaction pathways and to build networks of functional units reacting on remote control.

4.2 Lateral organization of lipophilic nucleic acids in lipid membranes

Lateral inhomogeneous membranes can act as a template for a two dimensional sorting of membrane compounds. To this end, molecules have to be used that show a distinct partitioning behavior in membranes. A special attention should be drawn to the design of the membrane anchor that interacts with the lipids of different domains. As many molecules do not bind to lipid membranes they have to be connected to a lipophilic moiety to functionalize the membrane. Therefore, the domain targeting molecule is ideally addressable with a variety of functional molecules without changing the partitioning behavior, as it might be given for lipophilic nucleic acids. Thus, it would enable the domain specific functionalization of lipid domains on demand.

Cholesteryl-TEG-modified DNA was incorporated into DOPC/SSM/Chol GUVs that show a liquid-liquid phase-separation. As it is known that the *lo* phase is enriched in cholesterol, it might be expected that the cholesteryl-TEG-based oligonucleotide also favorably partitions into this phase in DOPC/SSM/Chol GUVs. In fact, the construct partitioned equally into the *lo* and the *ld* phase, independent whether the construct was anchored via one or two cholesteryl-TEG moieties. Beales and Vanderlick revealed a 2:1 partitioning into the *lo* phase of oligonucleotides anchored with two cholesteryl-TEG moieties in the membrane of DOPC/DPPC/Chol GUVs. ^{2}H and ^{31}P NMR experiments showed that both the cholesteryl-TEG anchor alone and the lipophilic oligonucleotides show a different behavior in lipid membranes compared to cholesterol.[118] When incorporated into POPC membranes cholesterol enhances the order of the lipid chains. For the cholesteryl-TEG anchor and the cholesterol-based oligonucleotides only minor effects were found. Therefore, it is reasonable to assume that the cholesterol anchor has a different orientation and insertion depth inside the

membrane compared to cholesterol resulting in a different phase partitioning behavior in the DOPC/SSM/Chol GUVs.

Insertion and lateral partitioning of cholesterol-modified DNA in DOPC/POPS/SSM/Chol GUVs was also tested. At a low ionic strenght the charge of the oligonucleotides was not shielded by counterions, and the electrostatic repulsion prevented the lipophilic DNA from inserting into the lipid membrane. At a higher ionic strength the insertion was comparable to insertion into zwitterionic membranes. As the cholesterol-modified DNA is an amphiphilic molecule, lipophilic DNA already incorporated into the lipid membrane will presumably be extracted out of the membrane, when the ionic strength is reduced. When inserted into the lipid membrane, the cholesterol-modified oligonucleotides partitioned equally into both phases of DOPC/POPS/SSM/Chol GUVs. No influence of the negatively charged POPS on the lateral partitioning behavior of the negatively charged oligonucleotides was observed, although the POPS was enriched in one domain (*ld*). The negative charge of the oligonucleotides was shielded by counterions. The observation that the cholesterol-based DNA inserts into negatively charged, liquid-disordered membranes in presence of counterions has direct implications on biotechnological applications: It turned out, that a mixture of POPC and POPS (molar ratio: 1:1) is suited better than other lipid mixtures for a continuous and homogeneous covering of LbL particles enhancing their biocompatibility.[107] For a functionalization of these membrane-coated particles, lipophilic nucleic acids should be used, that insert into this membrane that is (i) highly negatively charged, and (ii) in a liquid-disordered state. The cholesteryl-TEG-DNA presented in this work fulfills these criteria, and showed that it stably inserts into the lipid coated LbL particles (Figure 32).[118]

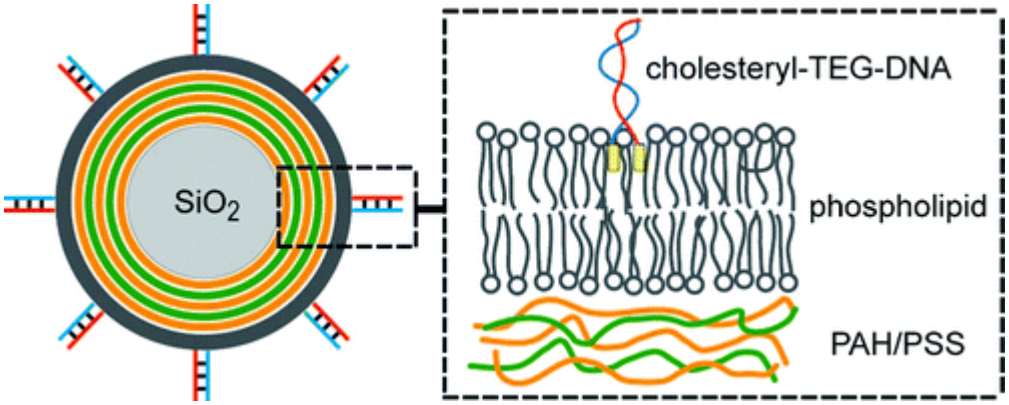

Figure 32: Membrane coated LbL particles, funtionalized with cholesterol-modified DNA. Taken from[118]

FLIM measurements revealed FRET between the oligonucleotides labeled with a FRET donor (FAM) and the marker for the *ld* phase *N*-Rh-PE as a FRET acceptor. FRET efficiency was dependent on the used lipophilic oligonucleotide system. When the cholesterol-based DNA was anchored with one cholesterol moiety (chol_DNA1*), the energy transfer was higher compared to the anchoring with two cholesterol moieties (chol_DNA1*/chol_DNA2). This can be explained by the difference in the distance between FRET donor (FAM) and acceptor (Rh). Upon hybridization of chol_DNA1* and chol_DNA2 a stiff double helix was formed protruding away from the lipid bilayer as it was already reported.[23,119] In consequence, the distance between the FAM label on the oligonucleotide and *N*-Rh-PE inserted into the membrane was increased and FRET efficiency was reduced. In the presented work transfer efficiencies were used to correct the fluorescence intensities in the *ld* phase, for the calculation of the relative concentrations of cholesterol-based oligonucleotides in both lipid domains. Beyond that, the FLIM measurements revealed that the cholesterol-modified DNA, labeled with FAM, can be used as a sensor to detect target DNA complementary to the cholesterol-based DNA.

Palmitoylated PNA was incorporated into the membranes of domain-forming GUVs, GPMVs and the plasma membrane of eukaryotic cells. It could be shown that this lipophilic PNA partitioned almost exclusively into the *lo* phase of DOPC/SSM/Chol GUVs and GPMVs

derived from CHO-K1 cells. These observations indicate that palmitoylated PNA possibly targets lipid rafts in eukayotic cells. Multiple palmitoylation drives rafts partitioning of many membrane proteins.[98] It is known that lipid rafts are involved in clathrin-independent endocytosis.[96] Thus, cellular uptake of the PNA or functional moieties linked via complementary DNA strands to PNA could be enhanced by using palmitoylated PNA. As PNA can bind with a high sensitivity for single base pair mismatches to single and double stranded DNA and RNA[14] it can be used for nucleic acid detection inside cells[120] and gene silencing.[14] These applications afford an efficient uptake into the cells, and palmitoylated PNA is a promising candidate to enhance the uptake.

By incorporation of tocopherol modified DNA and palmitoylated PNA into liquid-liquid phase-separated GUVs and GPMVs Janus vesicles were built. Both constructs segregated almost exclusively to the different domains. Due to hybridization with complementary DNA or RNA the different domains can be functionalized on demand. In this way the *ld* and *lo* phase can be labeled with nucleic acids exhibiting specific recognition sites for ligands,[121] or proteins,[122] so-called aptamers. Furthermore, the domains can be equipped with nucleic acid based enzymes as DNAzymes or ribozymes,[123] or, using conjugates of DNA, with various fluorophores,[80] peptides,[80] or proteins.[82] This enables the building of micropatterned surfaces by the use of phase-separated membranes of GUVs, GPMVs or supported lipid membranes that can be functionalized with a plethora of functions. For instance, such a two dimensional organization can find application in lipid-based microarrays.[39]

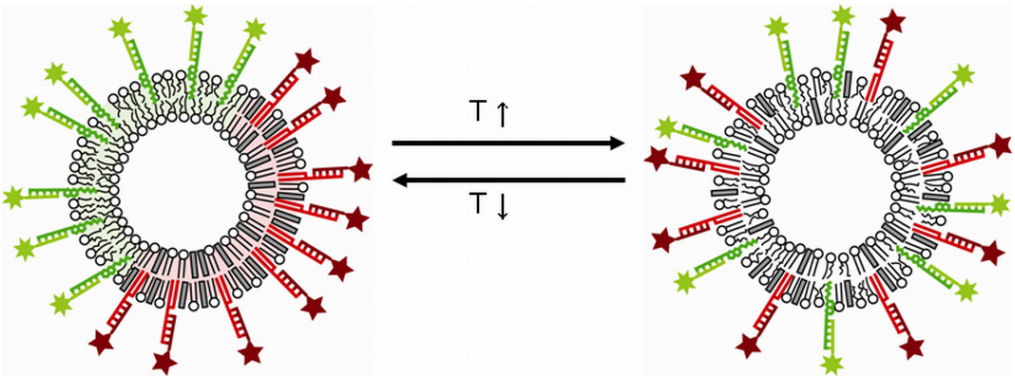

Figure 33: Temperature controlled mixing and separation of lipophilic nucleic acids incorporated into phase-separated GUVs.

Temperature controlled mixing and separation of the tocopherol based DNA and the palmitoylated PNA was also demonstrated (Figure 33). Upon heating over the phase transition temperature the lipid phases of the Janus vesicles vanished forming one *ld* phase, and both constructs were spread homogeneously over the whole membrane. When the temperature dropped again below the phase-separation temperature lipid domains were re-formed and the lipophilic nucleic acids again segregated into different domains. The DNA/DNA and DNA/PNA hybrids did not melt upon heating, showing that the phase transition temperature was still below the melting temperatures of the duplexes: Mixing and separation of functional moieties attached to the complementary DNA strands was also achieved. The domain formation by cooling resembles in some way one of the underlying principles of the formation of lipid rafts: Here, nanoscaled assemblies of sphingolipids, cholesterol, and raft partitioning proteins are combined to functional platforms, e.g. by the oligomerization of raft proteins in response to external signals.[7] Thus, similar to the membranes of eukaryotic cells, specific functions can be induced by remote triggers, e.g. signaling cascades. Apart of this, domain mixing by heating leads to mixing of the molecules associated to the different phases and interactions between the molecules become possible. For instance, by attaching reactants to the complementary DNA, chemical reactions could be triggered. It is also possible to functionalize one domain with an enzyme and the other one

with its substrate. In this way temperature controlled microreactors can be fabricated. When the resulting product of the reaction can be detected, e.g. by its fluorescence, the Janus vesicles become temperature sensors. In conclusion, Janus vesicles, equipped with lipophilic nucleic acids are versatile tools for biotechnical applications, e.g microarrays, model systems for eukaryotic cell membranes, temperature sensitive microreactors, and sensors.

Finally, both concepts – assembly of vesicles by DNA hybridization, and the domain specific partitioning of lipophilic nucleic acids – might be combined. Figure 34 illustrates how a directed vesicle assembly without a template could be achieved. First, complementary lipophilic nucleic acids that insert into the same domain could be incorporated into liquid-liquid phase-separated vesicles (Figure 34a and b). This would presumably result in relatively small assemblies. Second, liquid-liquid phase-separated vesicles could be functionalized with complementary lipophilic oligonucloetides that partition into different domains (Figure 34c). In this way larger assemblies could be achieved where the domains of the vesicles are oriented in one direction.

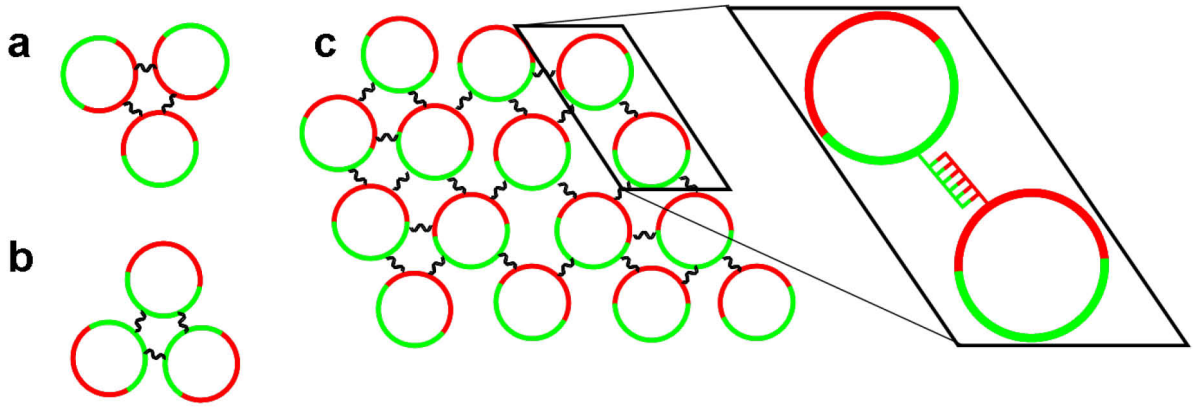

Figure 34: Assembly of liquid-liquid phase-separated vesicles using complementary lipophilic nucleic acids. When the lipophilic nucleic acids both partition into the *lo* (red) or the *ld* (green) phase, most likely small assemblies will be formed (a and b). When one lipophilic nucleic acid partitions into the *lo* and one into the *ld* domain, larger assemblies could be formed (c). Here, a directed orientation of the vesicles' domains might be achieved.

Using lipid coated particles, GPMVs, or GUVs showing a phase-separation, the concept of the assembling of vesicles on a solid support could also be expanded. Different types of vesicles could be bound to different domains using for example palmitoylated PNA and tocopherol-based DNA as tethers for the *lo* and the *ld* phase, respectively (Figure 35). Thus, vesicles could also be laterally organized.

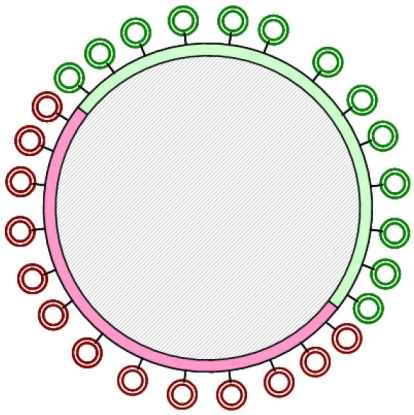

Figure 35: Assembly of vesicles on lipid coated particles, GUVs, or GPMVs. A liquid-liquid phase-separated membrane provides a lateral sorting of the vesicles: Palmitoylated PNA, partitioning into the *lo* phase (rose), and tocopherol-modified DNA located to the *ld* phase (light green), tether different types of vesicles with incorporated complementary lipophilic nucleic acids (green, red) on different lipid domains.

5 Outlook

Future prospects on vesicles assembled on LbL particles and the domain specific anchored lipophilic nucleic acids focus on biotechnological approaches.

Vesicles assembled on LbL particles might serve as nanoreactors. For example, encapsulation of enzymes inside the assembled vesicles should be studied. Among many different methods to entrap active enzymes inside vesicles the dehydration-rehydration method with a subsequent extrusion step seems to be one of the most promising ones, as it ensures high encapsulation values.[51] By an external trigger the enzyme would be released to start a reaction with a substrate that is present outside the vesicles. More complex reactors with control over the reaction place can be constructed by encapsulation of both enzyme and substrate (or two reactants) separately into the vesicles assembled on the LbL particles (Figure 36). Fusion of the vesicles would lead to a content mixing and induce the reaction. The fusion of vesicles, however, is often accompanied by a transient leakage. Therefore, a method for an induced fusion without the loss of content should be applied for the mixing of the reactants or the enzyme/substrate system, e.g. a phospholipase C/sphingomyelinase triggered fusion.[124] Another way to avoid the loss of reactants could be the use of membrane associated reactants or enzyme/substrate pairs, that will not diffuse away when the lipid bilayers becomes leaky. An application for such nanoreactor systems could be the construction of delivery systems for prodrugs that are converted to the desired molecule just at the defined place. For this aim the product should be released from the vesicles after the reaction. When the membrane is permeable for the reaction product, it can escape from the lumen and reach its destiny.

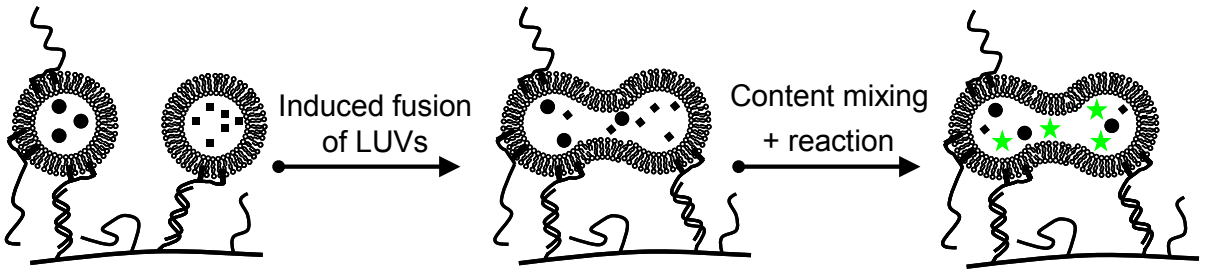

Figure 36: Scheme of two vesicles immobilized on a LbL particle by DNA hybridization. The vesicles are loaded with two reactants. Upon fusion of the vesicles, e.g. by the addition of melittin, the contents mix and a chemical reaction between the reactants starts resulting in the synthesis of a certain product (indicated as green stars). Alternatively, the vesicles can be loaded with an enzyme and its substrate. A release of the product will be obtained when the product can pass the membrane.

For cholesterol-modified DNA and palmitoylated PNA the partitioning inside the plasma membrane of cells will be of great interest: Targeting to lipid rafts will have an impact on the uptake of the construct. In this way the efficient cellular delivery of nucleic acids, or any molecule attached to an oligonucleotide complementary to the lipohilic nucleic acid might be enabled. To investigate the lateral partitioning of membrane compounds inside cellular membranes, several methods have been developed, e.g. using FLIM,[6] or stimulated emission depletion microscopy (STED).[125]

Finally, the partitioning behavior of lipophilic nucleic acids in phase-separated membranes can be tuned by a combination of different lipophilic anchors. Figure 37 shows a hybrid of a tocopherol-based oligonucleotide and palmitoylated PNA. As both constructs on their own partition into different lipid phases in liquid-liquid phase-separated lipid membranes, the partitioning behavior of lipophilic nucleic acids with one tocopherol and two palmitoyl anchors will be different for at least one of the constructs. By the cleavage of the dsDNA both lipophilic nucleic acids will again be separated resulting in a repartitioning of at least one of the lipophilic nucleic acids. Thus, it is possible to mimic the behavior of membrane proteins, whose partitioning behavior inside the cellular membrane into raft or non-raft regions is dependent on the modification with specific lipophilic moieties, to rebuild or study cellular processes like signaling pathways.

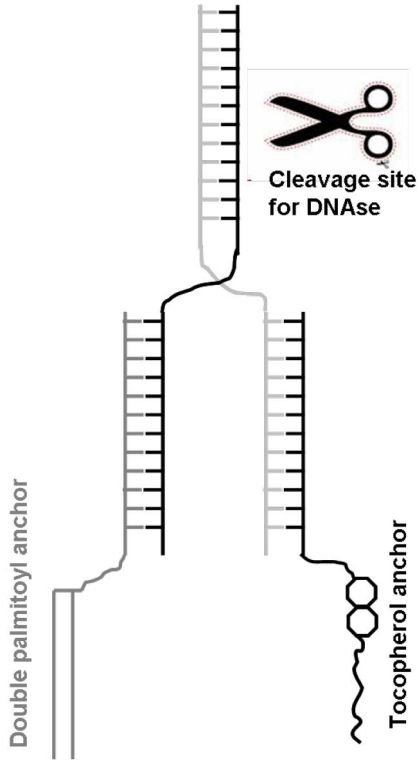

Figure 37: Hybrid of palmitoylated (dark grey) and tocopherol-based (black) nucleic acids, kept together by two DNA strands (black and light grey). A specific cleavage site allows separation of both lipophilic constructs that will result in a repartitioning of at least one of the lipophilic nucleic acids, when incorporated into the membrane of a liquid-liquid phase-separated GUV.

Appendum

Bibliography

[1] van Meer, G.; Voelker, D. R. and Feigenson, G. W. (2008): Membrane lipids: where they are and how they behave, Nat Rev Mol Cell Biol (vol. 9), No. 2, pp. 112-24. URL: http://www.ncbi.nlm.nih.gov/entrez/query.fcgi?cmd=Retrieve&db=PubMed&dopt=Citation&list_uids=18216768

[2] Voet, D.; Voet, D.G. and Pratt, C.W. (2002), Lehrbuch der Biochemie pp. 706-719, Wiley-VCH.

[3] Jahn, R. and Scheller, R. H. (2006): SNAREs--engines for membrane fusion, Nat Rev Mol Cell Biol (vol. 7), No. 9, pp. 631-43. URL: http://www.ncbi.nlm.nih.gov/entrez/query.fcgi?cmd=Retrieve&db=PubMed&dopt=Citation&list_uids=16912714

[4] Lingwood, D.; Kaiser, H. J.; Levental, I. and Simons, K. (2009): Lipid rafts as functional heterogeneity in cell membranes, Biochem Soc Trans (vol. 37), No. Pt 5, pp. 955-960. URL: http://www.ncbi.nlm.nih.gov/entrez/query.fcgi?cmd=Retrieve&db=PubMed&dopt=Citation&list_uids=19754431

[5] Lingwood, D. and Simons, K. (2010): Lipid rafts as a membrane-organizing principle, Science (vol. 327), No. 5961, pp. 46-50. URL: http://www.ncbi.nlm.nih.gov/entrez/query.fcgi?cmd=Retrieve&db=PubMed&dopt=Citation&list_uids=20044567

[6] Scolari, S.; Engel, S.; Krebs, N.; Plazzo, A. P.; De Almeida, R. F.; Prieto, M.; Veit, M. and Herrmann, A. (2009): Lateral distribution of the transmembrane domain of influenza virus hemagglutinin revealed by time-resolved fluorescence imaging, J Biol Chem (vol. 284), No. 23, pp. 15708-16. URL: http://www.ncbi.nlm.nih.gov/entrez/query.fcgi?cmd=Retrieve&db=PubMed&dopt=Citation&list_uids=19349276

[7] Simons, K. and Gerl, M. J. (2010): Revitalizing membrane rafts: new tools and insights, Nat Rev Mol Cell Biol (vol. 11), No. 10, pp. 688-99. URL: http://www.ncbi.nlm.nih.gov/entrez/query.fcgi?cmd=Retrieve&db=PubMed&dopt=Citation&list_uids=20861879

[8] Soutschek, J.; Akinc, A.; Bramlage, B.; Charisse, K.; Constien, R.; Donoghue, M.; Elbashir, S.; Geick, A.; Hadwiger, P.; Harborth, J.; John, M.; Kesavan, V.; Lavine, G.; Pandey, R. K.; Racie, T.; Rajeev, K. G.; Rohl, I.; Toudjarska, I.; Wang, G.; Wuschko, S.; Bumcrot, D.; Koteliansky, V.; Limmer, S.; Manoharan, M. and Vornlocher, H. P. (2004): Therapeutic silencing of an endogenous gene by systemic administration of modified siRNAs, Nature (vol. 432), No. 7014, pp. 173-8. URL: http://www.ncbi.nlm.nih.gov/entrez/query.fcgi?cmd=Retrieve&db=PubMed&dopt=Citation&list_uids=15538359

[9] Wolfrum, C.; Shi, S.; Jayaprakash, K. N.; Jayaraman, M.; Wang, G.; Pandey, R. K.; Rajeev, K. G.; Nakayama, T.; Charrise, K.; Ndungo, E. M.; Zimmermann, T.;

Koteliansky, V.; Manoharan, M. and Stoffel, M. (2007): Mechanisms and optimization of in vivo delivery of lipophilic siRNAs, Nat Biotechnol (vol. 25), No. 10, pp. 1149-57. URL: http://www.ncbi.nlm.nih.gov/entrez/query.fcgi?cmd=Retrieve&db=PubMed&dopt=Citation&list_uids=17873866

[10] Lorenz, C.; Hadwiger, P.; John, M.; Vornlocher, H. P. and Unverzagt, C. (2004): Steroid and lipid conjugates of siRNAs to enhance cellular uptake and gene silencing in liver cells, Bioorg Med Chem Lett (vol. 14), No. 19, pp. 4975-7. URL: http://www.ncbi.nlm.nih.gov/entrez/query.fcgi?cmd=Retrieve&db=PubMed&dopt=Citation&list_uids=15341962

[11] Chen, Q.; Butler, D.; Querbes, W.; Pandey, R. K.; Ge, P.; Maier, M. A.; Zhang, L.; Rajeev, K. G.; Nechev, L.; Kotelianski, V.; Manoharan, M. and Sah, D. W. (2010): Lipophilic siRNAs mediate efficient gene silencing in oligodendrocytes with direct CNS delivery, J Control Release (vol. 144), No. 2, pp. 227-32. URL: http://www.ncbi.nlm.nih.gov/entrez/query.fcgi?cmd=Retrieve&db=PubMed&dopt=Citation&list_uids=20170694

[12] Musacchio, T.; Vaze, O.; D'Souza, G. and Torchilin, V. P. (2010): Effective stabilization and delivery of siRNA: reversible siRNA-phospholipid conjugate in nanosized mixed polymeric micelles, Bioconjug Chem (vol. 21), No. 8, pp. 1530-6. URL: http://www.ncbi.nlm.nih.gov/entrez/query.fcgi?cmd=Retrieve&db=PubMed&dopt=Citation&list_uids=20669936

[13] Pandey, V. N.; Upadhyay, A. and Chaubey, B. (2009): Prospects for antisense peptide nucleic acid (PNA) therapies for HIV, Expert Opin Biol Ther (vol. 9), No. 8, pp. 975-89. URL: http://www.ncbi.nlm.nih.gov/entrez/query.fcgi?cmd=Retrieve&db=PubMed&dopt=Citation&list_uids=19534584

[14] Achim, C.; Armitage, B. A.; Ly, D. H. and Schneider, J. W. (2008): Peptide Nucleic Acids, Wiley Encyclopedia of Chemical Biology, pp. 1-9.

[15] Koppelhus, U. and Nielsen, P. E. (2003): Cellular delivery of peptide nucleic acid (PNA), Adv Drug Deliv Rev (vol. 55), No. 2, pp. 267-80. URL: http://www.ncbi.nlm.nih.gov/entrez/query.fcgi?cmd=Retrieve&db=PubMed&dopt=Citation&list_uids=12564980

[16] Janowski, B. A.; Huffman, K. E.; Schwartz, J. C.; Ram, R.; Hardy, D.; Shames, D. S.; Minna, J. D. and Corey, D. R. (2005): Inhibiting gene expression at transcription start sites in chromosomal DNA with antigene RNAs, Nat Chem Biol (vol. 1), No. 4, pp. 216-22. URL: http://www.ncbi.nlm.nih.gov/entrez/query.fcgi?cmd=Retrieve&db=PubMed&dopt=Citation&list_uids=16408038

[17] Savard, J. M.; Grosser, S. T. and Schneider, J. W. (2008): Length-dependent DNA separations using multiple end-attached peptide nucleic acid amphiphiles in micellar electrokinetic chromatography, Electrophoresis (vol. 29), No. 13, pp. 2779-2789. URL: http://www.ncbi.nlm.nih.gov/entrez/query.fcgi?cmd=Retrieve&db=PubMed&dopt=Citation&list_uids=18546164

[18] Mologni, L.; Marchesi, E.; Nielsen, P. E. and Gambacorti-Passerini, C. (2001): Inhibition of promyelocytic leukemia (PML)/retinoic acid receptor-alpha and PML expression in acute promyelocytic leukemia cells by anti-PML peptide nucleic acid, Cancer Res (vol. 61), No. 14, pp. 5468-73. URL: http://www.ncbi.nlm.nih.gov/entrez/query.fcgi?cmd=Retrieve&db=PubMed&dopt=Citation&list_uids=11454693

[19] Koppelhus, U.; Shiraishi, T.; Zachar, V.; Pankratova, S. and Nielsen, P. E. (2008): Improved cellular activity of antisense peptide nucleic acids by conjugation to a cationic peptide-lipid (CatLip) domain, Bioconjug Chem (vol. 19), No. 8, pp. 1526-34. URL: http://www.ncbi.nlm.nih.gov/entrez/query.fcgi?cmd=Retrieve&db=PubMed&dopt=Citation&list_uids=18646838

[20] Hu, J. and Corey, D. R. (2007): Inhibiting gene expression with peptide nucleic acid (PNA)--peptide conjugates that target chromosomal DNA, Biochemistry (vol. 46), No. 25, pp. 7581-7589. URL: http://www.ncbi.nlm.nih.gov/entrez/query.fcgi?cmd=Retrieve&db=PubMed&dopt=Citation&list_uids=17536840

[21] Filipovska, A.; Eccles, M. R.; Smith, R. A. and Murphy, M. P. (2004): Delivery of antisense peptide nucleic acids (PNAs) to the cytosol by disulphide conjugation to a lipophilic cation, FEBS Lett (vol. 556), No. 1-3, pp. 180-186. URL: http://www.ncbi.nlm.nih.gov/entrez/query.fcgi?cmd=Retrieve&db=PubMed&dopt=Citation&list_uids=14706847

[22] Borisenko, G. G.; Zaitseva, M. A.; Chuvilin, A. N. and Pozmogova, G. E. (2009): DNA modification of live cell surface, Nucleic Acids Res (vol. 37), No. 4, p. e28. URL: http://www.ncbi.nlm.nih.gov/entrez/query.fcgi?cmd=Retrieve&db=PubMed&dopt=Citation&list_uids=19158188

[23] Kurz, A.; Bunge, A.; Windeck, A. K.; Rost, M.; Flasche, W.; Arbuzova, A.; Strohbach, D.; Müller, S.; Liebscher, J.; Huster, D. and Herrmann, A. (2006): Lipid-anchored oligonucleotides for stable double-helix formation in distinct membrane domains, Angew Chem Int Ed Engl (vol. 45), No. 27, pp. 4440-4444. URL: http://www.ncbi.nlm.nih.gov/entrez/query.fcgi?cmd=Retrieve&db=PubMed&dopt=Citation&list_uids=16789049

[24] Bunge, A.; Kurz, A.; Windeck, A. K.; Korte, T.; Flasche, W.; Liebscher, J.; Herrmann, A. and Huster, D. (2007): Lipophilic oligonucleotides spontaneously insert into lipid membranes, bind complementary DNA strands, and sequester into lipid-disordered domains, Langmuir (vol. 23), No. 8, pp. 4455-4464. URL: http://www.ncbi.nlm.nih.gov/entrez/query.fcgi?cmd=Retrieve&db=PubMed&dopt=Citation&list_uids=17367171

[25] Svedhem, S.; Pfeiffer, I.; Larsson, C.; Wingren, C.; Borrebaeck, C. and Höök, F. (2003): Patterns of DNA-labeled and scFv-antibody-carrying lipid vesicles directed by material-specific immobilization of DNA and supported lipid bilayer formation on an Au/SiO2 template, ChemBioChem (vol. 4), No. 4, pp. 339-43. URL: http://www.ncbi.nlm.nih.gov/entrez/query.fcgi?cmd=Retrieve&db=PubMed&dopt=Citation&list_uids=12672114

[26] Yoshina-Ishii, C. and Boxer, S. G. (2003): Arrays of mobile tethered vesicles on supported lipid bilayers, J Am Chem Soc (vol. 125), No. 13, pp. 3696-7. URL: http://www.ncbi.nlm.nih.gov/entrez/query.fcgi?cmd=Retrieve&db=PubMed&dopt=Citation&list_uids=12656589

[27] Heuvingh, J.; Pincet, F. and Cribier, S. (2004): Hemifusion and fusion of giant vesicles induced by reduction of inter-membrane distance, Eur Phys J E Soft Matter (vol. 14), No. 3, pp. 269-76. URL: http://www.ncbi.nlm.nih.gov/entrez/query.fcgi?cmd=Retrieve&db=PubMed&dopt=Citation&list_uids=15338438

[28] Maruyama, T.; Yamamura, H.; Hiraki, M.; Kemori, Y.; Takata, H. and Goto, M. (2008): Directed aggregation and fusion of lipid vesicles induced by DNA-surfactants, Colloids Surf B Biointerfaces (vol. 66), No. 1, pp. 119-24. URL:

http://www.ncbi.nlm.nih.gov/entrez/query.fcgi?cmd=Retrieve&db=PubMed&dopt=Citation&list_uids=18617375
[29] Beales, P. A. and Vanderlick, T. K. (2007): Specific Binding of Different Vesicle Populations by the Hybridization of Membrane-Anchored DNA, J Phys Chem A (vol. 111), No. 49, pp. 12372-12380. URL: http://pubs3.acs.org/acs/journals/doilookup?in_doi=10.1021/jp075792z
[30] Ajo-Franklin, C. M.; Yoshina-Ishii, C. and Boxer, S. G. (2005): Probing the Structure of Supported Membranes and Tethered Oligonucleotides by Fluorescence Interference Contrast Microscopy, Langmuir (vol. 21), No. 11, p. 4976. URL: http://pubs3.acs.org/acs/journals/doilookup?in_doi=10.1021/la0468388
[31] Yoshina-Ishii, C.; Miller, G. P.; Kraft, M. L.; Kool, E. T. and Boxer, S. G. (2005): General method for modification of liposomes for encoded assembly on supported bilayers, J Am Chem Soc (vol. 127), No. 5, pp. 1356-7. URL: http://www.ncbi.nlm.nih.gov/entrez/query.fcgi?cmd=Retrieve&db=PubMed&dopt=Citation&list_uids=15686351
[32] Pfeiffer, I. and Höök, F. (2004): Bivalent cholesterol-based coupling of oligonucletides to lipid membrane assemblies, J Am Chem Soc (vol. 126), No. 33, pp. 10224-5. URL: http://www.ncbi.nlm.nih.gov/entrez/query.fcgi?cmd=Retrieve&db=PubMed&dopt=Citation&list_uids=15315417
[33] Shohda, K.; Toyota, T.; Yomo, T. and Sugawara, T. (2003): Direct visualization of DNA duplex formation on the surface of a giant liposome, ChemBioChem (vol. 4), No. 8, pp. 778-81. URL: http://www.ncbi.nlm.nih.gov/entrez/query.fcgi?cmd=Retrieve&db=PubMed&dopt=Citation&list_uids=12898631
[34] Beales, P. A. and Vanderlick, T. K. (2009): DNA as membrane-bound ligand-receptor pairs: duplex stability is tuned by intermembrane forces, Biophys J (vol. 96), No. 4, pp. 1554-65. URL: http://www.ncbi.nlm.nih.gov/entrez/query.fcgi?cmd=Retrieve&db=PubMed&dopt=Citation&list_uids=19217872
[35] Chan, Y. H.; Lenz, P. and Boxer, S. G. (2007): Kinetics of DNA-mediated docking reactions between vesicles tethered to supported lipid bilayers, Proc Natl Acad Sci U S A (vol. 104), No. 48, pp. 18913-8. URL: http://www.ncbi.nlm.nih.gov/entrez/query.fcgi?cmd=Retrieve&db=PubMed&dopt=Citation&list_uids=18025472
[36] van Lengerich, B.; Rawle, R. J. and Boxer, S. G. (2010): Covalent attachment of lipid vesicles to a fluid-supported bilayer allows observation of DNA-mediated vesicle interactions, Langmuir (vol. 26), No. 11, pp. 8666-72. URL: http://www.ncbi.nlm.nih.gov/entrez/query.fcgi?cmd=Retrieve&db=PubMed&dopt=Citation&list_uids=20180548
[37] Maru, N.; Shohda, K. and Sugawara, T. (2004): Assembling liposomes by means of an oligonucleotide tagged with a lipophilic unit, Nucleic Acids Symp Ser (Oxf), No. 48, pp. 95-6. URL: http://www.ncbi.nlm.nih.gov/entrez/query.fcgi?cmd=Retrieve&db=PubMed&dopt=Citation&list_uids=17150495
[38] Jakobsen, U.; Simonsen, A. C. and Vogel, S. (2008): DNA-controlled assembly of soft nanoparticles, J Am Chem Soc (vol. 130), No. 32, pp. 10462-10463. URL: http://www.ncbi.nlm.nih.gov/entrez/query.fcgi?cmd=Retrieve&db=PubMed&dopt=Citation&list_uids=18642914
[39] Städler, B.; Falconnet, D.; Pfeiffer, I.; Höök, F. and Vörös, J. (2004): Micropatterning of DNA-tagged vesicles, Langmuir (vol. 20), No. 26, pp. 11348-54. URL:

http://www.ncbi.nlm.nih.gov/entrez/query.fcgi?cmd=Retrieve&db=PubMed&dopt=Citation&list_uids=15595756
[40] Gartner, Z. J. and Bertozzi, C. R. (2009): Programmed assembly of 3-dimensional microtissues with defined cellular connectivity, Proc Natl Acad Sci U S A (vol. 106), No. 12, pp. 4606-10. URL: http://www.ncbi.nlm.nih.gov/entrez/query.fcgi?cmd=Retrieve&db=PubMed&dopt=Citation&list_uids=19273855
[41] Jakobsen, U.; Simonsen, A. C. and Vogel, S. (2008): DNA controlled assembly of liposomes, Nucleic Acids Symp Ser (Oxf), No. 52, pp. 21-2. URL: http://www.ncbi.nlm.nih.gov/entrez/query.fcgi?cmd=Retrieve&db=PubMed&dopt=Citation&list_uids=18776233
[42] Stengel, G.; Zahn, R. and Höök, F. (2007): DNA-induced programmable fusion of phospholipid vesicles, J Am Chem Soc (vol. 129), No. 31, pp. 9584-5. URL: http://www.ncbi.nlm.nih.gov/entrez/query.fcgi?cmd=Retrieve&db=PubMed&dopt=Citation&list_uids=17629277
[43] Chan, Y. H.; van Lengerich, B. and Boxer, S. G. (2009): Effects of linker sequences on vesicle fusion mediated by lipid-anchored DNA oligonucleotides, Proc Natl Acad Sci U S A (vol. 106), No. 4, pp. 979-84. URL: http://www.ncbi.nlm.nih.gov/entrez/query.fcgi?cmd=Retrieve&db=PubMed&dopt=Citation&list_uids=19164559
[44] Sutton, R. B.; Fasshauer, D.; Jahn, R. and Brunger, A. T. (1998): Crystal structure of a SNARE complex involved in synaptic exocytosis at 2.4 A resolution, Nature (vol. 395), No. 6700, pp. 347-53. URL: http://www.ncbi.nlm.nih.gov/entrez/query.fcgi?cmd=Retrieve&db=PubMed&dopt=Citation&list_uids=9759724
[45] Danion, A.; Brochu, H.; Martin, Y. and Vermette, P. (2007): Fabrication and characterization of contact lenses bearing surface-immobilized layers of intact liposomes, J Biomed Mater Res A (vol. 82), No. 1, pp. 41-51. URL: http://www.ncbi.nlm.nih.gov/entrez/query.fcgi?cmd=Retrieve&db=PubMed&dopt=Citation&list_uids=17265438
[46] Drulis-Kawa, Z. and Dorotkiewicz-Jach, A. (2010): Liposomes as delivery systems for antibiotics, Int J Pharm (vol. 387), No. 1-2, pp. 187-98. URL: http://www.ncbi.nlm.nih.gov/entrez/query.fcgi?cmd=Retrieve&db=PubMed&dopt=Citation&list_uids=19969054
[47] Cukierman, E. and Khan, D. R. (2010): The benefits and challenges associated with the use of drug delivery systems in cancer therapy, Biochem Pharmacol (vol. 80), No. 5, pp. 762-70. URL: http://www.ncbi.nlm.nih.gov/entrez/query.fcgi?cmd=Retrieve&db=PubMed&dopt=Citation&list_uids=20417189
[48] Ruiz-Arguello, M. B.; Basanez, G.; Goni, F. M. and Alonso, A. (1996): Different effects of enzyme-generated ceramides and diacylglycerols in phospholipid membrane fusion and leakage, J Biol Chem (vol. 271), No. 43, pp. 26616-21. URL: http://www.ncbi.nlm.nih.gov/entrez/query.fcgi?cmd=Retrieve&db=PubMed&dopt=Citation&list_uids=8900135
[49] Ong, W.; Yang, Y.; Cruciano, A. C. and McCarley, R. L. (2008): Redox-triggered contents release from liposomes, J Am Chem Soc (vol. 130), No. 44, pp. 14739-44. URL: http://www.ncbi.nlm.nih.gov/entrez/query.fcgi?cmd=Retrieve&db=PubMed&dopt=Citation&list_uids=18841890
[50] Guo, X.; MacKay, J. A. and Szoka, F. C., Jr. (2003): Mechanism of pH-triggered collapse of phosphatidylethanolamine liposomes stabilized by an ortho ester

polyethyleneglycol lipid, Biophys J (vol. 84), No. 3, pp. 1784-95. URL: http://www.ncbi.nlm.nih.gov/entrez/query.fcgi?cmd=Retrieve&db=PubMed&dopt=Citation&list_uids=12609880

[51] Walde, P. and Ichikawa, S. (2001): Enzymes inside lipid vesicles: preparation, reactivity and applications, Biomol Eng (vol. 18), No. 4, pp. 143-77. URL: http://www.ncbi.nlm.nih.gov/entrez/query.fcgi?cmd=Retrieve&db=PubMed&dopt=Citation&list_uids=11576871

[52] Simone, E. A.; Dziubla, T. D.; Colon-Gonzalez, F.; Discher, D. E. and Muzykantov, V. R. (2007): Effect of polymer amphiphilicity on loading of a therapeutic enzyme into protective filamentous and spherical polymer nanocarriers, Biomacromolecules (vol. 8), No. 12, pp. 3914-21. URL: http://www.ncbi.nlm.nih.gov/entrez/query.fcgi?cmd=Retrieve&db=PubMed&dopt=Citation&list_uids=18038999

[53] Ranquin, A.; Versees, W.; Meier, W.; Steyaert, J. and Van Gelder, P. (2005): Therapeutic nanoreactors: combining chemistry and biology in a novel triblock copolymer drug delivery system, Nano Lett (vol. 5), No. 11, pp. 2220-4. URL: http://www.ncbi.nlm.nih.gov/entrez/query.fcgi?cmd=Retrieve&db=PubMed&dopt=Citation&list_uids=16277457

[54] Vriezema, D. M.; Garcia, P. M.; Sancho Oltra, N.; Hatzakis, N. S.; Kuiper, S. M.; Nolte, R. J.; Rowan, A. E. and van Hest, J. C. (2007): Positional assembly of enzymes in polymersome nanoreactors for cascade reactions, Angew Chem Int Ed Engl (vol. 46), No. 39, pp. 7378-82. URL: http://www.ncbi.nlm.nih.gov/entrez/query.fcgi?cmd=Retrieve&db=PubMed&dopt=Citation&list_uids=17705203

[55] van Dongen, S. F.; Nallani, M.; Cornelissen, J. J.; Nolte, R. J. and van Hest, J. C. (2009): A three-enzyme cascade reaction through positional assembly of enzymes in a polymersome nanoreactor, Chemistry (vol. 15), No. 5, pp. 1107-14. URL: http://www.ncbi.nlm.nih.gov/entrez/query.fcgi?cmd=Retrieve&db=PubMed&dopt=Citation&list_uids=19072950

[56] Quinn, J. F.; Johnston, A. P.; Such, G. K.; Zelikin, A. N. and Caruso, F. (2007): Next generation, sequentially assembled ultrathin films: beyond electrostatics, Chem Soc Rev (vol. 36), No. 5, pp. 707-18. URL: http://www.ncbi.nlm.nih.gov/entrez/query.fcgi?cmd=Retrieve&db=PubMed&dopt=Citation&list_uids=17471396

[57] Jewell, C. M. and Lynn, D. M. (2008): Multilayered polyelectrolyte assemblies as platforms for the delivery of DNA and other nucleic acid-based therapeutics, Adv Drug Deliv Rev (vol. 60), No. 9, pp. 979-99. URL: http://www.ncbi.nlm.nih.gov/entrez/query.fcgi?cmd=Retrieve&db=PubMed&dopt=Citation&list_uids=18395291

[58] Tang, Z.; Wang, Y.; Podsiadlo, P. and Kotov, N. A. (2006): Biomedical Applications of Layer-by-Layer Assembly: From Biomimetics to Tissue Engineering, Advanced Materials (vol. 18), pp. 3203-3224.

[59] Fischlechner, M.; Zschornig, O.; Hofmann, J. and Donath, E. (2005): Engineering virus functionalities on colloidal polyelectrolyte lipid composites, Angew Chem Int Ed Engl (vol. 44), No. 19, pp. 2892-5. URL: http://www.ncbi.nlm.nih.gov/entrez/query.fcgi?cmd=Retrieve&db=PubMed&dopt=Citation&list_uids=15827976

[60] Peyratout, C. S. and Dähne, L. (2004): Tailor-made polyelectrolyte microcapsules: from multilayers to smart containers, Angew Chem Int Ed Engl (vol. 43), No. 29, pp. 3762-83. URL:

http://www.ncbi.nlm.nih.gov/entrez/query.fcgi?cmd=Retrieve&db=PubMed&dopt=Citation&list_uids=15258935

[61] Zelikin, A. N.; Li, Q. and Caruso, F. (2006): Degradable polyelectrolyte capsules filled with oligonucleotide sequences, Angew Chem Int Ed Engl (vol. 45), No. 46, pp. 7743-5. URL: http://www.ncbi.nlm.nih.gov/entrez/query.fcgi?cmd=Retrieve&db=PubMed&dopt=Citation&list_uids=17075936

[62] Zelikin, A. N.; Becker, A. L.; Johnston, A. P.; Wark, K. L.; Turatti, F. and Caruso, F. (2007): A general approach for DNA encapsulation in degradable polymer microcapsules, ACS Nano (vol. 1), No. 1, pp. 63-9. URL: http://www.ncbi.nlm.nih.gov/entrez/query.fcgi?cmd=Retrieve&db=PubMed&dopt=Citation&list_uids=19203131

[63] Caruso, F.; Trau, D.; Möhwald, H. and Renneberg, R. (2000): Enzyme Encapsulation in Layer-by-Layer Engineered Polymer Multilayer Capsules, Langmuir (vol. 16), pp. 1485-1488.

[64] De Koker, S.; De Geest, B. G.; Singh, S. K.; De Rycke, R.; Naessens, T.; Van Kooyk, Y.; Demeester, J.; De Smedt, S. C. and Grooten, J. (2009): Polyelectrolyte microcapsules as antigen delivery vehicles to dendritic cells: uptake, processing, and cross-presentation of encapsulated antigens, Angew Chem Int Ed Engl (vol. 48), No. 45, pp. 8485-9. URL: http://www.ncbi.nlm.nih.gov/entrez/query.fcgi?cmd=Retrieve&db=PubMed&dopt=Citation&list_uids=19810070

[65] Mitragotri, S. and Lahann, J. (2009): Physical approaches to biomaterial design, Nat Mater (vol. 8), No. 1, pp. 15-23. URL: http://www.ncbi.nlm.nih.gov/entrez/query.fcgi?cmd=Retrieve&db=PubMed&dopt=Citation&list_uids=19096389

[66] Hadorn, M. and Eggenberger Hotz, P. (2010): DNA-mediated self-assembly of artificial vesicles, PLoS One (vol. 5), No. 3, p. e9886. URL: http://www.ncbi.nlm.nih.gov/entrez/query.fcgi?cmd=Retrieve&db=PubMed&dopt=Citation&list_uids=20360854

[67] Lynch, N. J.; Kilpatrick, P. K. and Carbonell, R. G. (1996): Aggregation of ligand-modified liposomes by specific interactions with proteins. I: Biotinylated liposomes and avidin, Biotechnol Bioeng (vol. 50), No. 2, pp. 151-68. URL: http://www.ncbi.nlm.nih.gov/entrez/query.fcgi?cmd=Retrieve&db=PubMed&dopt=Citation&list_uids=18626932

[68] Bolinger, P. Y.; Stamou, D. and Vogel, H. (2004): Integrated nanoreactor systems: triggering the release and mixing of compounds inside single vesicles, J Am Chem Soc (vol. 126), No. 28, pp. 8594-5. URL: http://www.ncbi.nlm.nih.gov/entrez/query.fcgi?cmd=Retrieve&db=PubMed&dopt=Citation&list_uids=15250679

[69] Kisak, E. T. (2002): Nanocompartments Enclosing Vesicles, Colloids, and Macromolecules via Interdigitated Lipid Bilayers, Langmuir (vol. 18), pp. 284-288.

[70] Boyer, C. and Zasadzinski, J. A. (2007): Multiple lipid compartments slow vesicle contents release in lipases and serum, ACS Nano (vol. 1), No. 3, pp. 176-82. URL: http://www.ncbi.nlm.nih.gov/entrez/query.fcgi?cmd=Retrieve&db=PubMed&dopt=Citation&list_uids=18797512

[71] Bäumler, H. and Georgieva, R. (2010): Coupled enzyme reactions in multicompartment microparticles, Biomacromolecules (vol. 11), No. 6, pp. 1480-7. URL: http://www.ncbi.nlm.nih.gov/entrez/query.fcgi?cmd=Retrieve&db=PubMed&dopt=Citation&list_uids=20486658

[72] Delcea, M.; Yashchenok, A.; Videnova, K.; Kreft, O.; Möhwald, H. and Skirtach, A. G. (2010): Multicompartmental micro- and nanocapsules: hierarchy and applications in biosciences, Macromol Biosci (vol. 10), No. 5, pp. 465-74. URL: http://www.ncbi.nlm.nih.gov/entrez/query.fcgi?cmd=Retrieve&db=PubMed&dopt=Citation&list_uids=20166231

[73] Städler, B.; Chandrawati, R.; Price, A. D.; Chong, S. F.; Breheney, K.; Postma, A.; Connal, L. A.; Zelikin, A. N. and Caruso, F. (2009): A microreactor with thousands of subcompartments: enzyme-loaded liposomes within polymer capsules, Angew Chem Int Ed Engl (vol. 48), No. 24, pp. 4359-62. URL: http://www.ncbi.nlm.nih.gov/entrez/query.fcgi?cmd=Retrieve&db=PubMed&dopt=Citation&list_uids=19418505

[74] Walther, A. and Müller, A. H. (2008): Janus particles, Soft Matter (vol. 4), pp. 663-668.

[75] Yuet, K. P.; Hwang, D. K.; Haghgooie, R. and Doyle, P. S. (2010): Multifunctional superparamagnetic Janus particles, Langmuir (vol. 26), No. 6, pp. 4281-7. URL: http://www.ncbi.nlm.nih.gov/entrez/query.fcgi?cmd=Retrieve&db=PubMed&dopt=Citation&list_uids=19842632

[76] Christian, D. A.; Tian, A.; Ellenbroek, W. G.; Levental, I.; Rajagopal, K.; Janmey, P. A.; Liu, A. J.; Baumgart, T. and Discher, D. E. (2009): Spotted vesicles, striped micelles and Janus assemblies induced by ligand binding, Nat Mater (vol. 8), No. 10, pp. 843-9. URL: http://www.ncbi.nlm.nih.gov/entrez/query.fcgi?cmd=Retrieve&db=PubMed&dopt=Citation&list_uids=19734886

[77] Wurm, F. and Kilbinger, A. F. (2009): Polymeric janus particles, Angew Chem Int Ed Engl (vol. 48), No. 45, pp. 8412-21. URL: http://www.ncbi.nlm.nih.gov/entrez/query.fcgi?cmd=Retrieve&db=PubMed&dopt=Citation&list_uids=19798704

[78] Jiang, S.; Chen, Q.; Tripathy, M.; Luijten, E.; Schweizer, K. S. and Granick, S. (2010): Janus particle synthesis and assembly, Adv Mater (vol. 22), No. 10, pp. 1060-71. URL: http://www.ncbi.nlm.nih.gov/entrez/query.fcgi?cmd=Retrieve&db=PubMed&dopt=Citation&list_uids=20401930

[79] Suci, P. A.; Kang, S.; Young, M. and Douglas, T. (2009): A streptavidin-protein cage Janus particle for polarized targeting and modular functionalization, J Am Chem Soc (vol. 131), No. 26, pp. 9164-5. URL: http://www.ncbi.nlm.nih.gov/entrez/query.fcgi?cmd=Retrieve&db=PubMed&dopt=Citation&list_uids=19522495

[80] Singh, Y.; Murat, P. and Defrancq, E. (2010): Recent developments in oligonucleotide conjugation, Chem Soc Rev (vol. 39), No. 6, pp. 2054-70. URL: http://www.ncbi.nlm.nih.gov/entrez/query.fcgi?cmd=Retrieve&db=PubMed&dopt=Citation&list_uids=20393645

[81] Medintz, I. L.; Berti, L.; Pons, T.; Grimes, A. F.; English, D. S.; Alessandrini, A.; Facci, P. and Mattoussi, H. (2007): A reactive peptidic linker for self-assembling hybrid quantum dot-DNA bioconjugates, Nano Lett (vol. 7), No. 6, pp. 1741-8. URL: http://www.ncbi.nlm.nih.gov/entrez/query.fcgi?cmd=Retrieve&db=PubMed&dopt=Citation&list_uids=17530814

[82] Niemeyer, C. M. (2002): The developments of semisynthetic DNA-protein conjugates, Trends Biotechnol (vol. 20), No. 9, pp. 395-401. URL: http://www.ncbi.nlm.nih.gov/entrez/query.fcgi?cmd=Retrieve&db=PubMed&dopt=Citation&list_uids=12175771

[83] Gunnarsson, A.; Sjövall, P. and Höök, F. (2010): Liposome-based chemical barcodes for single molecule DNA detection using imaging mass spectrometry, Nano Lett (vol. 10), No. 2, pp. 732-7. URL: http://www.ncbi.nlm.nih.gov/entrez/query.fcgi?cmd=Retrieve&db=PubMed&dopt=Citation&list_uids=20085369

[84] Lynch, N. J.; Kilpatrick, P. K. and Carbonell, R. G. (1996): Aggregation of ligand-modified liposomes by specific interactions with proteins. II: Biotinylated liposomes and antibiotin antibody, Biotechnol Bioeng (vol. 50), No. 2, pp. 169-83. URL: http://www.ncbi.nlm.nih.gov/entrez/query.fcgi?cmd=Retrieve&db=PubMed&dopt=Citation&list_uids=18626933

[85] Granéli, A.; Edvardsson, M. and Höök, F. (2004): DNA-based formation of a supported, three-dimensional lipid vesicle matrix probed by QCM-D and SPR, ChemPhysChem (vol. 5), No. 5, pp. 729-33. URL: http://www.ncbi.nlm.nih.gov/entrez/query.fcgi?cmd=Retrieve&db=PubMed&dopt=Citation&list_uids=15179728

[86] Goksu, E. I.; Vanegas, J. M.; Blanchette, C. D.; Lin, W. C. and Longo, M. L. (2009): AFM for structure and dynamics of biomembranes, Biochim Biophys Acta (vol. 1788), No. 1, pp. 254-66. URL: http://www.ncbi.nlm.nih.gov/entrez/query.fcgi?cmd=Retrieve&db=PubMed&dopt=Citation&list_uids=18822269

[87] Veatch, S. L. and Keller, S. L. (2005): Seeing spots: complex phase behavior in simple membranes, Biochim Biophys Acta (vol. 1746), No. 3, pp. 172-85. URL: http://www.ncbi.nlm.nih.gov/entrez/query.fcgi?cmd=Retrieve&db=PubMed&dopt=Citation&list_uids=16043244

[88] Korlach, J.; Schwille, P.; Webb, W. W. and Feigenson, G. W. (1999): Characterization of lipid bilayer phases by confocal microscopy and fluorescence correlation spectroscopy, Proc Natl Acad Sci U S A (vol. 96), No. 15, pp. 8461-6. URL: http://www.ncbi.nlm.nih.gov/entrez/query.fcgi?cmd=Retrieve&db=PubMed&dopt=Citation&list_uids=10411897

[89] Veatch, S. L. and Keller, S. L. (2003): Separation of liquid phases in giant vesicles of ternary mixtures of phospholipids and cholesterol, Biophys J (vol. 85), No. 5, pp. 3074-3083. URL: http://www.ncbi.nlm.nih.gov/entrez/query.fcgi?cmd=Retrieve&db=PubMed&dopt=Citation&list_uids=14581208

[90] Baumgart, T.; Hammond, A. T.; Sengupta, P.; Hess, S. T.; Holowka, D. A.; Baird, B. A. and Webb, W. W. (2007): Large-scale fluid/fluid phase separation of proteins and lipids in giant plasma membrane vesicles, Proc Natl Acad Sci U S A (vol. 104), No. 9, pp. 3165-3170. URL: http://www.ncbi.nlm.nih.gov/entrez/query.fcgi?cmd=Retrieve&db=PubMed&dopt=Citation&list_uids=17360623

[91] Schneider, M. B.; Chan, W. K. and Webb, W. W. (1983): Fast diffusion along defects and corrugations in Pβ′ phospholipid Liquid Crystals, Biophys J(vol. 43), pp. 157 - 165.

[92] Brown, D. A. (2001): Seeing is believing: visualization of rafts in model membranes, Proc Natl Acad Sci U S A (vol. 98), No. 19, pp. 10517-8. URL: http://www.ncbi.nlm.nih.gov/entrez/query.fcgi?cmd=Retrieve&db=PubMed&dopt=Citation&list_uids=11553797

[93] Baumgart, T.; Hunt, G.; Farkas, E. R.; Webb, W. W. and Feigenson, G. W. (2007): Fluorescence probe partitioning between Lo/Ld phases in lipid membranes, Biochim Biophys Acta (vol. 1768), No. 9, pp. 2182-94. URL:

http://www.ncbi.nlm.nih.gov/entrez/query.fcgi?cmd=Retrieve&db=PubMed&dopt=Citation&list_uids=17588529

[94] Sengupta, P.; Hammond, A.; Holowka, D. and Baird, B. (2008): Structural determinants for partitioning of lipids and proteins between coexisting fluid phases in giant plasma membrane vesicles, Biochim Biophys Acta (vol. 1778), No. 1, pp. 20-32. URL: http://www.ncbi.nlm.nih.gov/entrez/query.fcgi?cmd=Retrieve&db=PubMed&dopt=Citation&list_uids=17936718

[95] Lingwood, D.; Ries, J.; Schwille, P. and Simons, K. (2008): Plasma membranes are poised for activation of raft phase coalescence at physiological temperature, Proc Natl Acad Sci U S A (vol. 105), No. 29, pp. 10005-10. URL: http://www.ncbi.nlm.nih.gov/entrez/query.fcgi?cmd=Retrieve&db=PubMed&dopt=Citation&list_uids=18621689

[96] Hanzal-Bayer, M. F. and Hancock, J. F. (2007): Lipid rafts and membrane traffic, FEBS Lett (vol. 581), No. 11, pp. 2098-2104. URL: http://www.ncbi.nlm.nih.gov/entrez/query.fcgi?cmd=Retrieve&db=PubMed&dopt=Citation&list_uids=17382322

[97] Beales, P. A. and Vanderlick, T. K. (2009): Partitioning of membrane-anchored DNA between coexisting lipid phases, J Phys Chem B (vol. 113), No. 42, pp. 13678-13686. URL: http://www.ncbi.nlm.nih.gov/entrez/query.fcgi?cmd=Retrieve&db=PubMed&dopt=Citation&list_uids=19827842

[98] Shogomori, H.; Hammond, A. T.; Ostermeyer-Fay, A. G.; Barr, D. J.; Feigenson, G. W.; London, E. and Brown, D. A. (2005): Palmitoylation and intracellular domain interactions both contribute to raft targeting of linker for activation of T cells, J Biol Chem (vol. 280), No. 19, pp. 18931-42. URL: http://www.ncbi.nlm.nih.gov/entrez/query.fcgi?cmd=Retrieve&db=PubMed&dopt=Citation&list_uids=15753089

[99] Kang, J.; Loew, M.; Arbuzova, A.; Andreou, I. and Dähne, L. (2010): Nucleic acid diagnostic FRET particles based on layer-by-layer technology, Adv Mater (vol. 22), No. 32, pp. 3548-52. URL: http://www.ncbi.nlm.nih.gov/entrez/query.fcgi?cmd=Retrieve&db=PubMed&dopt=Citation&list_uids=20665568

[100] Flasche, W.; Cismas, C.; Herrmann, A. and Liebscher, J. (2004): Lipophilic Nucleosides by Sonogashira Coupling, Synthesis (vol. 14), pp. 2335-2341.

[101] Hope, M. J.; Bally, M. B.; Webb, G. and Cullis, P. R. (1985): Production of large unilamellar vesicles by a rapid extrusion procedure.
Characterization of size distribution, trapped volume and ability to maintain a membrane potential, Biochim Biophys Acta (vol. 812), pp. 55-65.

[102] Angelova, M. I.; Soleau, S.; Meleard, P.; Faucon, J. H. and Bothorel, P. (1992): Preparation of giant vesicles by external AC fields. Kinetics and application., Progr Colloid Polym Sci (vol. 89), pp. 127-131.

[103] Stöckl, M.; Fischer, P.; Wanker, E. and Herrmann, A. (2008): Alpha-synuclein selectively binds to anionic phospholipids embedded in liquid-disordered domains, J Mol Biol (vol. 375), No. 5, pp. 1394-404. URL: http://www.ncbi.nlm.nih.gov/entrez/query.fcgi?cmd=Retrieve&db=PubMed&dopt=Citation&list_uids=18082181

[104] Zacharias, D. A.; Violin, J. D.; Newton, A. C. and Tsien, R. Y. (2002): Partitioning of lipid-modified monomeric GFPs into membrane microdomains of live cells, Science (vol. 296), No. 5569, pp. 913-6. URL:

http://www.ncbi.nlm.nih.gov/entrez/query.fcgi?cmd=Retrieve&db=PubMed&dopt=Citation&list_uids=11988576
[105] Lakowicz, J.R. (2006): Principles of fluorescence spectroscopy, Third. ed., Springer.
[106] Boxer, S. G. (2000): Molecular transport and organization in supported lipid membranes, Curr Opin Chem Biol (vol. 4), No. 6, pp. 704-9. URL: http://www.ncbi.nlm.nih.gov/entrez/query.fcgi?cmd=Retrieve&db=PubMed&dopt=Citation&list_uids=11102877
[107] Fischlechner, M.; Zaulig, M.; Meyer, S.; Estrela-Lopis, I.; Cuéllar, L.; Irigoyen, J.; Pescador, P.; Brumen, M.; Messner, P.; Moya, S. and Donath, E. (2008): Lipid layers on polyelectrolyte multilayer supports, Soft Matter (vol. 4), pp. 2245-2258.
[108] De la Maza, A. and Parra, J. L. (1994): Vesicle-micelle structural transition of phosphatidylcholine bilayers and Triton X-100, Biochem J (vol. 303 (Pt 3)), pp. 907-14. URL: http://www.ncbi.nlm.nih.gov/entrez/query.fcgi?cmd=Retrieve&db=PubMed&dopt=Citation&list_uids=7980461
[109] Benachir, T. and Lafleur, M. (1995): Study of vesicle leakage induced by melittin, Biochim Biophys Acta (vol. 1235), No. 2, pp. 452-60. URL: http://www.ncbi.nlm.nih.gov/entrez/query.fcgi?cmd=Retrieve&db=PubMed&dopt=Citation&list_uids=7756355
[110] Van Hoogevest, P.; De Gier, J. and De Kruijff, B. (1984): Determination of the size of the packing defects in dimyristoylphoshatidylcholine bilayers, present at the phase transition temperature, FEBS Lett (vol. 171), No. 2, pp. 160-164.
[111] Dempsey, C. E. (1990): The actions of melittin on membranes, Biochimica et Biophysica Acta (vol. 1031), pp. 143-161.
[112] Düzgüneş, N.; Allen, T. M.; Fedor, J. and Papahadjopoulos, D. (1987): Lipid mixing during membrane aggregation and fusion: why fusion assays disagree, Biochemistry (vol. 26), No. 25, pp. 8435-42. URL: http://www.ncbi.nlm.nih.gov/entrez/query.fcgi?cmd=Retrieve&db=PubMed&dopt=Citation&list_uids=3442666
[113] Jin, R.; Wu, G.; Li, Z.; Mirkin, C. A. and Schatz, G. C. (2003): What controls the melting properties of DNA-linked gold nanoparticle assemblies? J Am Chem Soc (vol. 125), No. 6, pp. 1643-54. URL: http://www.ncbi.nlm.nih.gov/entrez/query.fcgi?cmd=Retrieve&db=PubMed&dopt=Citation&list_uids=12568626
[114] Pfeiffer, I. and Hook, F. (2006): Quantification of oligonucleotide modifications of small unilamellar lipid vesicles, Anal Chem (vol. 78), No. 21, pp. 7493-8. URL: http://www.ncbi.nlm.nih.gov/entrez/query.fcgi?cmd=Retrieve&db=PubMed&dopt=Citation&list_uids=17073417
[115] Benachir, T.; Monette, M.; Grenier, J. and Lafleur, M. (1997): Melittin-induced leakage from phosphatidylcholine vesicles is modulated by cholesterol: a property used for membrane targeting, Eur Biophys J (vol. 25), pp. 201-210.
[116] Hossann, M.; Wang, T.; Wiggenhorn, M.; Schmidt, R.; Zengerle, A.; Winter, G.; Eibl, H.; Peller, M.; Reiser, M.; Issels, R. D. and Lindner, L. H. (2010): Size of thermosensitive liposomes influences content release, J Control Release. URL: http://www.ncbi.nlm.nih.gov/entrez/query.fcgi?cmd=Retrieve&db=PubMed&dopt=Citation&list_uids=20727921
[117] Tannock, I. F. and Rotin, D. (1989): Acid pH in tumors and its potential for therapeutic exploitation, Cancer Res (vol. 49), No. 16, pp. 4373-84. URL: http://www.ncbi.nlm.nih.gov/entrez/query.fcgi?cmd=Retrieve&db=PubMed&dopt=Citation&list_uids=2545340

[118] Bunge, A.; Loew, M.; Pescador, P.; Arbuzova, A.; Brodersen, N.; Kang, J.; Dähne, L.; Liebscher, J.; Herrmann, A.; Stengel, G. and Huster, D. (2009): Lipid membranes carrying lipophilic cholesterol-based oligonucleotides--characterization and application on layer-by-layer coated particles, J Phys Chem B (vol. 113), No. 51, pp. 16425-34. URL: http://www.ncbi.nlm.nih.gov/entrez/query.fcgi?cmd=Retrieve&db=PubMed&dopt=Citation&list_uids=19957915

[119] Banchelli, M.; Betti, F.; Berti, D.; Caminati, G.; Bombelli, F. B.; Brown, T.; Wilhelmsson, L. M.; Norden, B. and Baglioni, P. (2008): Phospholipid membranes decorated by cholesterol-based oligonucleotides as soft hybrid nanostructures, J Phys Chem B (vol. 112), No. 35, pp. 10942-52. URL: http://www.ncbi.nlm.nih.gov/entrez/query.fcgi?cmd=Retrieve&db=PubMed&dopt=Citation&list_uids=18693696

[120] Jarikote, D. V.; Köhler, O.; Socher, E. and Seitz, O. (2005): Linear and divergent solid-phase synthesis of peptide nucleic acids containing thiazole orange as artificial base, Eur J Org Chem (vol. 2005), No. 15, pp. 3187-3195.

[121] Ellington, A. D. and Szostak, J. W. (1990): In vitro selection of RNA molecules that bind specific ligands, Nature (vol. 346), No. 6287, pp. 818-22. URL: http://www.ncbi.nlm.nih.gov/entrez/query.fcgi?cmd=Retrieve&db=PubMed&dopt=Citation&list_uids=1697402

[122] Bouchard, P. R.; Hutabarat, R. M. and Thompson, K. M. (2010): Discovery and development of therapeutic aptamers, Annu Rev Pharmacol Toxicol (vol. 50), pp. 237-57. URL: http://www.ncbi.nlm.nih.gov/entrez/query.fcgi?cmd=Retrieve&db=PubMed&dopt=Citation&list_uids=20055704

[123] Fiammengo, R. and Jäschke, A. (2005): Nucleic acid enzymes, Curr Opin Biotechnol (vol. 16), No. 6, pp. 614-21. URL: http://www.ncbi.nlm.nih.gov/entrez/query.fcgi?cmd=Retrieve&db=PubMed&dopt=Citation&list_uids=16257198

[124] Montes, L. R.; Ibarguren, M.; Goni, F. M.; Stonehouse, M.; Vasil, M. L. and Alonso, A. (2007): Leakage-free membrane fusion induced by the hydrolytic activity of PlcHR(2), a novel phospholipase C/sphingomyelinase from Pseudomonas aeruginosa, Biochim Biophys Acta (vol. 1768), No. 10, pp. 2365-72. URL: http://www.ncbi.nlm.nih.gov/entrez/query.fcgi?cmd=Retrieve&db=PubMed&dopt=Citation&list_uids=17560896

[125] Eggeling, C.; Ringemann, C.; Medda, R.; Schwarzmann, G.; Sandhoff, K.; Polyakova, S.; Belov, V. N.; Hein, B.; von Middendorff, C.; Schonle, A. and Hell, S. W. (2009): Direct observation of the nanoscale dynamics of membrane lipids in a living cell, Nature (vol. 457), No. 7233, pp. 1159-62. URL: http://www.ncbi.nlm.nih.gov/entrez/query.fcgi?cmd=Retrieve&db=PubMed&dopt=Citation&list_uids=19098897

Acknowledgement

This work was done at the Humboldt University Berlin in the group Molecular Biophysics. I would like to thank all the people who helped me with my thesis during the past four years.

At first, I like to thank Prof. Dr. Andreas Herrmann who provided the possibility to work on this exciting topic in his group. His ideas and motivation had a great account for my work.

I am very grateful to Dr. Anna Arbuzova for the guidance throught experiment development, the excessive discussions of results, proof reading, and all the essential hints and advice she gave me. Thank you.

I have to thank Prof. Dr. Jürgen Liebscher and his group, especially Dr. Oliver Kaczmarek, Dr. Nicolai Brodersen, and Ralph Springer. They did not only provide the lipophilic nucleic acids but also gave much input for the progress of my work.

Many thanks go to Prof. Dr. Daniel Huster and his group, especially Dr. Andreas Bunge and Dr. Paula Pescador for the great co-operation and the help with the manuscripts.

I have to thank Dr. Lars Dähne and Jing Kang from Surflay Nanotec GmbH for their great LbL particles and also the very close co-operation.

I like to thank Prof. Dr. Oliver Seitz and Frank Altenbrunn for providing the lipophilic PNA.

I would also like to thank Dr. Christoph Böttcher and Dr. Kai Ludwig for the Cryo-TEM microscopy and the discussion about the results.

Many thanks go to Dr. Silvia Scolari and Roland Schwarzer. They prepared the cells and the GPMVs and showed me how to work with this biological system.

I have to thank Dr. Thomas Korte and Dr. Martin Stöckl who introduced me to the confocal microscope and the FLIM measurements.

Many thanks got to Christian Sieben for his smiling help with the optical tweezer.

I would also like to thank the whole group of Molecular Biophysics for the help and the great working atmosphere.

I am grateful to my family for their support over the past years.

I would like to thank Nadine Jungnick just for being herself. She believed in me even when I didn’t.

Publications

Posters

Loew, M.; Kang, J.; Dähne, L.; Kaczmarek, O.; Liebscher, J.; Pescador, P.; Bunge, A.; Huster, D.; Herrmann, A.; Arbuzova, A. (2010) Controlled release in time and space: Assembly of nanocontainers on a carrier system via DNA hybridization; Particles 2010, Orlando (Florida).

Loew, M.; Kang, J.; Dähne, L.; Kaczmarek, O.; Liebscher, J.; Huster, D.; Ludwig, K.; Böttcher, C.; Herrmann, A.; Arbuzova, A.; (2009) Controlled assembly of vesicle-based nanocontainers on Layer-by-Layer particles via DNA hybridization Biophysical Society, 53rd Meeting, Boston (Massachusetts).

Loew, M.; Kang, J.; Dähne, L.; Kaczmarek, O.; Liebscher, J.; Pescador, P.; Huster, D.; Herrmann, A.; Arbuzova, A.; (2009) Controlled assembly of vesicle-based nanocontainers on Layer-by-Layer particles via DNA hybridization; Nanotech Europe 2009, Berlin.

Manuscripts

(1) Loew, M.; Springer, R.; Scolari, S.; Altenbrunn, F.; Seitz, O.; Liebscher, J.; Huster, D.; Herrmann, A.; Arbuzova, A. *J Am Chem Soc* **2010**.
(2) Pescador, P.; Brodersen, N.; Scheidt, H. A.; Loew, M.; Holland, G.; Bannert, N.; Liebscher, J.; Herrmann, A.; Huster, D.; Arbuzova, A. *Chem Commun (Camb)* **2010**, *46*, 5358-5360.
(5) Kang, J.; Loew, M.; Arbuzova, A.; Andreou, I.; Dahne, L. *Adv Mater* **2010**, *22*, 3548-3552.
(3) Bunge, A.; Loew, M.; Pescador, P.; Arbuzova, A.; Brodersen, N.; Kang, J.; Dahne, L.; Liebscher, J.; Herrmann, A.; Stengel, G.; Huster, D. *J Phys Chem B* **2009**, *113*, 16425-16434.
(4) Loew, M.; Kang, J.; Dahne, L.; Hendus-Altenburger, R.; Kaczmarek, O.; Liebscher, J.; Huster, D.; Ludwig, K.; Bottcher, C.; Herrmann, A.; Arbuzova, A. *Small* **2009**, *5*, 320-323.
(6) Bunge, A.; Fischlechner, M.; Loew, M.; Arbuzova, A.; Herrmann, A.; Huster, D. *Soft Matter* **2009**, *5*, 3331-3335.

Martin Loew